Republic of Iraq

Ministry of Higher Education and Scientific Research

University of Babylon

College of science for women

Chemistry Department

Preparation and Characterization of New Micro/Nano SA-g-P(AAc-co-VBS)/ZnO Hydrogel Surface as a Superior Removal of Pollutants and Biological Activity.

A Thesis Submitted to the Council of the College of Science for Women, University of Babylon as a Partial Fulfilment of the Requirements for the Degree of Master of Chemistry

By

Hadeel Kadhim Abbas Kalaf Al-Bdairi

B.Sc. Chemistry, College of Science, Babylon University, 2000-2001

Supervised by

Asst. Prof. Dr. Aseel Mushtaq Aljeboree

2022 A.D **1443A.**

Supervisor Certification

I certify that this thesis entitled

Preparation and Characterization of New Micro/Nano SA-g-P(AAc-co-VBS)/ZnO Hydrogel Surface as a Superior Removal of Pollutants and biological Activity.

Was prepared under my supervision at the University of Babylon / College of Science for Women as a partial Requirement for the degree of Master in Chemistry Science .

Signature
Dr. Aseel Mushtaq Kadum
Scientific Order: Asst. Prof.
Address:
University of Babylon / College of
Science for Women
Date: / /2022

Recommendation of Head of Chemistry Department

According to the available recommendation, I forward this thesis for Discussion.

Signature of Chemistry Department
Dr/ Hazim Yahya Mohammed
Scientific order: Asst. Prof.
Address: Head of Chemistry Department
University of Babylon / College of
Science for Women
Date: / /2022

Dedications

To My father soul , mother, husband and family members who supported me all the time.

To my supervisor, Assistant Professor Dr. ***Aseel Mushtaq Al-Jeboree.***

To my teacher ***Dr. Ayad Alkaim*** *And To all department of chemistry staff .*

To all my postgraduate colleagues.

Researcher

Acknowledgments

Praise be to God, Lord of the worlds. Praise be to God, who helped me and gave me the strength, patience, and endurance to complete this thesis.

I would like to thank and appreciate my supervisor Assistant Professor ***Dr. Aseel Mushtaq Aljeboree*** , for her suggestions and supporting, definitely without her continuous advice and valuable guidance, the research work could not be completed.

I also would like to extend my sincere thanks and appreciation to professor **Dr. Ayad Alkaim** for his continuous support and encouragement.

I also express my thanks and gratitude to the deanship of the college of science for women department of chemistry and all other lecturers who helped me and gave their valuable comments to make my thesis in good form.

Finally, I would like to express my sincere thanks and appreciation to the members of my family, especially, my husband and my children who encouraged me until I reached this stage.

Researcher

Summary

Synthesis Superabsorbent polymer was prepared by the free radical graft copolymerization method. where the work included the preparation of two surfaces of hydrogel, the first Sodium Alginate-g-(poly acrylic acid-co-Sodium4-VinylBenzeneSulfonate), (SA-g-(PAAc-co-VBS) and the second surface hydrogel after loading Zinc oxide nannoparticals (SA-g-(PAAc-co-VBS)/ZnO NPs) and these new surfaces were prepared from different monomers, for the removal of three pollutants (Crystal Violet (CV) dye, Tetracycline (TC) drug, and Phenol PH). The physical characterizations of these prepared materials have been studied. The obtained powders are characterized by using different techniques like Ultraviolet-Visible Spectroscopy (UV–Vis), Fourier Transform Infrared (FT-IR), Thermo gravimetric analysis (TGA), Field Emission Scanning Electron Microscopy (FE-SEM), Transmission Electron Microscopy (TEM), Energy Dispersive X-Ray (EDX) and X-ray Diffraction Spectroscopy (XRD).

The practical experiments included calculation of the maximum wavelength and study of optimum condition of the effect of adsorption parameters are: Effect of contact time, Effect of adsorbent dose, Effect of pH solution, Effect of temperature solution, Adsorbent regeneration experiments (Desorption), Comparative adsorption between different surfaces to removal three pollutant , A comparative between the amount of zinc oxide decorated of hydrogel, Removal of laboratory sample aqueous pollutants, Tetracycline (TC) drug loading , In vitro drug release, Biological activity bacterial test and Treating mice wounds using a surface prepared from SA-g-(PAAc-co-VBS)/ZnO NPs.

The results of the adsorption study show that percentage of removal increases with the increase of the weight of the surfaces; and contact time. The optimized value of agitation time is 2 hr. after which the adsorption becomes constant. The increase of adsorbent amount about rang (0.01 - 0.1)g, the percentage removal E% of CV dye, TC drug and PH increase from (72.9 - 99.8%), (60.639% - 97.085%), (48.71% - 94.05%) and adsorption capacity (Qe mg/g) decrease from (1599 – 200 mg/g), (606.39 – 97.08 mg/g), (487.1831- 94.456mg/g) onto (SA-g-(PAAC-co-VBS)/ZnO NPs at the same order about 2h of adsorption time. The enthalpy (ΔH) values are positive indicating that the adsorption process is an endothermic reaction. All processes of adsorption considered spontaneous from the negative value of Gibes free energy (ΔG), While, entropy (ΔS) have positive value that refer the interaction of molecules caused random of the total system. The Freundlich and Langmuir models are also introduced. It has been found that all results follow the Freundlich model in the presence of three pollutant; this nonlinearity is higher when using the Freundlich model.

Comparative between ((SA-g-(PAAc-co-VBS)/ZnO NPs, (SA-g-(PAAc-co-VBS) and ZnO NPs) surfaces as adsorbents. The best results of the percentage of removal (E%) of three pollutant (Crystal violet (CV) dye, Tetracycline(TC) drug and phenol PH) arrange in order increasing (SA-g-(PAAc-co-VBS)/ZnO NPs > SA-g-(PAAc-co-VBS) > ZnO NPs), The good results of the percentage of removal (E%) of SA-g-(PAAc-co-VBS)/ZnO NPs, (92,451%, and 87.56% and 82.56) for CV, TC and PH at the same order. Also comparative between the amount of Zinc oxide nanoparticals (ZnO NPs) decorated of (SA-g-(PAAc-co-VBS) by using (0.05, 0.08, 0.1 and 0.15 g). The good results of the percentage of removal (E%) of three pollutant (CV,TC, PH) about 0.1 g ZnO NPs.

Recyclability and Desorption studies indicated the best recycling performance of the prepared composite. Based on the results, the prepared SA-g-(PAAc-co-VBS)/ZnO NPs can be useful as a promising, eco-friendly , cost-effective, and efficient material for dyes decontamination .Studies was carry out utilizing several desorption agents at concentration (0.01N) like H_2SO_4, NaOH, H_3PO_4, HCl, HNO_3, and water. The (SA-g-(PAAc-co-VBS)/ZnO NPs) was regeneration with 100% can be desorbed in diluted HCl (0.01N).

Kinetics adsorption models of three pollutant on SA-g-(PAAc-co-VBS)/ZnO NPs was studied and modeled using three kinetic models. The classification of the kinetic models according to the simulation of the adsorption study is Pseudo first order > Psuedo second order > Chemisorption.

The release of Tetracycline (TC) drug was studied in conditions similar to the human body in terms of acidity and temperature. Drug release of 28% and 21.56%, in the first 1 h was observed for TC drug. The cumulative release of TC drug in 3 h was 50.65 %, 42.33% from pH=7.5 and pH 1.2 at the same order.

The results of the inhibition regions of the three compounds (SA-g-(PAAc-co-VBS)/ZnO NPs, SA-g- (PAAc-co-VBS), ZnO NPs), where it was given that the compound (SA-g-(PAAc-co-VBS)/ZnO NPs) had high antibacterial activity, (30mm) against *Staphylococcus aureus*, (25 mm) against *Streptococcus epigenetics*, (13 mm, 12 mm) against *E.coli*, and *Klebsiella spp*. That is, it had a higher effect on the Gram-positive bacteria than on the Gram-negative bacteria, respectively. The compound ((SA-g-(PAAC-co-VBS)) has antibacterial activity against *Staphylococcus aureus* (15 mm), against *Streptococcus epigenetics* (20 mm), had very low activity against E coli and *Klebsiella spp*. That is, it

had an effect on the Gram-positive bacteria and had low effect on the Gram-negative bacteria and the compound (ZnO NPs) had very low anti-bacterial activity for Gram-positive bacteria and Gram-negative bacteria.

It was studied, treating rat wounds with a surface prepared from SA-g-(PAAc-co-VBS)/ZnO NPs, which was observed within two to seven days, according to the results, there is complete healing of the mice and the return of the skin to its natural colour. This is due to the fact that SA-g-(PAAc-co-VBS)/ZnO NPs have high effective efficiency in treating and healing mice. It is considered environmentally friendly, non-toxic, and also considered anti-inflammatory. In addition, there is biocompatibility with mammalian cells.

الخلاصة

تخليق بوليمر فائق الامتصاص يتم تحضيره بطريقة البلمرة المشتركة بتطعم الجذور الحرة. حيث اشتمل العمل على تحضير سطحين , الهلام المائي الاول , صوديوم الجنيت (بولي أكريليك أسيد - g - 4 صوديوم 4 - فينيل بنزين سلفونات) (SA-g- (PAAc-co-VBS) ، وسطح الهلام المائي الثاني بعد تحميل أكسيد الزنك النانوي عليه SA-g-(PAAc-co-VBS) / ZnO) وهذه الأسطح الجديدة تم تحضيرها من مونومرات مختلفة لإزالة ثلاثة ملوثات (صبغة البلوره البنفسجية (CV) ، دواء تتراسايكلين (TC) ، الفينول PH).

تمت دراسة الخصائص الفيزيائية لهذه السطوح المحضره التي تم الحصول عليها باستخدام تقنيات مختلفة مثل باستخدام التحليل الطيفي للأشعة فوق البنفسجية المرئية (UV-Vis) ، مطيافية الاشعه تحت الحمراء (FT-IR) ، التحليل الحراري الوزني (TGA) ، المجهر الكتروني الماسح ذو المجال المنبعث (FESEM) ، المجهر الإلكتروني النافذ (TEM) ، الأشعة السينية المشتتة للطاقة (EDX) حيود الاشعه السينيه (XRD).

تضمنت التجارب العملية حساب الطول الموجي الاعظم ودراسة الظروف المثلى المؤثره على عملية الامتزاز وتشمل : تأثير زمن الاتزان ، تأثير جرعة الممتزات ، تأثير محلول الأس الهيدروجيني ، تأثير محلول درجة الحرارة ، تجارب تجديد وتنشيط السطح ، مقارنة الامتزاز بين الأسطح المختلفة لإزالة ثلاثة ملوثات ، مقارنة بين كمية أكسيد الزنك نانوي المحمله على الهيدروجيل ، وإزالة الملوثات المائية الحقيقية ، وتحميل دواء التتراسيكلين (TC) ، وإطلاق الأدوية في المختبر ، والنشاط البيولوجي ، والاختبار البكتيري ، وعلاج جروح الفئران باستخدام (SA-g-(PAAC-co-VBS) / ZnO NPs).

تظهر نتائج دراسة الامتزاز أن نسبة الإزالة تزداد مع زيادة وزن السطح. وزمن الاتزان . حيث كانت الظروف المثلى لزمن الاتزان 2 ساعة. وبعد ذلك يصبح الامتزاز ثابتا. زيادة كمية الممتزات حوالي (g 0.1-0.01)، وزيادة النسبة المئوية لإزالة صبغة CV ودواء TC و PH من (72.9% – 99.8٪) ، (60.63٪ - 98.80٪) ، (48.66٪ - 94.76٪) ,وكفاءة الامتزاز تقل من (1599 - 200 mg/g) ، (606.45 mg/g - 97.77) ، (487.134- 94.445 mg/g) على (SA-g- (PAAC-co-VBS) / ZnO NPs) بنفس الترتيب حوالي خلال زمن اتزان ساعتين . تم دراسه الدوال الثرموديناميك , حيث تكون قيمة الانثالبي HΔ موجبة مما يشير إلى أن عملية الامتزاز تفاعل ماص للحرارة. تعتبر جميع عمليات الامتزاز تلقائية من

القيمة التغير طاقة جبس الحره لـ GΔ. في حين أن الانتروبي SΔ لها قيمة موجبة تشير إلى تفاعل الجزيئات الناتج بشكل عشوائي من النظام الكلي ، كما تم تقديم ايزوثيرمات الامتزاز Freundlich و Langmuir. لقد وجد أن جميع النتائج تتبع موديل Freundlich في وجود ثلاثة ملوثات .

تم دراسة مقارنة بين الاسطح المحضره ((SA-g- (PAAc-co-VBS) / ZnO NPs، SA-g- (PAAc-co-VBS)) و ZnO NPs) كمواد مازه. أفضل النتائج لنسبة الإزالة (E٪) لثلاثة ملوثات (صبغة كريستال بنفسجية (CV)، دواء Tetracycline (TC) وفينول PH) مرتبة بالترتيب ((SA-g- (PAAc-co-VBS) / ZnO NPs> SA-g- (PAAc- co-VBS> ZnO NPs) ، النتائج للنسبة المئوية للإزالة (E٪) من SA-g- (PAAc-co-VBS) /ZnO NPs، (92،451٪ ، و 87.56٪ و% 83.56) لكل من CV ، و TC و PH بنفس الترتيب وايضا تم دراسة مقارنه بين كمية أكسيد الزنك (ZnO NPs) المحمله بـ SA-g- (PAAc-co-VBS) باستخدام (0.01, 0.05, 0.1 , 0.15 g) النتائج للنسبة المئوية من إزالة (٪ E) لثلاثة ملوثات (CV، TC ، PH) حوالي 0.1 gm من اوكسيد الزنك نانوي .

تمت دراسة حركيات الامتزاز لثلاثة ملوثات بتركيز مختلفه على سطح الهلام المائي

SA-g- (PAAC-co-VBS) / ZnO NPs باستخدام ثلاثة موديلات حركية. تصنيف النماذج الحركية وفقًا لدراسة الامتزاز Psuedo-second order> > Psuedo-first- order Chemisorption.

تمت دراسة إطلاق دواء تتراسيكلين في ظروف مشابهة لجسم الإنسان من حيث درجة الحموضه ودرجة الحرارة. لوحظ تحرر الدواء بنسبة 28٪ و 21.56٪ في أول ساعة من دواء TC. كان التحرر التراكمي لـ TC في 3 ساعات 50,65 ٪ ، 42,33٪ من pH = 7.5 و pH 1.2 بنفس الترتيب.

تم دراسة مناطق التثبيط للمركبات الثلاثة (SA-g-(PAAc-co-VBS)/ZnO NPs ، SA-g- (PAAC-co-VBS)، ZnO NPs) ، حيث تم إعطاء المركب

(SA -g- (PAAC-co-VBS) / ZnONPs) له نشاط مضاد للجراثيم مرتفع ، (30mm) ضد المكورات العنقودية الذهبية ، (25 mm) ضد Streptococcus epigenetics، (13 ، 12) mm ضد الإشريكية القولونية ، و Klebsiella spp. أي أنه كان له تأثير أعلى على

البكتيريا موجبة الجرام مقارنة بالبكتيريا سالبة الجرام ، على التوالي. اما بالنسبه لسطح الهلام المائي (PAAC-co-VBS) -SA-g له نشاط مضاد للجراثيم ضد *Staphylococcus aureus* (mm 15) ، ضد *Streptococcus epigenetics* (20mm) ، وتاير ضعيف ضد E coli و Klebsiella spp.اي كان له تأثير على البكتيريا موجبة الجرام و تأثير منخفض على البكتيريا سالبة الجرام والمركب (ZnO NPs) له نشاط مضاد للبكتيريا منخفض جدًا للبكتيريا موجبة الجرام والبكتيريا سالبة الجرام.

تمت دراسته ، علاج جروح الفئران باستخدام السطح المحضر

SA-g- (PAAc-co-VBS)/ZnO NPs، والذي لوحظ في غضون يومين إلى سبعة أيام ، وفقًا للنتائج ، هناك شفاء كامل للفئران و عودة الجلد إلى لونه الطبيعي. هذا يرجع إلى حقيقة أن

SA-g- (PAAc-co-VBS)/ZnO NPs، تتمتع بكفاءة عالية في علاج الفئران وشفائها. يعتبر صديقًا للبيئة وغير سام ومضاد للالتهابات. بالإضافة إلى ذلك ، هناك توافق حيوي مع خلايا الثدييات.

Chapter One

Introduction

1- Introduction

1-1 General Introduction:

Rapid industrialization and urbanization around the world has lead to the recognition and understanding of relationship between the environmental pollutants and public health . Among the different types of environmental pollution, water pollution is regarded as the most serious problem where effluents from different dye-based industries serve as the major source of contamination. Industries generating dye-containing wastewater include pigment manufacture, textile, printing, dyeing, leather, food and cosmetic industries (Heloise Beatriz Quesada 2021).

Pollution is the most widespread major problem that has caused a defect in the ecosystem, as well as a dangerous problem that threatens human life. Therefore, it is difficult to obtain clean water in the existence the ratio of water pollution that affects the human system is increased(Heloise Beatriz Quesada 2021; Mahdi 2021) .The most hazardous compounds are heavy metals, oils, drug, phenol compound and dyes. Especially, Organic dyes are produced in many different local industries for example textile ,paper, plastic, leather, food, cosmetic, etc.(Gamoudi and Srasra 2019; Martínez-Huitle 2019; Mohib Ullah 2020; Aljeboree 2021).Textile dyes have a strong color even in extremely low concentrations. These Pollutions are non degradable, bioaccumulation in living organisms and stable toward light, biological and chemical treatments. Additionally , they display high biotoxicity and potential mutagenic and carcinogenic effects. The dye pollutions in water incline to preclude light penetration and therefore, affect photosynthesis considerably.(Arif Chowdhury 2020) .Numerous dyes are difficult to remove from contaminated water solutions due to complex structure and synthesis. These Pollutions are not effectively removed by using traditional techniques. Numerous methods can be used to remove these Pollutions with high efficiency such as ion exchange, coagulation /flocculation, adsorption, chemical oxidation, ozone treatment, membrane filtration , sono-chemical and electrochemical methods, photo catalysis economical innovation because of its high effectiveness, naivety of design and simplicity of operation (Chen J.P. 2012).

1-2 Dye

Dyes are basically chemical compounds that can connect themselves to surfaces or fabrics to impart colour. Synthetic dyes are widely used in

many fields of advanced technology, e.g., in various kinds of the textile , paper , leather tanning , food processing, plastics, cosmetics, rubber, printing and dye manufacturing industries . Synthetic dyes are also employed in ground water tracing , for the determination of specific surface area of activated sludge , sewage and wastewater treatment , etc. Their discharges into hydrosphere possess a significant source of pollution due to their recalcitrance nature. This will give undesirable colour to the water body which will reduce sunlight penetration and resist photochemical and biological attacks to aquatic life(Mustafa T. Yagub ;Tushar Kanti Sen 2014) .In the dye molecules there are two important components: chromophores which are responsible for producing the color and auxochromes which enhance the affinity of the dye toward the fibers . Generally, the dyes used in the textile industry are basic dyes, acid dyes, reactive dyes, direct dyes, azo dyes, mordant dyes, vat dyes, disperse dyes and sulfur dyes , where azo derivatives are the major class of dyes that are used in the industry today (Mohamad A Salleh 2020).

1-2-1 Crystal Violet

Crystal violet dye is an industrial dye classified under Dyes Basic or cationic dyes, and its scientific name according to the IUPAC system is Tris(4-(dimethylamino)phenyl)methylium chloride ,and it has a molecular formula of $C_{25}N_3H_{30}Cl$, and molecular weight = 407.98 g/mol, solubility in water 16 g/L at 25 ^{0}C, and the degree of Its melting point is 205 ^{o}C, and it registers a wavelength of 590 nm when it absorbs visible rays. it belongs to the Triphenylmethane group, and its aqueous solution gives a violet color, and it has wide uses in the textile industries represented in dyeing cotton, silk, wool and nylon, and in the

manufacture of printing inks, As well as coloring various products, such as detergents and fertilizers, it is also used by coloring bacterial cells in order to identify and diagnose them (Sakin 2019), as shown in Figure (1-1).

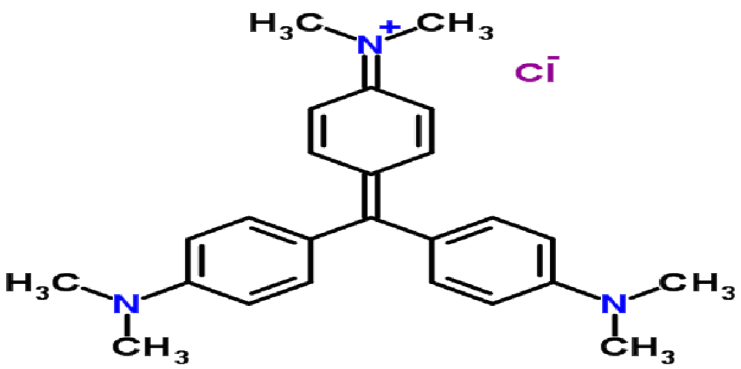

Figure (1-1): Chemical structure Crystal violet (CV) dye (Sadeghi 2019).

1-3 Pharmaceuticals compound

Pharmaceuticals are chemicals used to diagnose, treat, change and prevent diseases. The definition is extended to veterinary compounds and can also be applied to illicit drugs . A wide variety of human medicines including antibiotics, synthetic hormones, antiinflammatories, statins, and cytotoxins are produced and consumed, some of them in thousands of tons per year . Pharmaceuticals differ from other chemical contaminants due to the following characteristics (Wieczerzak 2019.): (a) They may be formed by innumerable complex molecules which vary in molecular weight, structure, functionality, and form; (b) They have the capacity to go by cellular membranes and consequently are relatively persistent, once

they are not inactivated before reaching the expected therapeutic effect; (c) They are polar molecules with more than one ionizable group and their degree of ionization, among other characteristics, depends on the pH of the medium; (d) They are lipophilic and some moderately soluble in water; (e) Drugs such as erythromycin, naproxen, and sulfamethoxazole may persist in the environment for more than one year; others, such as clofibric acid can persist for several years and become biologically active due to accumulation; (f) After administration, the molecules are absorbed in the human body, distributed and subjected to metabolic reactions that can modify their chemical structure (Quesada, Baptista et al. 2019).

1-3-1 Tetracycline

Tetracycline (TC) has been widely used in human therapy and animal husbandry , with the global annual production of more than 20,000 tons . As such, it has been one of the most frequently detected antibiotics in the wastewater treatment plants(Yazidi A Atrous 2020). used to treat a number of infections, including acne, cholera, brucellosis, plague, malaria, and syphilis. Common side effects include vomiting, diarrhea, rash, and loss of appetite. Formula: $C_{22}H_{24}N_2O_8$, Molecular weight 444.4 gm/mol and IUPAC (4S,6S,12aS)-4-(dimethylamino)-1,4,4a,5,5a,6,11,12a-octahydro-3,6,10,12,12apentahydroxy-6-methyl-1,11-dioxonaphthacene-2-carboxamide(Liu 2020) . as shown in Figure (1-2).

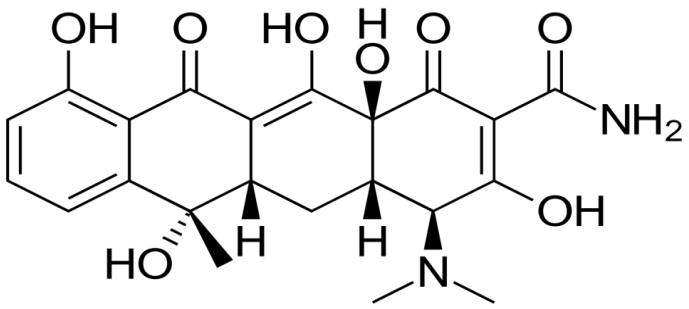

Figure (1-2): Chemical structure Tetracycline (TC) (Liu 2020) .

1-4 Phenols compound

Phenols compound are natural components of many substances like wine, smoked foods and tea. Phenols are present in animal wastes and decomposing organic material. Phenols can be generated from the industrial sources of contaminants such as oil refineries, coal gasification sites and petrochemical units. Phenols also released from the combustion of tobacco and fossil fuels. Furthermore, phenols are introduced into surface water from industrial effluents such as those from the coal tar, gasoline, plastic, rubber proofing, disinfectant, pharmaceutical and steel industries and domestic wastewaters, agricultural run-off and chemical spills. In the refinery and lubricant production, phenols used as anextracting solvent (Yang 2019). Due to their germicidal and local anestheticproperties, phenols used at preparation of shaving soaps and creams. Phenols also used as a reagent in chemical analysis and as a primary petrochemical intermediate. Phenols are biodegradable and at high concentrations can be toxic and mutagenic. Phenol is rapidly absorbed through the skin and can cause skin and eye burns upon contact. Therefore, it is important to remove these compounds from the effluents before it disposed into the wastewaters (Jun 2019).

1-4-1 Phenol

Phenol (also called carbolic acid , Phenylic acid Hydroxybenzene , Phenic acid) is an aromatic organic compound with the

molecular formula C_6H_5OH. It is a white crystalline solid that is volatile. The molecule consists of a phenyl group ($-C_6H_5$) bonded to a hydroxy group (−OH). Mildly acidic. Molecular weight 49.113 g/mol, (λmax) =270 nm, IUPAC name Benzonol . Phenol and its chemical derivatives are essential for production of polycarbonates, epoxies, Bakelite, nylon, detergents, herbicides such as phenoxy herbicides, and numerous pharmaceutical drugs (Dalia Khalid Mahmoud 2012; Mariana Alves Leite Dutra 2021) as shown in Figure (1-3).

.

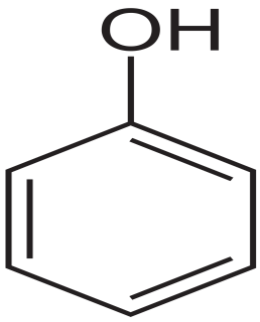

Figure (1-3): Chemical structure Phenol(Dalia Khalid Mahmoud 2012) .

1-5 Hydrogels

Hydrogels are hydrophilic polymer chains that are crosslinked to form gel structures that swell in aqueous solution and trap fluids for a long period without dissolving. Hydrogels may contain carboxylic, amine, imide, hydroxyl and sulfonyl groups in their 3D structure that are responsible for the hydrophilicity and swelling capacity(Ahmed EM

2019; Liang Y, Zhao X et al. 2019). The hydrogel must have the following properties, High absorption capacity; low residue monomer and soluble content; cost-effective .reusable .;high biodegradability and not produce harmful byproducts ;must retain neutral pH after swelling in water and easy recoverability(Li J, Ma J et al. 2019; Makhado E and Hato M 2021).

Depending on the nature of the hydrogel, it can be classified based on various properties. Classification of hydrogels (Figure 1-4) can be based on whether they are synthetic (involves the use of synthetic monomers), natural (involves using biopolymers) or a combination of synthetic and natural monomers resulting in a hybrid hydrogel. The polymeric composite classification can be based on the method used to synthesize the hydroge(Thakur S, Pandey S et al. 2019; Nompumelelo Malatji 2021):

a. Homopolymeric hydrogels: they are hydrogels consisting of the same type of monomer.

b. Copolymeric hydrogels: these hydrogels comprise two or more different kinds of monomers such that the network would have at least one hydrophilic component on the polymer network chain.

c. Multipolymer interpenetrating polymeric hydrogel (IPN): the hydrogel network consists of two components (natural and/or a synthetic polymer) that are independently cross-linked.

It was also demonstrated that hydrogels can be categorized based on whether they are(Wang 2020).

a. crystalline, b. amorphous or c. semi-crystalline: showing properties of both crystalline and amorphous phases.

The other classification is based on whether the crossinking of hydrogels .occurs via chemical or physical means(Xu J, Liu X et al. 2019) :

a. physical crosslinking in hydrogels may be through

1-formation of a hydrogen bond

2-hydrophobic interactions between chains.

3- crystallization.

b. Chemical crosslinking can be achieved by

1- using aldehydes such as acetaldehyde, glutaraldehyde (GA) and formaldehyde

2- formation free radical

3- free-radical polymerization .

In addition, the hydrogels may be classified based on the charge on their cross-linked polymer network. The charge may be a. ionic (cationic/anionic), b. non-ionic (neutral), c. amphoteric (comprising both basic and acidic groups) and d. zwitterionic (contains anionic and cationic components on each repeating structural unit). The net charge of the gel is zero (Garg S and Garg A 2016).

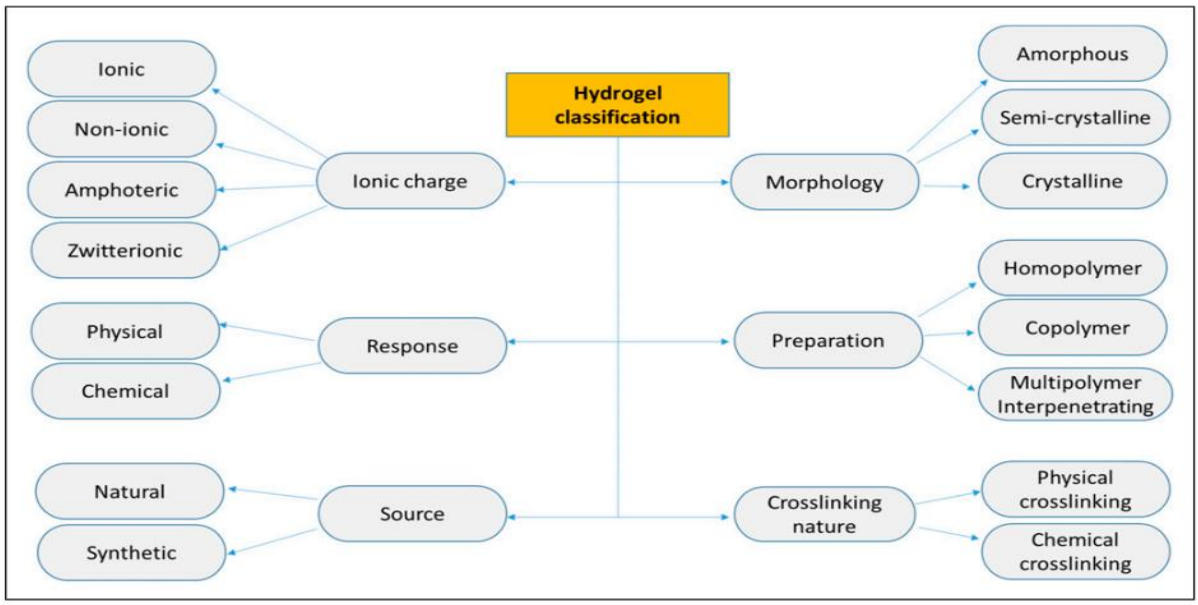

Figure (1- 4). Classification of hydrogels (Liang Y, Zhao X et al. 2019).

1-6 Zinc oxide–based hydrogels

Zinc oxide (ZnO) can be found in nature as a zincite mineral; however the majority of it is prepared synthetically. Its crystal structure can be found in a hexagonal wurtzite form or cubic zinc blende .The form that is most stable and commonly found at ambient temperature is the wurtzite structure. ZnO is commonly used for treating skin-related problems such as nappy rash, dandruff and incorporation in ointments used in wound dressing (Stefaniuk I, Cieniek B et al. 2019; Zhang M, Chang L et al. 2019).where adsorbent hydrogel incorporated with ZnO nanoparticles was used for removing pollutant from water. The group reported that incorporating ZnO nanoparticles improved the recovery of the adsorbent from the aqueous solution after the removal of pollutant . also , hydrogel was modified with ZnO for antimicrobial activity, Therefore, looking at these properties, the ZnO would be ideal for preparing hydrogels for adsorbing pollutant (Khan TA, Nazir M et al. 2018; Vahidhabanu S, Karuppasamy D et al. 2018).

1-7 Adsorption

The term adsorption refers to the accumulation of a substance at the interface between two phases (liquid–solid interface or gas–solid interface). The substance that accumulates at the interface is called adsorbate and the solid on which adsorption occurs is adsorbent . Adsorption can be classified into two types: chemical sorption and physical sorption (Salleh 2021). Chemical adsorption of chemisorption is illustrated by the formation of strong chemical associations between molecules or ions of adsorbate to the adsorbent surface, which is generally due to the exchange of electrons and thus chemical sorption generally is irreversible. Physical adsorption or physisorption is characterised by weak van der Waals intraparticle bonds between adsorbate and adsorbent and thus reversible in most cases (Yazidi A Atrous 2020) .

1-7-1 Factor Influencing Adsorption Process

1-7-1-1 Effect of amount of adsorbent

Adsorbent dosage is an important process parameter to determine the capacity of an adsorbent for a given amount of the adsorbent at the operating conditions. Generally the percentage removal increases with increasing adsorbent dosage, where the quantity of sorption sites at the surface of adsorbent will increase by increasing the amount of the adsorbent. The effect of adsorbent dosage gives an idea for the ability of a dye adsorption to be adsorbed with the smallest amount of adsorbent, so as to recognise the capability of a dye from an economical point of view (Hazem Hassan 2019).

1-7-1-2 Effect of initial concentration

The effect of initial concentration can be carried out by prepare adsorbent–adsorbate solution with fixed adsorbent dose and different initial concentration for different time intervals and shaken until equilibrium. The percentage removal of pollutant is highly dependent on the initial amount of dye concentration. The effect of the initial concentration factor depends on the immediate relation between the concentration of the pollutant and the available binding sites on an adsorbent surface (Hameed 2019).

1-7-1-3 Effect of solution pH

One of the most important factors affecting the capacity of adsorbent in wastewater treatment is solution pH . The efficiency of adsorption is dependent on the solution pH, since variation in pH leads to the variation in the degree of ionization of the adsorptive molecule and the surface properties of adsorbent(Yazidi A Atrous 2020) .

1-7-1-4 Effect of temperature

Effect of temperature is another significant physico-chemical process parameter because temperature will change the adsorption capacity of the adsorbent . If the amount of adsorption increases with increasing temperature then the adsorption is an endothermic process. This may be due to increasing mobility of the dye molecules and an increase in the number of active sites for the adsorption with increasing temperature. Whereas the decrease of adsorption capacity with increasing temperature indicates that the adsorption is an exothermic process. This may be due to increasing temperature decreasing the adsorptive forces between the pollutant species and the active sites on the adsorbent surface as a result of decreasing the amount of adsorption(Mahdi 2021) .

1-7-1-5 Ionic Strength

It is an important factor that control both electrostatic and non-electrostatic interactions between the adsorbate and the adsorbent surface. The solubility of ionic salts is effected in adsorption process, because when the ionic salts having solubility are better than the adsorbent substances caused increased in adsorption, or decrease because the ionic salts caused interference on the surface adsorption (Nadher 2019).

1-8 Adsorption Isotherm

The adsorption isotherm is significant for the explanation of how the adsorbent will interact with the adsorbate and give an idea of adsorption capacity. They play an important role in understanding the mechanism of adsorption. The surface phase may be considered as a monolayer or multilayer. Several isotherm models are presented in the literature . Langmuir and Freundlich models are the most widely used to describe the adsorption isotherm (A. H. Al-muhtaseb and T.Magee 2021).

1-8-1 Langmuir adsorption isotherm model

The Langmuir adsorption isotherm model assumed that adsorption takes place at specific homogeneous sites within the adsorbent, and it has been used successfully for many adsorption processes of monolayer adsorption. The Langmuir equation is expressed by the following relation(Langmuir 1918):

$$q_e = \frac{q_m K_a C_e}{1 + K_a C_e} \qquad (1\text{-}1)$$

Where C_e the residual concentration, q_e ,q_m is the adsorption capacity at equilibrium and the maximum adsorption capacity respectively, K_a Langmuir constant. The linear form of the equation of Langmuir isotherm is according to the following equation(Del Mar Orta 2019):

Where C_e the residual concentration, q_m, q_e is the adsorption capacity at equilibrium and the maximum adsorption capacity respectively, K_a Langmuir constant. The linear form of the equation of Langmuir isotherm is according to the following equation (Del Mar Orta 2019):

$$\frac{C_e}{q_e} = \frac{C_e}{q_m} + \frac{1}{K_a q_m} \qquad (1\text{-}2)$$

1-8-2 Freundlich adsorption isotherm model

The Freundlich adsorption isotherm model considers a heterogeneous adsorption surface that has unequal available sites with different energies of adsorption. The Freundlich adsorption isotherm model is represented as follows(Freundlich 1906) :

$$q_e = K_f C_e^{\frac{1}{n}} \qquad (1\text{-}3)$$

K_f, is a freundlich constant and their values depend on the nature of the absorbent material, the surface and the temperature. The linear form of freundlich isotherm can be expressed as follows:

$$\log q_e = \log k_f + \frac{1}{n} \log C_e \qquad (1\text{-}4)$$

1-9 Drug Release

The entrapped drug in hydrogels releases only when the water penetrates into the polymer networks and dissolves the drug. A drug solubilization is followed by diffusion through a network of fluid-filled pores and channels. In such cases, the control over the internal pore size, distribution, and connectivity would be useful for fine tuning formulation conditions and drug release kinetics (Liu L, Gao Q et al. 2019).

The release kinetics often deviates from the expected one and is strongly influenced by a variety of parameters. These parameters include device geometry, the physicochemical properties of the polymer matrix (molecular weight, swelling, crystallinity, and temperature), initial drug concentration profile, drug– matrix interactions, and osmotic pressure associated with drug solubility and its loading content . The release of drug is closely related to the swelling characteristics of the hydrogels, which in turn, is a, key function of chemical architecture of the hydrogels (Kumar T, Thakur A et al. 2018) as shown in Figure (1-5).

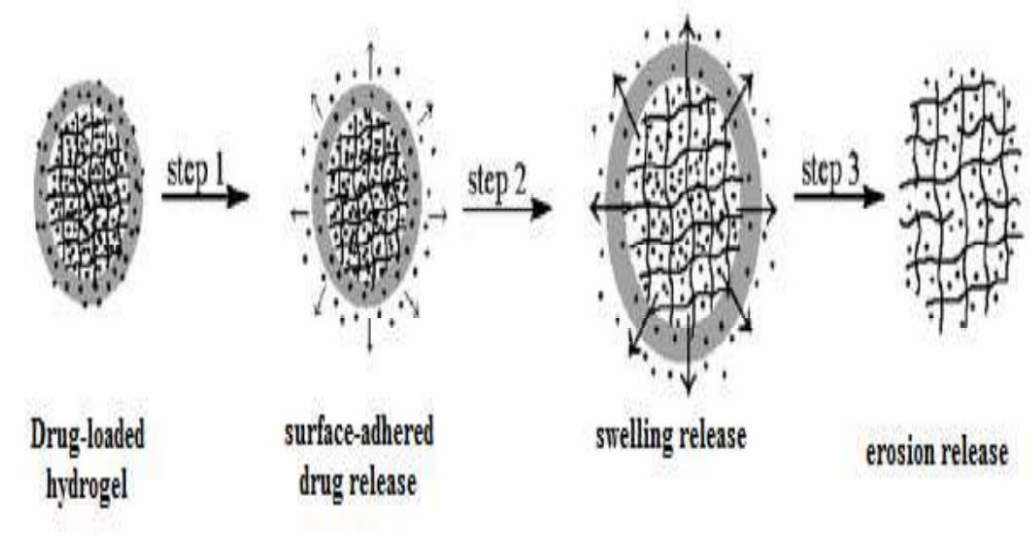

Figure(1-5): Drug release process for hydrogels (Kumar T, Thakur A et al. 2018).

1-10 Microorganisms

Microorganisms, the category of microbes includes a large group of living organisms including bacteria, fungi and algae. In this study, wear used two types of bacteria, like bacteria Gram-positive and bacteria Gram-negative .

1-**10-1** ***Escherichia coli***

Escherichia coli is a Gram-negative, facultative anaerobic, rod-shaped, coli form bacterium of the genus Escherichia that is commonly found in the environment, foods, and intestines of people and animals . Most E. coli strains are harmless, but some serotypes (EPEC, ETEC etc.) can cause serious food poisoning in their hosts, and are occasionally responsible for food contamination. Although most strains of E. coli are harmless, others can make you sick. Some kinds of E. coli can cause diarrhea, while others cause urinary tract infections, respiratory illness and pneumonia, and other illnesses (Jolanta Sarowsk 2019).

1-10-2- ***Klebsiella pneumonia***

Klebsiella pneumonia is a Gram-negative, non-motile, encapsulated, lactose-fermenting, facultatively anaerobic, rod-shaped bacterium. It appears as a mucoid lactose fermenter on MacConkey agar. Klebsiella species are found everywhere in nature. This is thought to be due to distinct sublineages developing specific niche adaptations, with associated biochemical adaptations which make them better suited to a particular environment. They can be found in water, soil, plants, insects and other animals including humans. The species of Klebsiella are all gram-negative and usually non-motile. They tend to be shorter and thicker when compared to others in the family Enterobacteriaceae. The

cells are rods in shape and generally measures 0.3 to 1.5 µm wide by 0.5 to 5.0 µm long. They can be found singly, in pairs, in chains or linked end to end. Klebsiella can grow on ordinary lab medium and do not have special growth requirements, like the other members of Enterobacteriaceae. The species are aerobic but facultatively anaerobic. Their ideal growth temperature is 35° to 37 °C, while their ideal pH level is about 7.2 (Clement Yaw Efah 2020).

1-10-3 *Staphylococcus aureus*

Staphylococcus aureus is a Gram-positive round-shaped bacterium, a member of the Firmicutes, and is a usual member of the microbiota of the body, frequently found in the upper respiratory tract and on the skin. It is often positive for catalase and nitrate reduction and is a facultative anaerobe that can grow without the need for oxygen. Although S. aureus usually acts as a commensal of the human microbiota it can also become an opportunistic pathogen, being a common cause of skin infections including abscesses, respiratory infections such as sinusitis, and food poisoning. Pathogenic strains often promote infections by producing virulence factors such as potent protein toxins, and the expression of a cell-surface protein that binds and inactivates antibodies(Katz AR 2019; V 2020).

1-10-4 *Streptococcus pyogenes*

Streptococcus pyogenes, (colloquially named “group A *streptococcus*” (GAS)), is a Gram positive bacterial pathogen that can cause both non-invasive and invasive disease (iGAS), as well as nonsuppurative sequelae. This includes pharyngitis, scarlet fever, impetigo,cellulitis, type II necrotizing fasciitis, streptococcal toxic shock

syndrome, acute rheumatic fever and post-streptococcal glomerulonephritis (Aziz RK 2018).

Group A streptococcus (GAS) is synonymous with Streptococcus pyogenes, the only species within this group of β-hemolytic streptococci. GAS is one of the leading pathogenic bacteria that infects children and adolescents, and is associated with a wide spectrum of infections and disease states. Worldwide, there are estimated to be >600 million cases of GAS pharyngitis (“strep throat”) and>100 million cases of GAS pyoderma annually(Kwinn LA 2019; Nelly Janira Avire 2021) .

1-11 Literature survey of application for removal of pollutants by using different surfaces:

The table below represents a comparison between the current work and previous research on the high ability of hydrogel to remove different types of pollutant . This was reported in Table(1-1):

Table (1-1): Removal of pollutant using different surfaces.

No.	Sorbent	Pollutant	T (°C)	pH	t (hr.)	Dose ($mg.L^{-1}$)	Q_e (mg/g)	E%	Co ($mg.L^{-1}$)	Ref.
1	SA-g-P(AAc-co-MA)/TiO_2	Brilliant green	25	6	1	0.05	1200	99.9	700	(Aljeboree 2022)
1	Chitosan-based hydrogel	Tetracycline	25	8	2	0.3	541.3	93	40	(Qiuyan Luo 2022)
2	(UCN-GO)hydrogel	Tetracycline	25	5	1	0.2	20.3	88.8	20	(Yiping Feng 2022)
3	(PAAm/Starch)hydrogel	phenol	25	6	2	0.12	20.12	90	100	(Mariana Alves Leite Dutra 2021)
4	(GO/PAA/PAM)-	Crystal violet	30	7	1	0.4	328	90.12	30	(Abd-Elhamid 2021)
5	Poly(AA-co-AMPSA)	crystal violet	25	7	1	0.5	370	80	100	(Hemant Mittal 2021)
6	Sodium alginate poly(acrylic acid)/zinc oxide	Methylene blue (MB)	25	6	1	0.1	1129	90.2	100	(Mohammad T. ALSamman 2021)
7	Rice bran/alginate hydrogel beads	Crystal violet	30	5	6	0.3	270	90.12	50	(Gui-Bing Hong 2021)
8	(PAAc/Lap) hydrogel	Methylene blue	25	6	3	0.5	3800	90	100	(Bo Gao 2021)
9	N-isopropyl acrylamide (NIPAM)	phenol	25	7	1	0.15	77.7	88.8	20	(Gaofeng Pan 2021)
10	Acrylamide bonded sodium alginate (AM-SA) hydrogel	crystal violet	30	8	3	0.1	62.07	92	10	(Sevda Pashaei-Fakhri)

No.	Sorbent	Pollutant	T (°C)	pH	t (hr.)	Dose ($mg.L^{-1}$)	Q_e (mg/g)	E%	Co ($mg.L^{-1}$)	Ref.
11	Acrylamide/graphene oxide bonded sodium alginate (AM-GO-SA)	Crystal violet	30	8	3	0.1	100.30	98.9	10	(Sevda Pashaei-Fakhri)
12	Polyacrylamide/ starch hybrid hydrogels	Phenol	25	2	6	0.1	20	60	50	(Mariana Alves Leite Dutra 2020)
13	(Y-GO-SA) hydrogel	Tetracycline	20	7	2	0.4	477.9	82.1	50	(Jinsong He 2020)
14	(SA-g-(PAA-co-PDMC)	Crystal violet	25	2	1	0.05	654	98.3	100	(Zhao Ying 2019)
15	Alginate/acid activated bentonite beads (A-AAB)	crystal violet	25	8	3	0.2	582.4	92.39	100	(Akeem Adeyemi Oladipo 2019)
16	Alginate/bentonite beads (AB),	Crystal violet	25	8	3	0.2	498.2	84.59	100	(Akeem Adeyemi Oladipo 2019)
17	SA-g-PAA	Methyl violet	25	6	1	0.3	655	86.55	100	(Thakur 2017)
18	SA-g-PAA/TiO2	Methyl violet	25	6	1	0.3	1156	98.2	100	(Thakur 2017)
19	poly(2-acrylamido-1-propane sulfonic acid-co-itaconic acid) hydrogels	Crystal violet	28	1	5.6	0.1	58.6	80.3	100	(Venkatesan Srinivasan 2014)
20	Hydrogel-palm kernel shell	phenol	25	2	6.8	0.1	19.6	-	50	Lamin Sanyang) (2013
21	(2-hydroxyethyl methacrylate/acrylamid opyridine) hydrogel	phenol	25	2	7.5	0.1	26.45	-	100	(Hany El-Hamshary 2007)

1-11 Objectives:

This work aims to investigate the following:

1- To synthesize new adsorbent surface by the free-radical-induced graft co-polymerization of acrylic acid in the presence of alginate bio-polymer and ZnO NPs for the uptake of Three pollutants (Crystal violet (CV) dye, Tetracycline (TC) drug ,and phenol PH) .

2- To characterize the adsorbent surface by using different techniques X-ray diffraction(XRD), Field Emission Scanning Electron Microscopes (FE-SEM), Energy Dispersive X-Ray (EDX) Thermo-gravimetric analysis (TGA) ,Fourier–transform-infrared-spectroscopy(FTIR), and Transmission Electron Microscopy (TEM).

3- To study optimum conditions to estimate Three pollutant .

4- Investigate the effectiveness of the (SA-g-(PAAc-co-VBS)/ZnO NPs).to adsorb selected three pollutants (CV,TC, and PH) through batch treatment processes.

5- Investigate the effects of contact time, adsorbent dosage, pH, temperature, during batch treatment methods.

6- Determine the applicability of Freundlich, and Langmuir approach to estimate design parameters characterizing the performance of the adsorption batch tests, and determine the adsorption constants of three pollutants onto hydrogel surfaces.

7- Estimate the thermodynamic parameters for three pollutants on the hydrogel surfaces.

8-Study the effect of adsorbent Regeneration , and In vitro drug release on the adsorption capacity.

9- Study the Removal of Real Aqueous Pollutants by Using ((SA-g-(PAAc-co-VBS)/ZnO NPs) by using several pollutants.

10- The biological effect of the surface prepared from ((SA-g-(PAAc-co-VBS)/ZnO NPs) on a class of Gram-positive bacteria and Gram-negative bacteria . And it was clear from this study that the surface ((SA-g-(PAAc-co-VBS)/ZnO NPs) has high effectiveness in inhibiting negative and positive bacteria effectively.

Chapter Two

Experimental part

Experimental Part

2-1 Instruments :

There are several techniques used in this current study, most of them are listed in Table (2-1).

Table (2-1): Devices used in the study and its manufacturers.

No.	Instrument	Model	Company supplied
1	[1] UV-Visible spectrophotometer, Double beam	PC 1650	Shimadzu, Japan
2	[1] UV-Visible spectrophotometer, Single beam	UV mini-1240	Shimadzu, Japan
3	[1] FTIR spectrophotometer	8400S	Shimadzu, Japan
4	[2] Field-Emission Scanning electron microscope (FE-SEM)	MIRA3	TESCAN ,Czechia Republic
5	[2] Transmission electron microscope (TEM)	912AB	Leo, Germany
6	[2] X-Ray diffraction (XRD)	D2 Phaser	Bruker AXS Gmbh, Germany
7	[2] Energy Dispersion X-ray (EDX)	MIRA3	TESCAN ,Czechia Republic
8	[1] Thermogravimetric analysis (TGA)	DTG-60	Shimadzu, Japan
9	[1] Shaker water bath	CL002	K&K Scientific, Korea
10	[1] Centrifuge	CL008	JANETZI - T5, Belgium
11	[1] Ultra-sonication	405 power sonic	Hwashin, Korea
12	[1] Oven	LDO-060e	Labtech, Korea

13	[1] pH meter	HI 83141	Hanna, Romania
14	[1] Autoclave and Stainless steel device	Binder	Germany
15	[1] Hot plate stirrer	LMS-1003	Labtech, Korea
16	Muffle furnace	42127	Aurora, IL USA

1-University of Babylon / College of science for women-Chemistry Department.
2 University of Tehran

2-2 Chemicals

Chemicals used in this study are shown in Table (2-2), some of them commercial and the other supplied from companies interesting in synthesis of chemicals compounds

Table(2-2):Materials used in the study, purity and their manufacturers

No	Material	Molecular Formula	Molar mass (g/mol)	Purity (%)	Supplier
1	Crystal violet	$C_{25}N_3H_{30}Cl$	407.98	99.0	Sigma-Aldrich
2	Tetracycline	$C_{22}H_{24}N_2O_8$	444.4	98.0	SDI-Iraq
3	Phenol	C_6H_6OH	49.113	98.0	Sigma-Aldrich
4	Sodium hydroxide	NaOH	40.00	98.0	Sigma-Aldrich
5	Phosphoric acid	H_3PO_4	97.9	98.0	Sigma-Aldrich
6	Sodium alginate	$C_6H_9NaO_7$	216.12	99.0	Sigma-Aldrich
7	Ethanol	C_2H_5OH	46.07	99.0	(B.D.H)
8	Methanol	CH_3OH	32.04	99.9	Sigma-Aldrich
9	Acrylic acid	$C_3H_4O_2$	72.063	98.0	Sigma–Aldrich
10	N´N-dimethylacrylamide	C_5H_9NO	99.13	> 99.5	Sigma –Aldrich
11	Sodium4-vinylbenzenesulfonate	$C_8H_7NaO_3S$	206.09	98.0	Sigma-Aldrich
12	Potassium persulfate	$K_2S_2O_8$	270.3	99.5	Sigma-Aldrich
13	Zinc Acetate dihydrate	$Zn(CH3COO)_2$.$2H_2O$	219.50	99.0	Sigma-Aldrich
14	Oxalic Acid	$C_2H_2O_4$	94.02	99.0	Sigma-Aldrich
15	Sulfuric acid*	H_2SO_4	36.07	98.0*	Sigma-Aldrich
16	Hydrochloric acid*	HCl	37.46	37.0* (w/w)	Sigma-Aldrich

2-3 Preparation of ZnO Nanocomposite :

Zinc oxide Nanocomposite was prepared by using a hydrothermal process. 10 g of zinc acetate, 5 g of oxalic acid, were mixed, then complete to 100mL with distilled water then mixed for half-hour to get a required solution. The resultant mixtures were kept at 160oC for 24 hr in an autoclave. The obtained color white precipitate was filtered, washed with distilled water then sonicated in10 minutes then dried at 80^{o}C for 24

hr. to get a fine powder as appear in Scheme (2-1) (Aseel M. Aljeboree 2021).

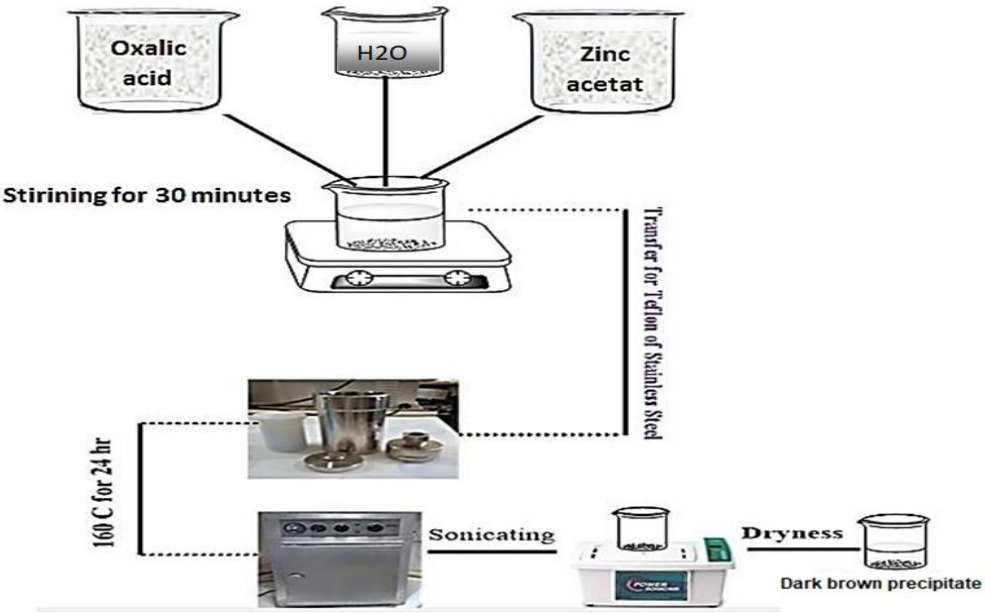

Scheme (2-1): Preparation of ZnO nanocomposite**.**

2-4 Preparation of superabsorbent polymer

Superabsorbent polymer was prepared by the free radical graft copolymerization method. Sodium alginate (SA) 1gm was dissolved in a 20 mL distilled water. In a reaction flask, quantity of ZnO NPs (0.1g) was taken in 20 ml of distilled water and shook for 5 hours followed by ultra-sonic for 2 hours. Then, it was gradually added to the solution sodium alginate , followed by stirring at 25 oC for 2 hrs until the formation of a

homo-geneous and gel well dispersed. At that point, the addition of Sodium4-vinylbenzenesulfonate VBS (0.5 g) followed by Acrylic acid AAC (3 ml) and consistent blending at 25 °C was conducted. and then 0.03 g of potassium per sulfate (KPS) in 1ml D.W was added with 5 min continuous mixing. After that, N,N-methylene-bis acrylamide (MBA) , (0.05 g) was added to the mixture with the purge of N2. finally set in a water bath at 70 °C to complete the co-polymerization reaction and obtain the (SA-g-(PAAc-co-VBS)/ZnO NPs)hydrogel nano-composite. The obtain hydrogel was cut into little pieces and washed by distilled water at several time and ethanol to get rid of unreacted chemicals, dried in an oven at 60 °C, and then stored in a desiccators as appear in Figure (2-2).

Based on these results, the formation mechanism of SA-g-(PAAc-co-VBS)/ZnO NPs is proposed as shown in Scheme (2-3a) . Free radicals are generated from the decomposition of initiator and transferred onto SA to initiate the polymerization of AAC and VBS. Both monomers are then grafted onto the SA backbone. Polymer chains are then cross-linked to form a three-dimensional (3D) network as the cross-linker added. Also, Scheme (2-3b) shows the proposed adsorption process of CV.

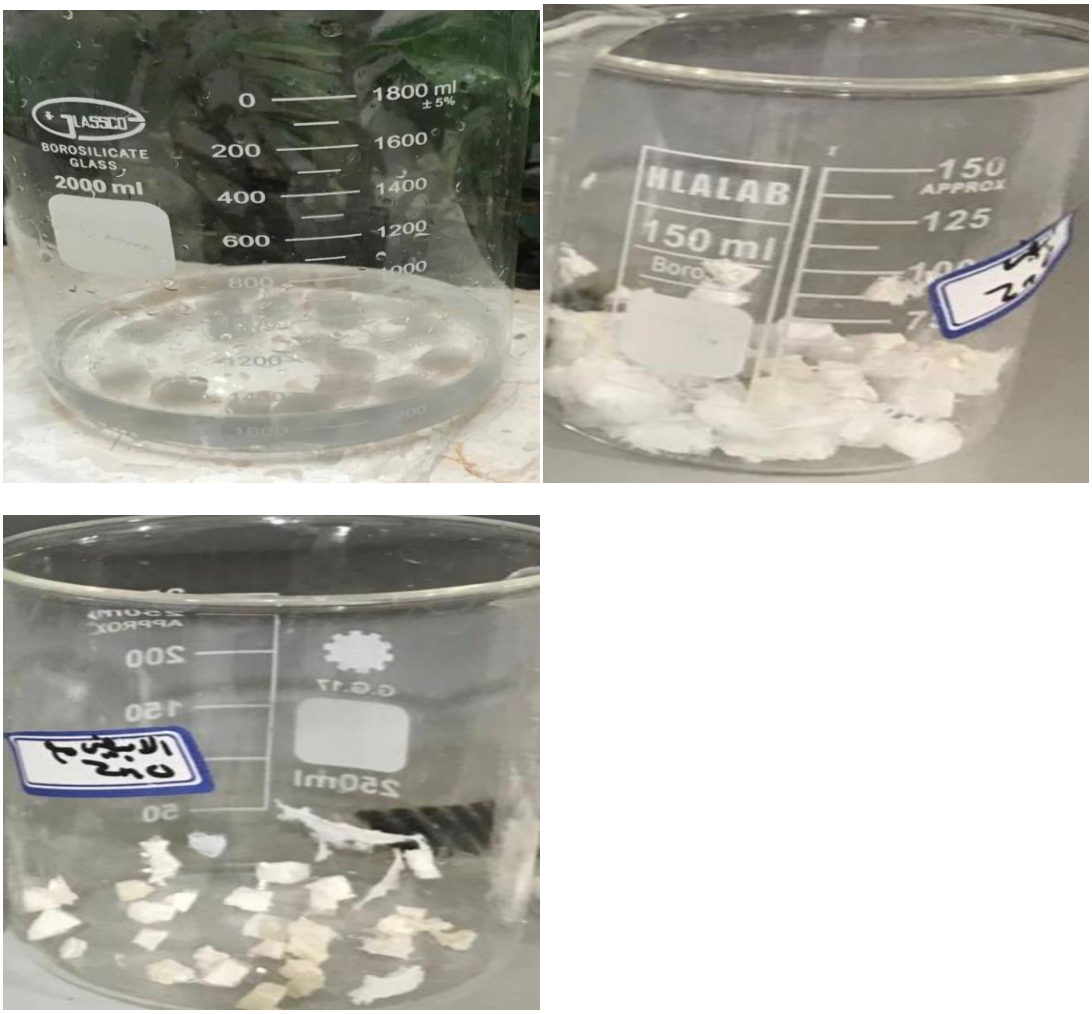

Figure (2-2) : **Preparation of superabsorbent** (SA-g-(PAAc-co-VBS)/ZnO) NPs hydrogel nano-composite.

a)

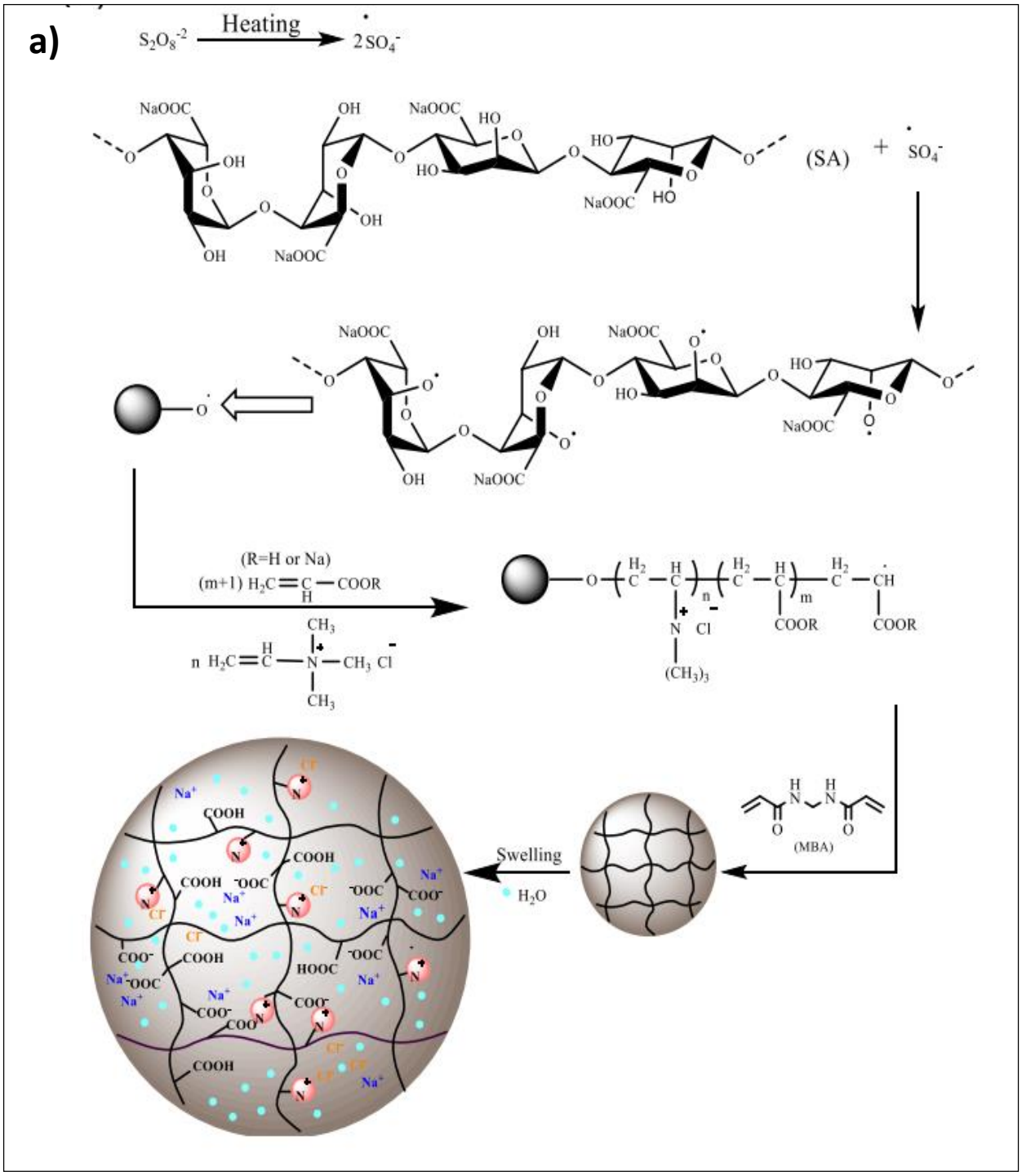

b)

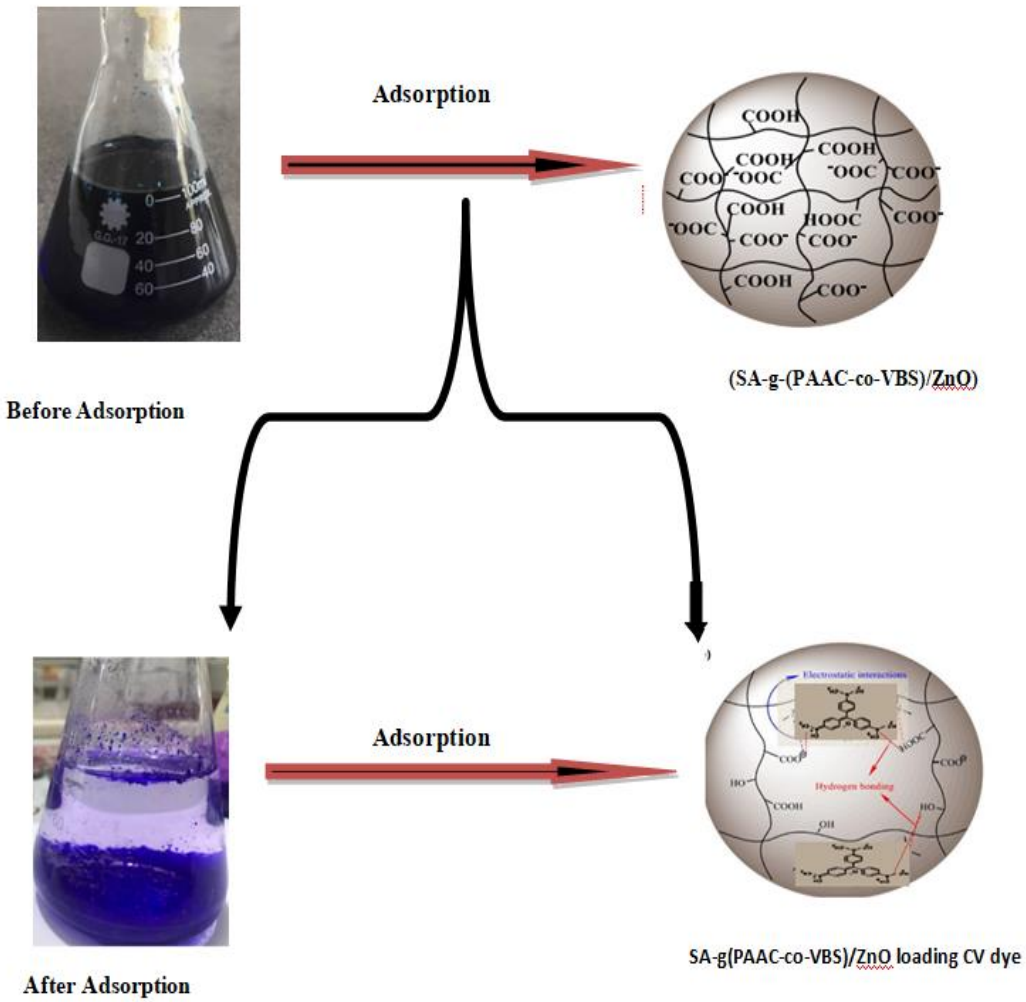

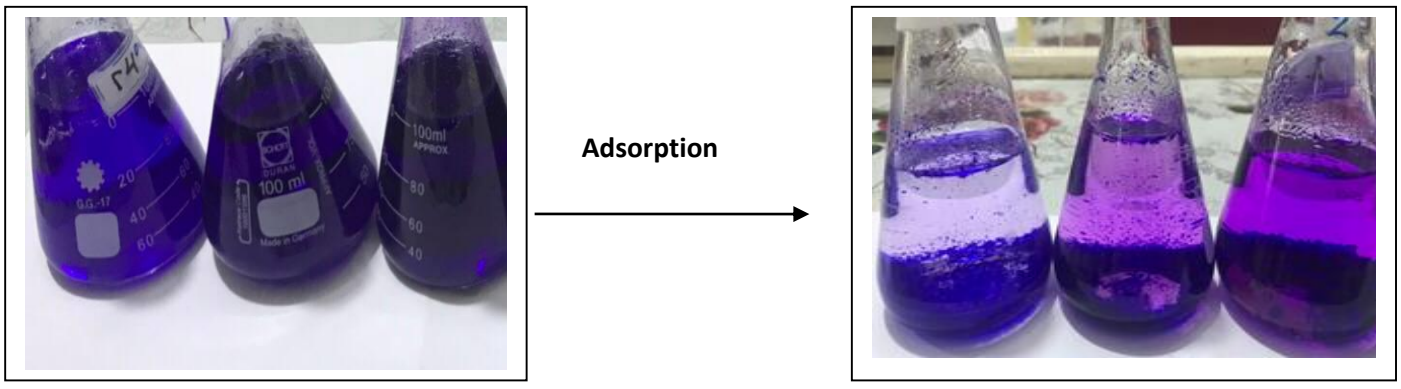

Scheme(2-3): Proposed reaction and swelling mechanism of SA-g-(PAAc-co-VBS)/ZnO NPs and schematic diagram for CV adsorption mechanism. (a) Reaction and swelling mechanism; (b) schematic diagram for CV adsorption process.

2-5 Characterization of the Prepared Nanocomposites

The samples were examined using the transmission electron microscopy (TEM) and Field emission scanning electron microscopy (FE-SEM) , X-ray diffraction spectroscopy (XRD) at Ferdowsi University, Mashhad, Iran.

2-5-1 Ultraviolet-Visible Spectroscopy (UV–Vis) :

An important technique used to measure absorption and transmission for dye solution. Where 0.1 $mg.mL^{-1}$ of the composite are placed in the dye solution and then filled the quartz cells for measurements(A. H. Al-muhtaseb and T.Magee 2021) .

2-5-2 Fourier Transform Infrared (FT-IR) Analysis :

The vibrational motions of the chemically bound constituents of matter have frequencies in the infrared region. The oscillations induced by certain vibrational modes provide a means for the matter to couple with an impinge beam of infrared electromagnetic radiation and exchange energy with it when the frequencies are in resonance. Consequently, the molecular vibration will be excited by infrared frequency causing the energy of molecular vibration to increase. In the meantime, the electromagnetic radiation with a specific frequency will be absorbed by the molecule because the photon energy is transferred to excite molecular vibrations. FTIR spectra were recorded using the FTIR instrument (Shimadzu. 8400S) in the 4000-400 cm^{-1} frequency range. Dried C/ZnO (1 mg) was mixed with KBr powder (10 mg) in an agate mortar. The mixture was pressed into a pellet under 10 tons load for 2–4 min, and the spectrum was recorded immediately (Yazidi A Atrous 2020).

2-5-3 Thermogravimetric analysis (TGA) :

The thermodynamic analysis is performed to determine the thermal stability of prepared nanomaterials and to determine the purity of these particles. The sample was heated from 10 °C to 600 °C and at a heating speed of 10 °C/min (Aseel M. Aljeboree 2021).

2-5-4-Field Emission Scanning Electron Microscopy (FE-SEM)

FE-SEM is a powerful device that is used in characterizing sample morphology such as grain size, particle size, particle distribution, crystal defects and surface structure. FE-SEM has several features like large depth of field, higher resolution and more control in the degree of amplification. Aboutb50µL of aqueous or ethanol suspension of sample was placed on a clean silicon wafer surface. Then dried at 80ºC to remove the solvent(Nompumelelo Malatji 2021) .

2-5-5 Transmission Electron Microscopy (TEM)

TEM is a microscopy technique used a beam of electrons transmitted across an ultra-thin sample where the electrons are transformed into light and form an image. TEM provides information on phase composition, structure and lattice defects. The mechanism for examining the sample by adding drops from the sample as aqueous solution on the carbon covered TEM networks. Then remove the solvent by simple drying (A. H. Al-muhtaseb and T.Magee 2021).

2-5-6 X-ray Diffraction Spectroscopy (XRD)

X-ray diffraction is a powerful nondestructive technique for characterizing crystalline materials. The crystalline properties of materials prepared using an X-ray deflection technique were studied using a single-wavelength light (1.5104nm) from the CuKα source with the use of nickel as a filter. Where the range taken from deviation angles (2Ɵ) in this measurement is between (0-80) degrees (Aseel M. Aljeboree 2021).

2-6 Removal of pollutant by using(SA-g-(PAAc-co-VBS)/ZnO NPs) surfaces as Adsorbents :

2-6-1 Determination of optimum wavelengths (λmax) and Calibration curves of (Crystal violet (CV) dye, Tetracycline(TC) drug and phenol (PH)) .

2-6-1-1 Crystal violet

A Crystal violet dye is a very well-known cationic dye that has a molecular formula ($C_{25}N_3H_{30}Cl$), and molecular weight (407.98 g/mol); the dye is odourless Violet powder used for various purposes, also extensively used in textile dying and paper printing. A stock solution (1000 mg L^{-1}) was prepared by dissolving (1.0 g) of dye in (1000 mL) D.W.

To determine the maximum wavelength of Crystal violet dye the ultraviolet-visible absorption spectra of Crystal violet dye solution was recorded within wavelengths of 200-800 nm. Where the maximum wavelength of the solution was determined from its highest absorption in the UV-Vis spectrum found at the wavelength λ_{max} CR= 590 nm in Figure (2-4).

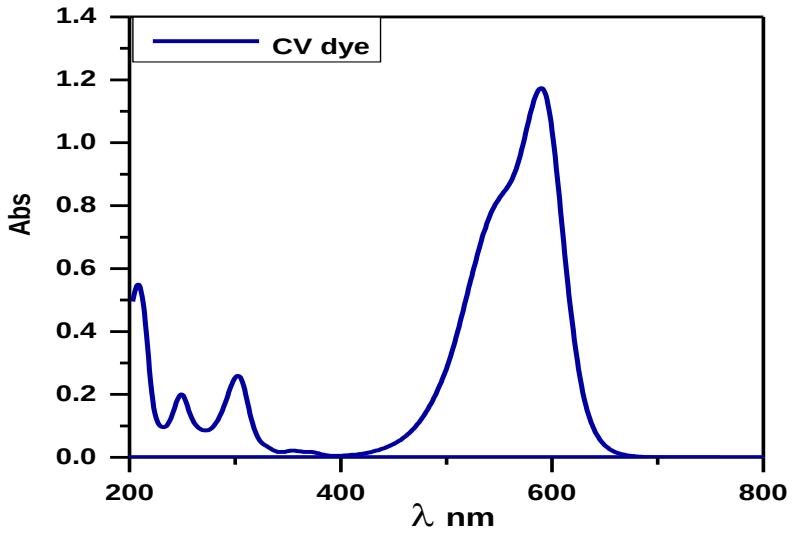

Figure(2-4): UV-Visible absorption spectra of Crystal violet (CV) dye .

The calibration curve of different concentration of Crystal violet dye was prepared in serial dilutions (2-100 mg/L). Absorbance was measured at the λ_{max} Crystal violet dye and plotted against the concentration values of Crystal violet dye in (Figure 2-5).

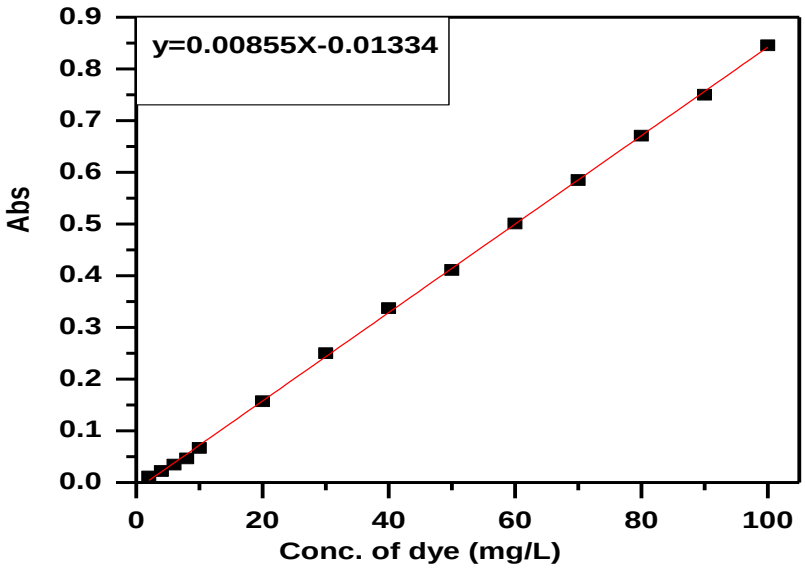

Figure (2-5): Calibration curve for Crystal violet (CV) dye .

2-6-1-2 Tetracycline

A Tetracycline(TC) drug is a very well-known antibiotic that has a molecular formula ($C_{22}H_{24}N_2O_8$), and molecular weight (444.4 g/mol); the drug is yellow powder used for various purposes, also extensively used human and veterinary medicine for the treatment of bacterial . A stock solution (1000 mg L^{-1}) was prepared by dissolving (1.0 g) of Amoxicillin in (1000 mL) D.W.

To determine the maximum wavelength of Tetracycline(TC) drug , the ultraviolet-visible absorption spectra of Tetracycline(TC) drug solution recorded within wavelengths of 200-800 nm. Where the maximum wavelength of the solution was determined from its highest absorption in the UV-Vis spectrum found at the wavelength λ_{max} TC= 350 nm ,in Figure (2-6).

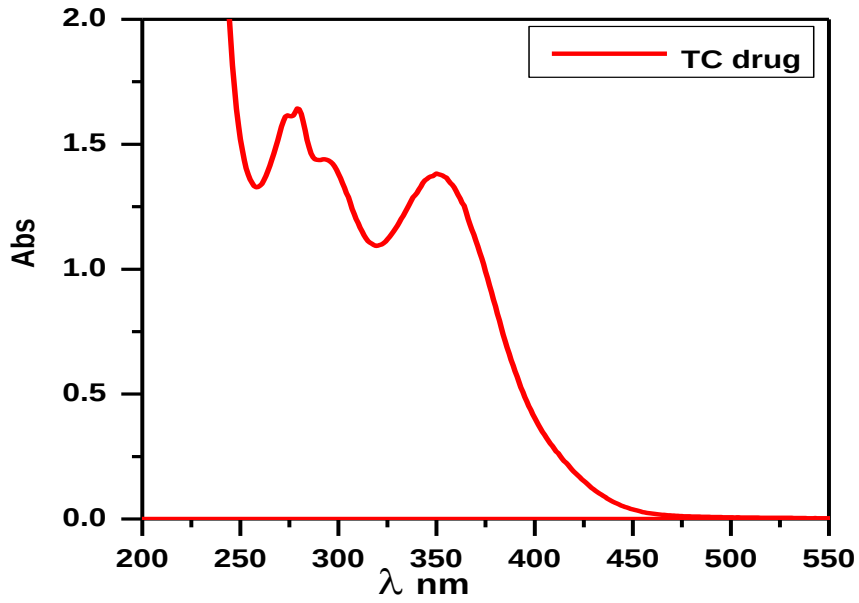

Figure(2-6): UV-Visible absorption spectra of Tetracycline(TC)drug

The calibration curve of different concentration of Tetracycline(TC) was prepared in serial dilutions (2-100 mg/L). Absorbance was measured at the λ_{max} for Tetracycline(TC) and plotted against the concentration values of Tetracycline(TC) in (Figure 2-7) .

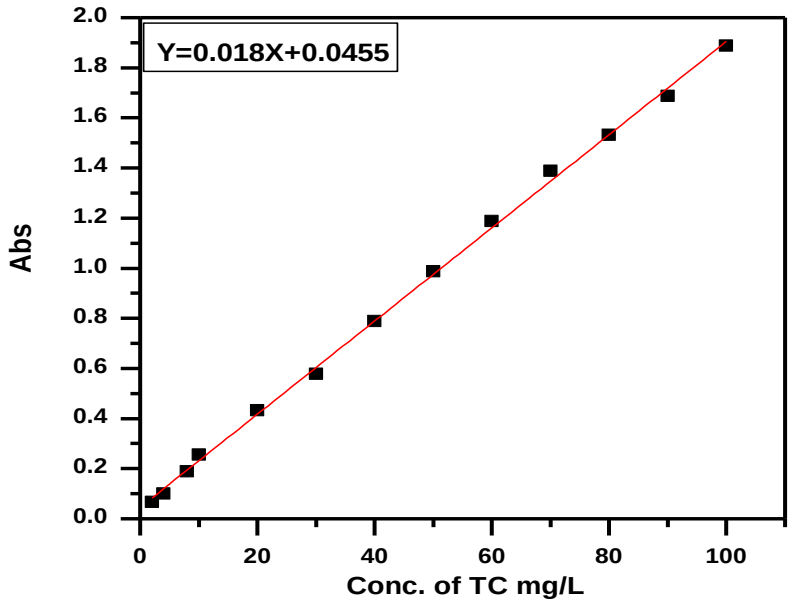

Figure (2-7): Calibration curve for Tetracycline(TC) drug

2-6-1-3 Phenol

Phenol PH is a very well-known pollutant that has a molecular formula (C_6H_6OH), and molecular weight (49.11g/mol); the phenol is colorless used on a large scales in chemical industry including the production of pharmaceuticals, pesticides and dyes . A stock solution (1000 mg L^{-1}) was prepared by dissolving (1ml) of phenol in (1000 mL) D.W.

To determine the maximum wavelength of phenol the ultraviolet-visible absorption spectra of phenol solution were recorded within wavelengths of 200-800 nm. Where the maximum wavelength of the solution was determined from its highest absorption in the UV-Vis spectrum found at the wavelength λ_{max} PH= 270 nm in Figure (2-8).

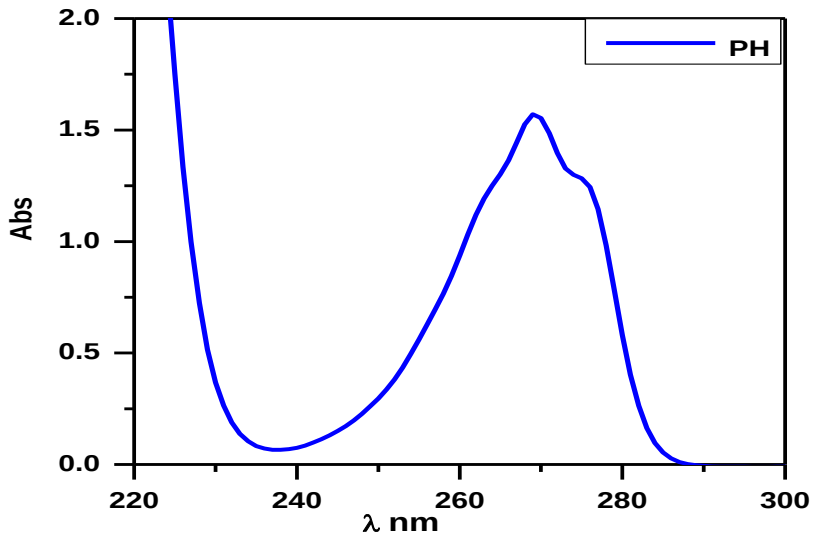

Figure(2-8): UV-Visible absorption spectra of Phenol (PH) .

The calibration curve of different concentration of Phenol was prepared in serial dilutions (2-100 mg/L). Absorbance was measured at the λ_{max} for Phenol (PH) and plotted against the concentration values of PH(Figure 2-11), (Figure 2-9) .

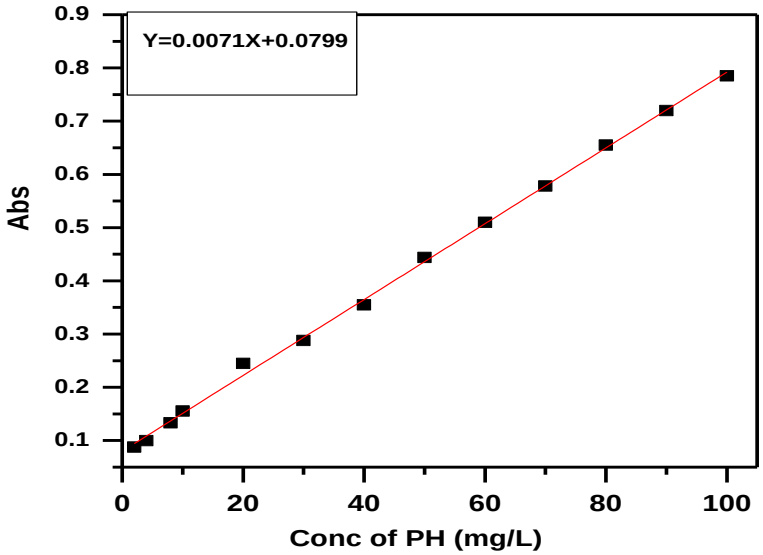

Figure (2-9): Calibration curve for Phenol (PH) .

In order to determine the precision and accuracy of the method, solutions containing ten different concentrations. The measured detection limit LOD, limits of Quantitation's, LOQ, relative standard deviations percent (R.S.D%) and standard deviation (S.D.), (Table 2-3) (Rangaraju and Chaitanya 2018).

The limit of detection (LOD) for the proposed method was calculated using equation (2-1). The signal-to-noise ratio (S/N) obtained by standard addition quantification and subsequent extrapolation to a S/N of 3.(Metrani, Jayaprakasha et al. 2018; Ashour and Bayram 2019)

$$\mathrm{LOD} = \frac{3\ \mathrm{S.D}}{\mathrm{b}} \qquad (2-1)$$

The limits of Quantitation's (LOQ) was experimentally calculated using equation (2-2) (Abdoon 2018; Ashour and Bayram 2019) :

$$\mathrm{LOQ} = \frac{10\ \mathrm{S.D}}{\mathrm{b}} \qquad (2\text{-}2)$$

S.D is the standard deviation and *b* is the sensitivity, namely the slope of the calibration graph.

Table (2-3): Statistics data of calibration for different concentrations of Crystal violet dye, Tetracycline(TC) drug , and Phenol (PH)

Parameters	**Proposed Method CV**	**Proposed Method TC**	**Proposed Method PH**
λ_{max} (nm)	595	335	272
Beer's law limit (µg/ml)	2-100	2–100	2–100
Regression equation	(Y = m X + C) Y=0.0085X- 0.013	(Y = m X + C) Y=0.0186X+0.0456)	(Y = m X + C) Y=0.0071+0.0799)
Slope (m)	0.0085	0.0186	0.0071
Intercept (C)	0.0133	0.0456	0.0799
Correlation coefficient (R^2)	0.9997	0.9988	0.9987
Color	Violet	Yellow	colorless
Detection limit LOD (µg/ml)	1.040*10-4	1.012*10-4	1.033*10-4
limit of Quantitation LOQ (µg/ml)	3.42*10-4	3.43*10-4	3.44*10-4
% Relative Standard deviation (RSD%)	90.198	75.3314	63.988
standard deviation (SD)	0.2947	0.6381	0.2445
Molar absorptivity (L/mol.cm)	3.508*103	8.226*104	6.681*103
Sandal's sensitivity (µg/cm)	0.116*10-6	0.054*10-6	0.0734*10-6

2-7 Effect of different parameters on the adsorption process:

2-7-1 Effect of contact time:

100 mL of pollutant solution (100 mg.L^{-1}) With different time periods (2,5,10,15,20,25,30,35,40,45,50,60,90,100,120 and 240min.) is prepared and put in a conical flask with adsorbent concentration (0.04 g/100 mL) of (SA-g-(PAAc-co-VBS)/ZnO NPs) at 30°C and 220 rpm Shaking speed and kept separately in a shaker the water bath controlled temperature. Pollutant concentration to be estimated spectrophotometrically at the wavelength corresponding to maximum absorbance, λ_{max}, using a single beam UV-Visible spectrophotometer. The samples at different interval times are separated by the centrifugation process. The absorbance of the solution is then measured, the dye concentration is to be measured after (2- 240) minute until equilibrium is reached.

The adsorption capacity was calculated from equation (2-1): (Tariq J. AlMusawi 2021)

$$qe = \frac{(C_0 - C_e) * V_L}{m_{gm}} \qquad (2-3)$$

Where: q_e = Amount of pollutant adsorbed per unit mass of adsorbent (mg/g).

C_o= Initial concentration (mg.L^{-1}).

C_e= Equilibrium concentration (mg.L^{-1}).

m = Dose of adsorbent (g).

V_L= is the volume of solution (L).

The percentage removal (E%) of the pollutant was calculated based on the reduction in absorbance at λ_{max} value of the pollutant as follows:(Tariq J. AlMusawi 2021)

$$E\ \% = \frac{C_0 - C_e}{C_0} * 100 \qquad (2-4)$$

Where: C_0 and C_e are initial and equilibrium concentrations, respectively.

2-7-2 Effect of dose of adsorbent :

The study was carried out with different doses (0.01,0.02, 0.04,0.06, 0.08, and 0.1) g for (SA-g-(PAAc-co-VBS)/ZnO NPs).The concentrations of the samples were (100) $mg.L^{-1}$. The solutions were kept in the shaker water bath at (220 rpm) about (2 hr.) at a fixed temperature (30 ^{0}C) the remaining pollutant concentration in the aqueous phase is measured spectrophotometrically for the chosen wavelength.

2-7-3 Effect of Initial Concentration of pollutant :

A series of different concentrations of 100 mL for pollutant has been used in this study (10-100) $mg.L^{-1}$, was added to a conical flask (Erlenmeyer) in the presence of (0.04g/100 mL) of (SA-g-(PAAc-co-VBS)/ZnO NPs) at 30°C and 220 rpm Shaking speed these series were putting in a shaker water bath for 2 hr. , after that the supernatant was separated by centrifuge and measured the remaining concentration of pollutant in the aqueous phase is measured spectrophotometrically for the chosen wavelength.

2-7-4 Effect of pH :

The effect of solution pH on the pollutant removal is examined by varying the initial pH solutions (3,4, 6,8, and 10) using conical flasks (100 mL) container concentrations (100 $mg.L^{-1}$) in 100 mL .The pH was adjusted by using (0.1N) HCl and/or (0.1N) sodium hydroxide (NaOH) and was measured using a pH meter. Then the amount of adsorbent surface (0.04 g/100 mL) of (SA-g-(PAAc-co-VBS)/ZnO NPs) adsorbents was set on the conical flask.

The flasks were put inside the shaker water bath (220 rpm fixed throughout the study) maintained at 30^{o}C and the final concentration of pollutant was measured using the single beam UV-Vis spectrophotometer

2-7-5 Effect of Temperature :

The adsorption experiments are performed at different temperatures (10, 20,30 and 40°C) in a thermostat water bath with a shaker. The effect of temperature was investigated with (0.04g) dose of adsorbent (SA-g-(PAAc-co-VBS)/ZnO NPs) mixing with (100mL) aqueous solution of different concentration of three pollutants and the sample was shaking at a period for (2 hr.) , then measured the remaining pollutant concentration in the aqueous phase is measured spectrophotometrically for the chosen wavelength.

2-8 Adsorbent Regeneration Experiments:

Reusability To investigate the reusability of the adsorbent, 0.5g of (SA-g-(PAAc-co-VBS)/ZnO NPs) adsorbent was added into 100 mL for each of three pollutant (CV,TC,PH) solution of concentration 500 mg/L at 30 oC temperature to achieve saturated adsorption. The (SA-g-(PAAc-co-VBS)/ZnO NPs) was regenerated in excess desorption studies were carried out using different desorption agents at different concentration

(0.1 N) such as H_2SO_4, NaOH, H_3PO_4 , HCl , HNO_3, and water to regenerate anionic binding sites and finally washed with excess distiller water prior to use in the next adsorption cycle. An adsorption and desorption cycle was repeated six additional times using 100 mL of pollutant solution of concentration 500 mg/L at 30^oC temperature .

2-9 A Comparative adsorption between different surfaces

A sample of 100 mL of three pollutant concentration (100 $mg.L^{-1}$) are used in this study, then added to a conical flask (Erlenmeyer) in the presence of 0.04 g from prepared ((SA-g-(PAAc-co-VBS)/ZnO NPs), (SA-g-(PAAC-co-VBS)), and ZnO NPs), and put in a shaker water bath for 2 hr., after that the supernatant was separated by centrifuge and measured the remaining concentration by using UV-Visible spectrophotometer for the chosen wavelength .

2-10 Removal of Pollutants (pharmaceutical) by Using ((SA-g-(PAAc-co-VBS)/ZnO NPs) .

A laboratory sample 100mL of pharmaceutical pollutants containing (Amoxicillin (AMX), phenylephrine hydrochloride (PHE), Tetracycline (TC) , paracetamol (PR) , Vitamin B6 (pyridoxine) Riboflavin (RF) with a riffle concentration were using in this study, then added to a conical flask (Erlenmeyer) in the presence of 0.04g from prepared ((SA-g-(PAAC-co-VBS)/ZnO), after that the mixture were putting in Shaker water bath for 2hr, after that the supernatant were separated by centrifuge and measured the remaining concentration by using UV-Visible spectrophotometer at the λmax 350 nm for TC drug .

2-10-1 Removal of Pollutants (Dyes) by Using by Using ((SA-g-(PAAc-co-VBS)/ZnO NPs) .

A laboratory sample 100mL of dyes pollutants containing (Congo red (CR), Crystal Violet (CV), Methylen Blue (MB) , Berllint Blue (BB) , Direct yellow (DY) ,Reactive blue (RB) with a riffle concentration were using in this study, then added to a conical flask (Erlenmeyer) in the presence of 0.04g from prepared ((SA-g-(PAAc-co-VBS)/ZnO NPs), after that the mixture were putting in Shaker water bath for 2hr, after that the supernatant were separated by centrifuge and measured the remaining concentration by using UV-Visible spectrophotometer at the λmax 595 nm for CV dye .

2-10-2 Removal of Pollutants (Dyes , pharmaceutical , and phenol compound)by Using ((SA-g-(PAAC-co-VBS)/ZnO)

A laboratory sample 100mL of pollutants containing (Phenol (PH), 4-Clorophenole (CPH), Amoxicillin (AMX), phenylephrine hydrochloride (PHE), Tetracycline (TC) , paracetamol (PR) , Vitamin B6 (pyridoxine) Riboflavin (RF) Congo red (CR), Crystal Violet (CV), Methylen Blue (MB) , Berllint Blue (BB) , Direct yellow (DY)) with a riffle concentration were using in this study, then added to a conical flask (Erlenmeyer) in the presence of 0.04g from prepared ((SA-g-(PAAc-co-VBS)/ZnO NPs), after that the mixture were putting in Shaker water bath for 2hr, after that the supernatant were separated by centrifuge and measured the remaining concentration by using UV-Visible spectrophotometer at the λmax 595 nm for CV, λmax 350 nm for TC, λmax 272 nm for PH at the same order .

2-11 Tetracycline (TC) drug Loading

About 0.5 gm of the SA-g-(PAAc-co-VBS)/ZnO NPs) is added to (100 ml) of the amoxicillin solution in concentration 500 mg/L and placed in a shaker device for a period of (2h) at a temperature (30 ^{o}C), after that the surface is separated from the solution and the drug-loading SA-g-(PAAc-co-VBS)/ZnO NPs) is dried in an oven at a temperature (70 ^{o}C) and then ground to obtain the powder .

2-12 In vitro drug release

The effect of the hydrogel loaded with a drug in different acidic media, as the release of the drug at (pH 1.2) and (pH 7.5) was studied. Where (0.1g) of the surface loaded with a drug was placed in (100ml) of different acidic media, and then placed in a shaker water bath , at a temperature (37 ^{o}C) in different time, the removal percentage and amount of drug release is calculated through the equations .

$$\text{Amount of drug release} = \frac{Ce\ V}{M} \qquad (2\ -5)$$

$$\text{Percentage drug release} = \frac{\text{amount of drug release}}{\text{amount of drug loading}}\ 100 \qquad (2-6)$$

2-13 Biological activity bacterial test

The two cultivars of Gram-positive bacteria (*Staphylococcus aureus and Streptococcus epigenetics*) and Gram-negative bacteria (*E.coli, and Klebsiella spp*.), were obtained from the Department of Life Sciences / College of Science - University of Babylon. hinton agar) and Mannitol salt agar as media for cultivation, isolation and differentiation between positive and negative bacteria.

2-13-1 Preparation of standard solutions for bacteria

Mueller hinton agar medium was prepared by dissolving (37 gm) of the culture medium in 1 liter of distilled water, then heat the mixture until the agar melts, then put the culture medium in an autoclave at a temperature of 120 ^{o}C for 15 minutes.) minutes), then pour the medium into sterilized glass dishes (petri disk) at a rate of (15-20) milliliters per plate and left until solidification completes, then the dishes were placed in the incubator for (24 hrs) at a temperature (37 ^{o}C) to make sure that there were no contaminate it.

2-14 Treating mice wounds using a surface prepared from SA-g-(PAAC-co-VBS)/ZnO NPs)

Mice were obtained from the animal house of the College of Veterinary Medicine at Al-Qadisiyah University, where the rats were wounded with a wound of medium depth and this wound was bandaged by loading (0.1 gm) of the surface prepared from the leaves of the castor plant and the rates of wound healing after surface loading were studied from (1-7)) days depending on the superior surface properties on wound healing and the ability to deliver it to the inside of the wound.

Chapter Three

Result and Discussion

3-1 Physicochemical characterization of adsorbents surfaces

3-1-1 FTIR characterization for adsorbent/adsorbate

FTIR technique was used to analyses the surface functional groups responsible for three pollutant (CV,TC, and PH) adsorption. Adsorbent surfaces (SA-g-(PAAc-co-VBS), (SA-g-(PAAc-co-VBS)/ZnO NPs), and pollutant -loaded adsorbent sample after adsorption was placed in an oven at 65 ◦C for 4 h. Samples were made as pellet and then the infrared spectra of three pollutant CV, TC and PH on adsorbents before and after

the adsorption process was recorded in the range 4000–400 cm^{-1} on an Infrared spectrophotometer, FTIR, 8000, Shimadzu-Japan. Results are shown in figures (3-1),(3-2) and (3-3).

Figures(3-1 to 3-3) shows a broad peak at 3000 to 3600 cm^{-1} in the spectrum of alginate and is attributed to the COOH groups, and little change was observed in peak intensity after modification of alginate with ZnO. The bands at 2923–2925 cm^{-1} in the spectra are attributed to the C–H stretch vibration from glucose units in alginate (Zhao Ying 2020).

The grafting of AA on SA is supported by a new characteristic adsorption band 1718 cm^{-1}, assigned to C=O stretching of poly(acrylic acid) in the spectrum of SA-g-(PAAc-co-VBS)/ZnO NPs. Moreover, the broad band at 450–800 cm^{-1} is assigned to the stretching band of (Zn-O-Zn) groups(Akeem Adeyemi Oladipo 2019; Mohammad 2019) .FTIR spectra of ZnO nanoparticles commonly shows these two main bands. The bands at 627(corresponding to stretching vibration of Zn–O) and 1404 cm^{-1} (corresponding to stretching vibrations of Zn–O–Zn) depict the presence of Zn NP in SA-g-(PAAc-co-VBS)/ZnO NPs. The presence of all these peaks confirms the successful graft co-polymerization of SA with the ZnO NPs (Peter Cass 2010; Zhao Ying 2020; Hanieh Gharehbakhsh 2022).

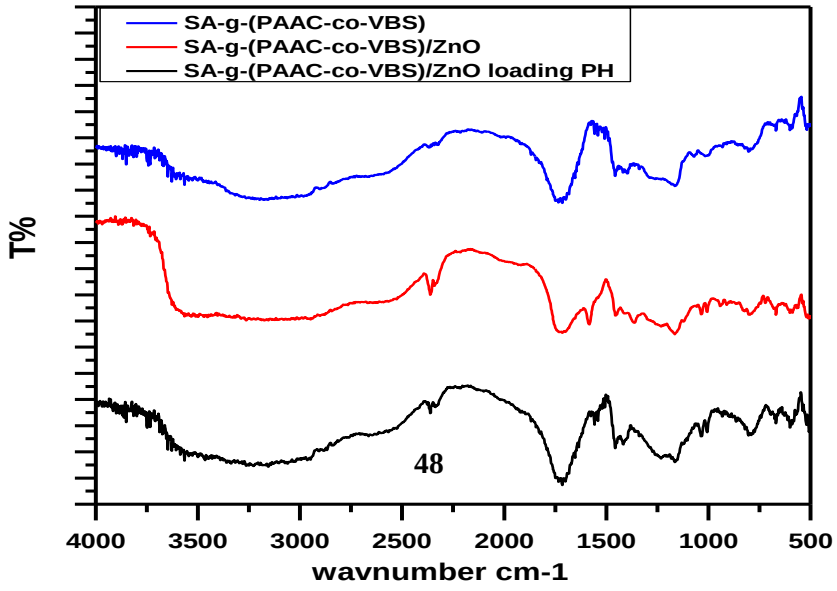

Figure (3-1) FT-IR spectra of(SA-g-(PAAc-co-VBS)and (SA-g-(PAAc-co-VBS)/ZnO NPS) surface before, and after adsorption of PH .

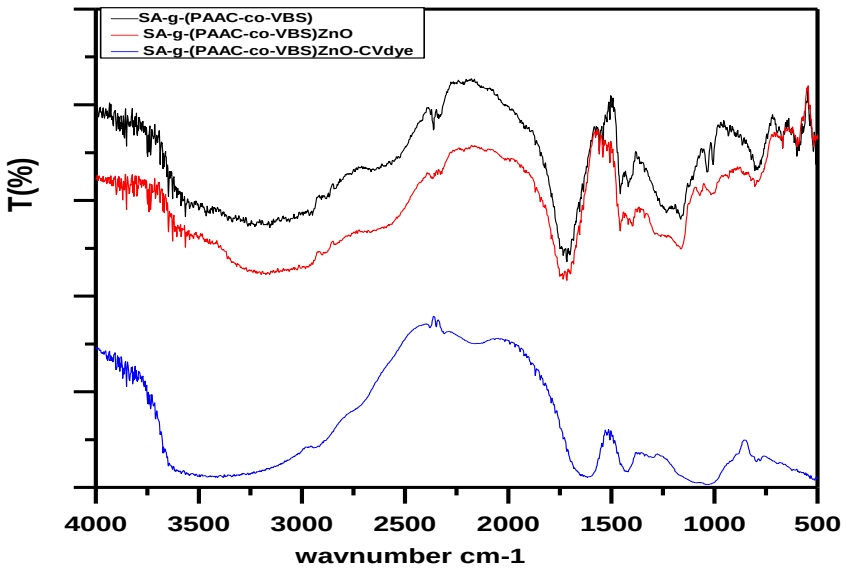

Figure (3-2) FT-IR spectra of(SA-g-(PAAC-co-VBS)and (SA-g-(PAAC-co-VBS) and (SA-g-(PAAC-co-VBS)/ZnO) surface before, and after adsorption of CV dye .

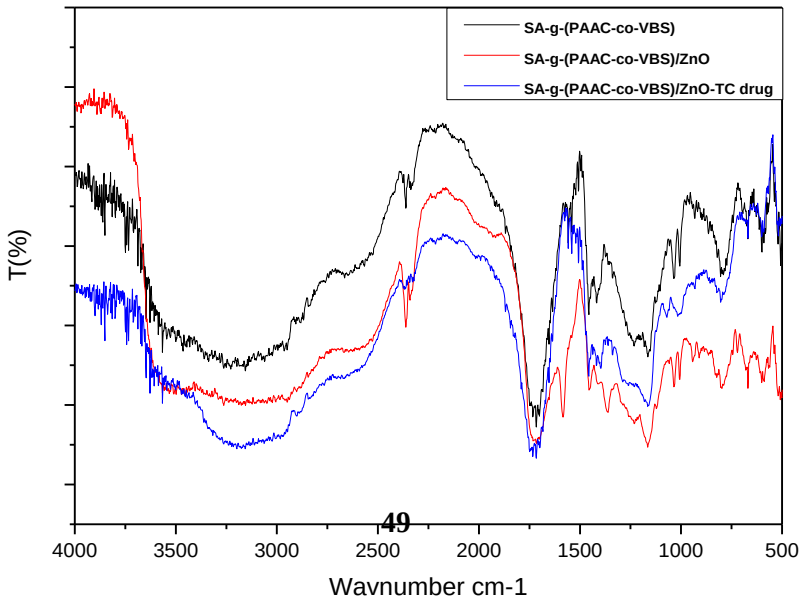

Figure (3-3) FT-IR spectra of(SA-g-(PAAc-co-VBS)and (SA-g-(PAAc-co-VBS)/ZnO NPs) surface before, and after adsorption of TC drug .

3-1-2 FE-SEM characterization for adsorbent/adsorbate:

Field Emission Scanning electron microscopy (FE-SEM) has been used as a primary tool for characterizing the surface morphology and fundamental physical properties of the adsorbent. ZnO nanoparticles were arranged in a flower-like pattern (Figure 3-4 (a)). These pores offered a strong opportunity for ZnO nanoparticles to get entangled within them(Banerjee and Chattopadhyaya 2017).The micrographs of(SA-g-(PAAC-co-VBS) appear that smooth porous surface (Figure 3-4(b)) ,and (SA-g-(PAAC-co-VBS)/ZnO) rough porous surface and showed changes in the morphology of phase for new irregular bulky particles presence on the surface(SA-g-(PAAc-co-VBS)/ZnO NPs) (Aseel M. Aljeboree 2021) . This leads to increased surface texture protuberance and coarseness .This increases the surfaces of the absorbents that facilitate water diffusion into the absorbent(Figure 3-4(c)) .FE-SEM of adsorbent material was taken before and after dye adsorption on (SA-g-(PAAc-co-VBS)/ZnO NPs) surface (Figure 3-4 (d) , 3-4 (e) and 3-4 (f)), respectively (Saeed Ullah Jan 2020; Hemant Mittal 2021).

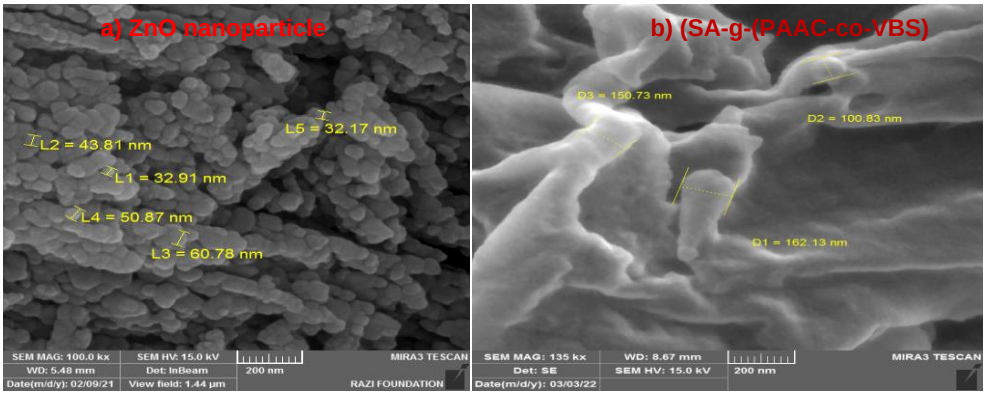

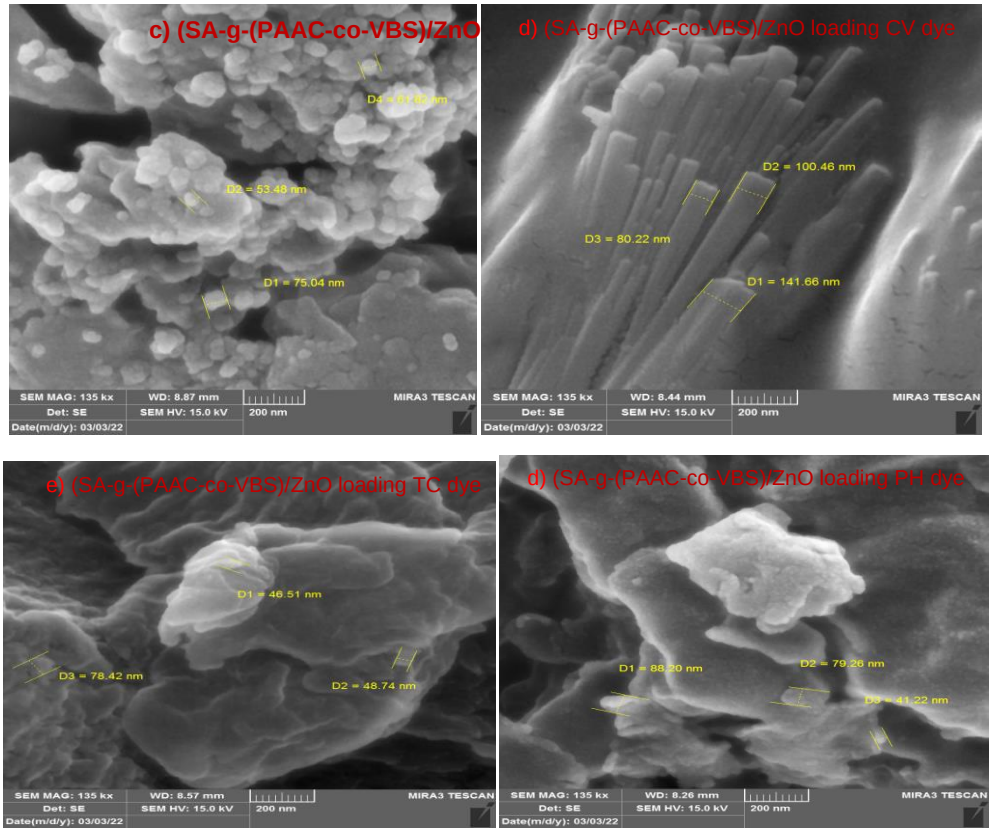

Figure (3-4): FESEM images of (a) ZnO NPs, (b) SA-g-(PAAc-co-VBS), (c) SA-g-(PAAC-co-VBS)/ZnONPs , (d) CV loaded SA-g-(PAAc-co-VBS)/ZnO NPs, (e) TC loaded SA-g-(PAAc-co-VBS)/ZnO NPs and (f) (d) PH loaded SA-g-(PAAc-co-VBS)/ZnO NPs **.**

3-1-3 Transmission Electron Microscopy (TEM) and Energy Dispersive X-Ray (EDX)

Figure(3-5(a and b)) shows the TEM images of ZnO NPs and SA-g-(PAAC-co-VBS)/ZnO, where ZnO NPs was observed embedded inside the SA-g-(PAAC-co-VBS). Also, incorporation of ZnO NPs in to SA-g-(PAAC-co-VBS) is supported via the presence of Zn and O peak in the EDS of SA-g-(PAAC-co-VBS)/ZnO as appear in Figure(3-5(c)) (Hemant Mittal 2021) . The synthesized nano-composite contains elements C, O, Zn, S, Ca, and, Al, which indicates the presence of ZnO onto SA-g-

(PAAC-co-VBS)/ZnO. values of the highest and lowest elements that existed in the modified SA-g-(PAAC-co-VBS)/ZnO by 63.4 wt.% and 0.3 wt.%, respectively(Ali M. El Shafey 2021).

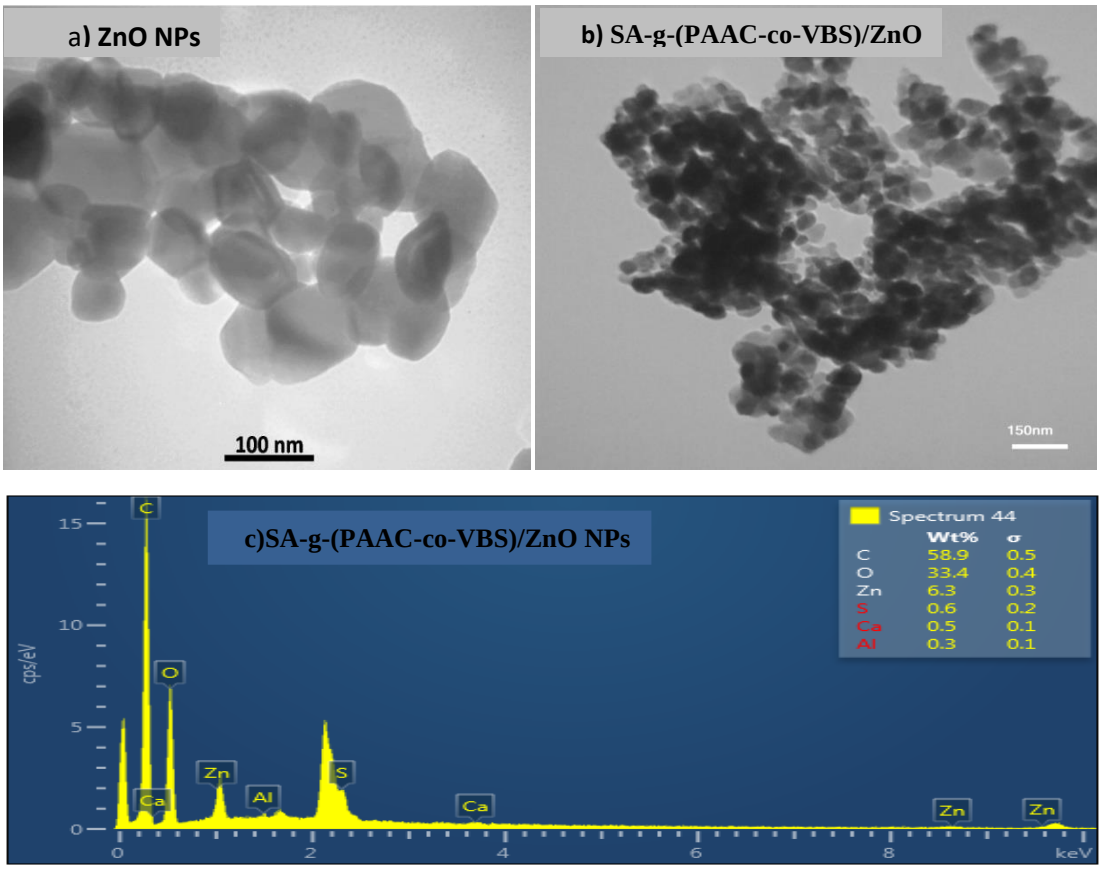

Figure (3-5): TEM images of (a)ZnO NPs , b) SA-g-(PAAC-co-VBS)/ZnO NPs and (c) EDX of SA-g-(PAAC-co-VBS)/ZnO NPs.

3-1-4 Thermal Gravimetric Analysis

The thermal gravimetric analysis of the SA-g-(PAAC-co-VBS) and SA-g-(PAAc-co-VBS)/ZnO NPs was investigated. That obtained at a heating rate of 5 ◦C/min up to 600 ◦C under a dry nitrogen flow is shown in (Fig. 3-6 and 3-7 respectively , one can see that the degradation process is different. It is well- known that any weight loss below 200 ◦C is due to the loss of unbound water, while the loss in the range of 200−800 ◦C is mainly due to organic matter degradation (Soulaima Chkirida 2021). By analyzing the thermograms of SA-g-(PAAc-co-VBS) and SA-g-

(PAAc-co-VBS)/ZnO NPs , it is quite clear that the incorporation of ZnO has an approving effect on the thermal stability of the matrix hydrogel since we have a decrease of the weight loss percentage. Similarly, by examining the thermograms of SA-g-(PAAc-co-VBS), SA-g-(PAAc-co-VBS)/ZnO NPs, we can detect an enhancement in thermal stability attributed to the ZnO loading (Ali M. El Shafey 2021). It is very common that the nanocomposite's thermal degradation is affected by the presence of organic and inorganic materials at their surface. In fact, in our case the bonds at the biocomposite surface are originated from the interaction between Zn atoms and COO− biopolymer groups. The reduced size and increased area of ZnO NPs on the surface of the hydrogel assure the good interactivity between them, which gives rise to more stable complexes. Thusly, SA-g-(PAAC-co-VBS)/ZnO NPs ameliorates the biocomposite thermal stability(H.M. Xiong 2008; X. Zhou 2009; Y. Guo 2009; Zhou 2013).

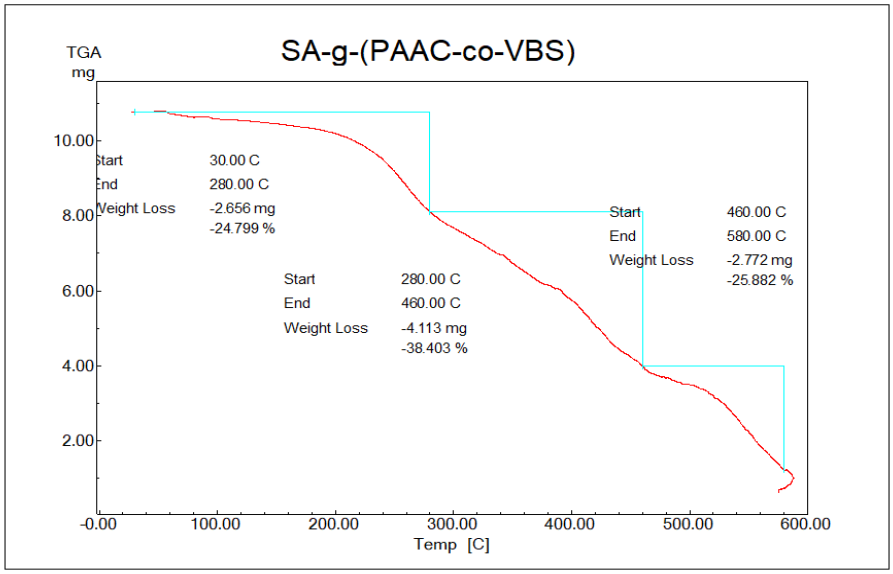

Figure (3-6): Thermal gravimetric analysis curve of the SA-g-(PAAC-co-VBS) .

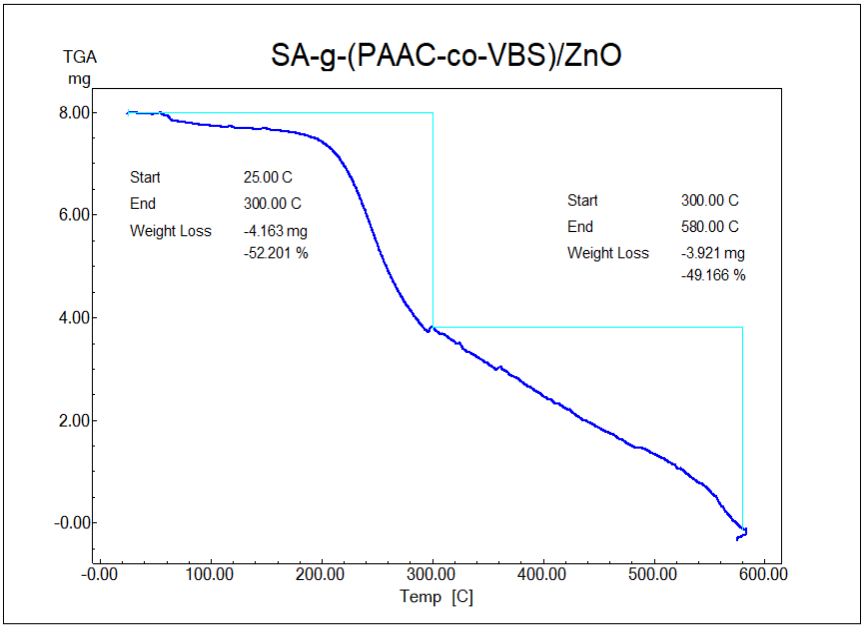

Figure (3-7) :Thermal gravimetric analysis curve of the SA-g-(PAAC-co-VBS)/ZnO NPs .

3-1-5 X-Ray Diffraction (XRD)

The XRD of ZnO NPs, SA-g-(PAAc-co-VBS)/ZnONPs and SA-g-(PAAC-co-VBS) shows in Figure 3-8. The ZnO NPs crystalline peaks that appear at 32º,34º,and 36º which confirm the presence of ZnO NPs .The broadness in peak is due to graft co-polymerization. The broadness confirms the grafting of poly(acrylic acid) chains onto SA(Inas A. Ahmed 2022). The disappearance of the crystalline peaks was observed after adding ZnO NPs to hydrogel. The transition from crystalline to amorphous may be due to the diffusion of ZnO NPs into the micro-pores and macro-pores of SA-g-(PAAc-co-VBS)/ZnONPs .The XRD patterns

of SA-g-(PAAc-co-VBS)/ZnO NPs that appear very little peak observed in the case of ZnO which confirm the incorporation of ZnO NPs with in SA-g-(PAAc-co-VBS) matrix(Hanieh Gharehbakhsh 2022).

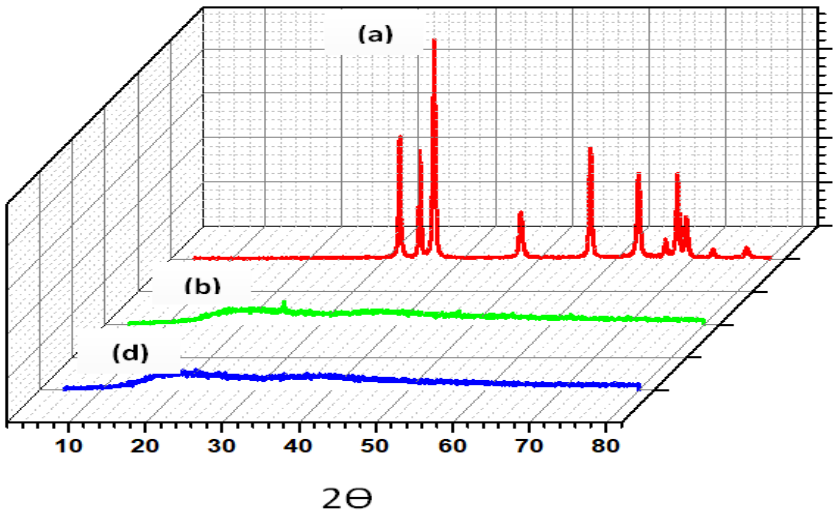

Figure(3-8):X-ray diffraction patterns for (a) ZnO NPs, (b) SA-g-(PAAC-co-VBS)/ZnO NPs,(d) SA-g-(PAAC-co-VBS) .

3-2 Effect of different parameters on the adsorption process of the removal CV dye :

3-2-1 Effect of contact time:

The contact time is one of the important parameters for the assessment of the practical application of the adsorption process. The experimental results of adsorption of initial CV dye concentrations of 200 $mg.L^{-1}$ on the adsorbent surfaces of the (SA-g-(PAAc-co-VBS)/ZnO NPs) with contact time. The equilibrium data are shown in Figures (3-9) which reveal that the adsorption increased rapidly in the first 15 min, and after that gradually increased till the equilibrium (Hameed 2017). Adsorption capacity increases with the increase in contact time to reach the

equilibrium, because with a time of adsorption increased, the active sites of absorbent surfaces will saturate, indicating that an apparent equilibrium is reached, Where an acceptable efficiency was found at a concentration of 200 $mg.L^{-1}$ and contact time of two hour as the increase in time will have a slight effect on the removal rate due to the fullness of the active sites(Yazidi A Atrous 2020; Soulaima Chkirid 2021) .

Figure (3-9) : Effect of contact time on removal percentage and adsorption capacity for removal of CV dye by (SA-g-(PAAc-co-VBS)/ZnO NPs) at pH 6.6, Temp. 30 ^{o}C and mass adsorbent 0.04 g .

3-2-2 Effect of dose of adsorbent

The study was carried out with different doses (0.01- 0.1) gm for (SA-g-(PAAC-co-VBS)/ZnO) . The concentrations of the CV dye (200 $mg.L^{-1}$). The solutions were kept in the shaker water bath at (220 rpm) about (2 hour) in a fixed temperature (30^{0}C) at pH 6.6 , then measured the remaining dye concentration in the aqueous phase is measured spectrophotometrically for the chosen wavelength. The results are illustrated in Table (3-1) and shown in Figures 3-10 .

Table (3-1): Effect of adsorbent dose on the removal percentage of CV dye on to (SA-g-(PAAC-co-VBS)/ZnO).

Co(mg.L^{-1})	W(g)	Abs.	Ce(mg.L^{-1})	E%	Qe mg/g
200	**0.01**	0.1767	53.5454	73.2272	1464.545
200	**0.02**	0.0977	29.6060	85.1969	851.9697
200	**0.04**	0.063	19.0909	90.4545	452.2727
200	**0.06**	0.0333	10.0909	94.9545	316.5152
200	**0.08**	0.0111	3.36363	98.3181	245.7955
200	**0.1**	0.0001	0.03030	99.9848	199.9697

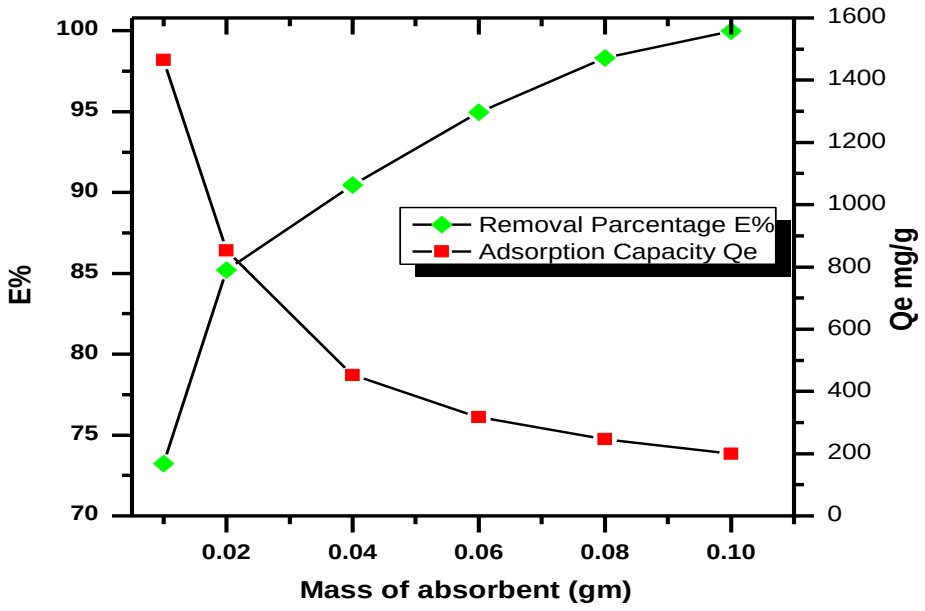

Figure (3-10): Effect of the mass amount of adsorbent (SA-g-(PAAC-co-VBS)/ZnO NPs) on the percent removal and amount of adsorbed CV dye, initial concentration = 200 mg.L^{-1}, Temp. = 30°C, contact time 2hr., pH=6.6.

An increase in the percentage of the dye removal with adsorbent mass was related to increases in the adsorbent surface areas, enhancing the number of adsorption sites available for adsorption as reported already in other cases (Wang 2020). The increase in removal of dye with adsorbent dose due to the introduction of more binding sites for adsorption (Yahya A. Faleh 2021). The primary factor explaining this characteristic is that adsorption sites remain unsaturated during the adsorption reaction whereas the number of sites available for adsorption site increases by increasing the adsorbent dose(Aljeboree, Alshirifi et al. 2017).The increase of adsorbent amount about rang 0.01 - 0.1g, the percentage removal of CV dye increase from 72.9 - 99.8% and adsorption capacity decrease from 1599 -200 mg/g onto (SA-g-(PAAc-co-VBS)/ZnO NPs) about 2h of adsorption time. This data is attributed to increasing the number of active sites caused via increasing mass of adsorbent (Mohammed A. Jawad 2021; Mohammed A. Jawad 2021).

3-2-3 Effect of pH

Solution pH play an important role in adsorption through is effect on the target compounds, the charge species and density on the surface of sorbent . In this work, the effect of pH is investigated at pH range from 3.0-10.0 .The results are illustrated in Table (3-2) and shown in Figures 3-11 .

Table (3-2): Effect of solution pH on adsorption CV dye onto (SA-g-(PAAC-co-VBS)/ZnO)

Co(mg/L)	pH	Abs	Ce(mg/L)	E%	Qe (mg/g)
200	3	0.432	130.9091	34.5454	172.7273

200	4	0.322	97.63636	51.1818	255.9091
200	6.6	0.063	19.09091	90.45455	452.2727
200	8	0.099	30	85	425
200	10	0.155	46.9697	76.5151	382.5758

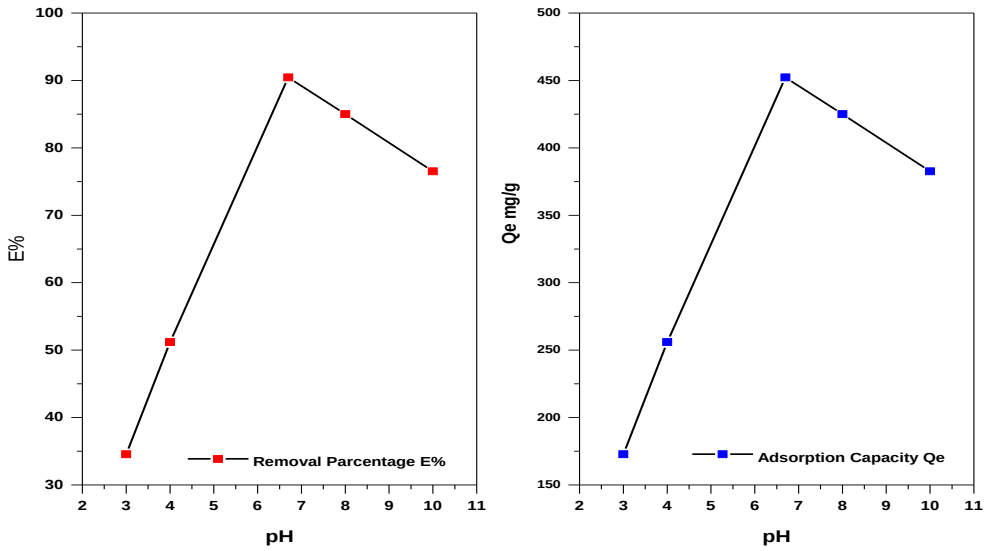

Figure (3-11): Effect of solution pH on the adsorption of CV dye on (SA-g-(PAAC-co-VBS)/ZnO) (Exp. Condition: Temp. = 30°C, contact time 1 h, and pH of solution 6.6).

The equilibrium sorption capacity of CV dye on (SA-g-(PAAC-co-VBS)/ZnO) very little in pH range of 3,4. The adsorption capacity (Qe mg/g) of pH 3 (158.5 mg/g) and pH4 (259.6 mg/g) , which suggests that (SA-g-(PAAC-co-VBS)/ZnO) is excellent adsorbents for CV dye removal from large volumes of aqueous solutions(Farabi Temel 2020; Saeed U J 2020). When the pH is greater than 4 the adsorption capacity (Qe mg/g) of CV dye on (SA-g-(PAAC-co-VBS)/ZnO) increases with increasing pH values at pH 6.6 after that decreasing to reach pH10 ,the adsorption capacity (Qe mg/g) decrease with increasing pH. Lower adsorption of dye at acidic pH is probably due to the presence of excess

H+ ions competing with the cation groups on the dye for adsorption sites . At higher pH, the surface may get positively charged, which enhances the negatively charged dye anion through electrostatic forces of attraction (Aseel M Aljeboree 2021; Hemant Mittal 2021) .

3-2-4 Effect of temperature

To determine whether the ongoing adsorption process was endothermic or exothermic. The adsorption isotherms were determined for various dye-adsorbent systems. The removal of CV dye has been studied at different temperature (283.15, 293.15, 303.15 and 313.15 K) in the presence of various initial concentrations (50-500 $mg.L^{-1}$) results are illustrated in Tables (3-3), and presented in Figures (3-12) .

Table (3-3)Adsorption isotherm for adsorption of CV dye on the (SA-g-(PAAC-co-VBS)/ZnO) **at different temperatures. (pH 6.6, mass adsorbent 0.04 gm/ 100 ml, contact time 2h).**

C_0 $mg.L^{-1}$	10 ºC			20 ºC			30 ºC			40ºC		
	C_e $mg.L^{-1}$	Q_e $mg.g^{-1}$	E%	C_e $mg.L^{-1}$	Q_e $mg.g^{-1}$	E %	C_e $mg.L^{-1}$	Q_e $mg.g^{-1}$	E%	C_e $mg.L^{-1}$	Q_e $mg.g^{-1}$	E%
50	1.654	120.8	96.6	1	122.5	98	0.666	123.33	98.6	0.639	123.4	98.7
100	6	235	94	3	242.5	97	2.666	243.33	97.3	2.548	243.6	97.4
150	10.39	349	93.0	8.415	353.9	94.3	5.151	362.12	96.5	4.696	363.2	96.8
200	23.63	440.9	88.1	23.93	440.1	88.0	19.09	452.27	90.4	15.51	461.2	92.2
300	60.30	599.2	79.8	50.12	624.6	83.2	40.30	649.24	86.5	24.69	688.2	91.7
400	84.84	787.8	78.7	84.51	788.7	78.8	74.24	814.39	81.4	60	850	85

500	121.2	946.9	75.7	117.4	956.3	76.5	110.9	972.72	77.8	94.27	1014.	81.1

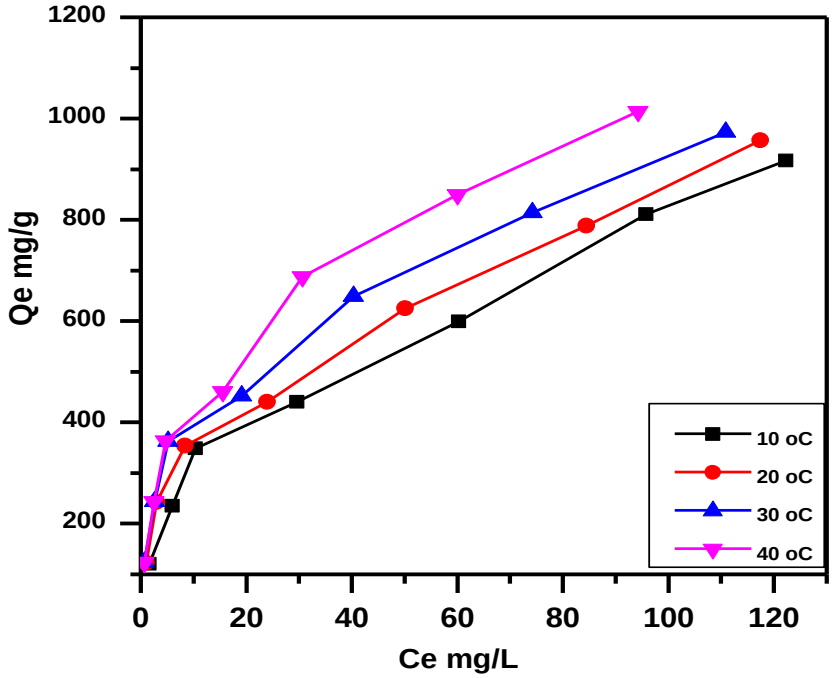

Figure (3-12): Effect of temperature on the adsorption of CV dye on the surface of (SA-g-(PAAC-co-VBS)/ZnO). (pH 6.6, mass adsorbent 0.04 gm/ 100 ml).

The result shows that the equilibrium adsorption capacity of CV dye was increased while increasing the solution temperature for all initial concentrations. As generally observed from Figures. (3.13), the uptake capacity of (SA-g-(PAAC-co-VBS)/ZnO) increases with increasing temperature, due to the enhanced magnitude of the reverse (desorption) step in the mechanism. This is possibly due to the endothermic effect of the surroundings during the adsorption process (Amer M. Alshamri 2021).

The study of the temperature effect on adsorption will also help in the calculation of the basic thermodynamic functions such as Gibbs free energy (ΔG), change enthalpy (ΔH), and change entropy (ΔS) of the adsorption process (Yahya A. Faleh 2021).

The equilibrium constant (K_e) of the adsorption process at each temperature, was calculated from the equations (3-1) (A. F. AlKaim 2007):

$$K_e = \frac{(Q_{max}) * Wt\ (0.04\ gm)}{(C_e) * V(0.1L)} \qquad 3-1$$

Where Q_{max} is the amount adsorbed in ($mg.gm^{-1}$), C_e is the equilibrium concentration of the adsorbent expressed in ($mg.L^{-1}$), 0.04 gm represents the weight of the (SA-g-(PAAC-co-VBS)/ZnO) adsorbent, and 0.1L represents the volume of the CV dye solution used in the adsorption process (Huda Salim Al-Niaeem 2022). The change in the free energy could be determined from the equation (3-2) :(Huda Salim Al-Niaeem 2022)

$$\Delta G = -RT \ln K_e \qquad 3-2$$

Where ΔG: Gibbs free energy ($J.K^{-1}.mol.^{-1}$), R is the gas constant (8.314 $J.K^{-1}.mole^{-1}$), T is the absolute temperature in Kelvin.

The enthalpy of adsorption may be obtained from the following equation (3-3) (Abdalghaffar M Osman 2020):

$$\ln X_m = -\frac{\Delta H^{\circ}}{RT} + Cons. \qquad 3-3$$

When $X_{m:}$ is the maximum value of adsorption at a certain value of equilibrium concentration (Ce). Table (3-4) gives X_m values at different temperatures CV dye. Plotting $\ln X_m$ versus (1/T) should produce a straight line with a slope -ΔH/R as shown in Figures (3-13) The value of ΔH and ΔS can be calculated from the slope and intercept respectively (Nasseh 2019).

Table (3-4) Maximum adsorption quantity Xm values of CV dye onto (SA-g-(PAAC-co-VBS)/ZnO) surfaces at different temperatures.

T(K)	1000/T(K^{-1})	C_e = 94	
		X_m	ln X_m
283	3.5335	795	6.6783
293	3.4129	840	6.7334
303	3.3003	900	6.8023
313	3.1948	1000	6.9077

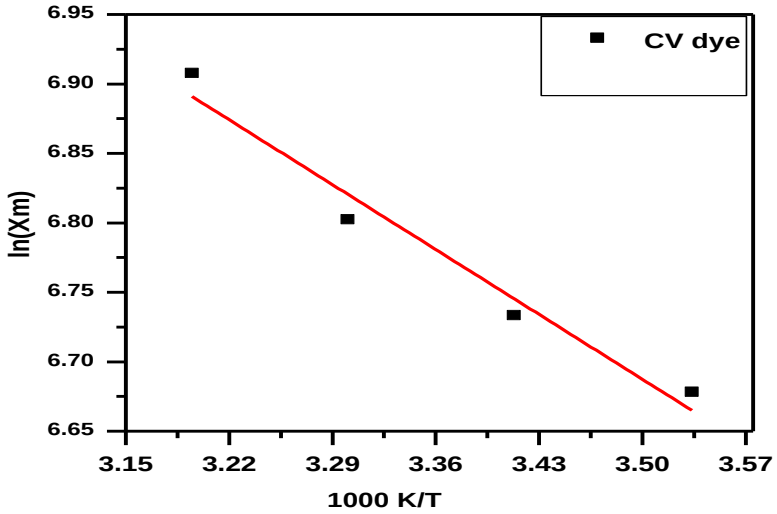

Figure (3-13): Plot ln X_m against the absolute temperature. of the adsorption (CV dye) onto (SA-g-(PAAc-co-VBS)/ZnO) .

The quantitative thermodynamic data of CV dye on the adsorbent surfaces (SA-g-(PAAC-co-VBS)/ZnO). are presented in Table 3-5. The Table 3-5 shows the ΔH values of CV dye is positive indicating that the adsorption process is endothermic reaction. All process of adsorption considered spontaneous from the negative value of ΔG. While, ΔS have positive value for CV dye that refer the interaction of molecules caused random of the total system (Abdalghaffar M. 2020; Adheem 2020).

From results in Table 3-5, the enthalpy change ΔH and entropy change ΔS for adsorption are assumed to be temperature independent The enthalpy of the adsorption ΔH is a measure of the energy barrier that must be overcome by reacting molecules (Sakin 2019; Shumei Zhao 2020.)..

Table 3-5: Thermodynamic functions ΔG, ΔS and, ΔH of CV dye adsorbed on the (SA-g-(PAAC-co-VBS)/ZnO NPs)..

(SA-g-(PAAC-co-VBS)/ZnONPs). adsorbent/ CV adsorbate				
Thermodynamics parameters / T/K	K_e	$-\Delta G^o$/ kJ.mol^{-1}	ΔH^o/ kJ.mol^{-1}	ΔS^o/ J.K^{-1}.mol^{-1}
283	8457.447	21.2765		
293	8936.17	22.1624		75.012
303	9574.468	23.0926		
313	10638.3	24.1289	5.548	

3-5 Effect of different parameters on the adsorption process for the removal TC drug :

3-5-1 Effect of contact time:

100 ml of TC drug solution (100 mg.L^{-1}) is to be prepared and placed in a conical flask with an adsorbent (0.04g/100ml) from (SA-g-(PAAc-co-VBS)/ZnO NPs and put in a shaker water bath at controlled temperature. A spectrophotometer will be used to estimate TC drug concentration spectrophotometrically at the wavelength equivalent to maximal absorbance, . Centrifugation is used to isolate samples at various time intervals. The results are illustrated in and shown in Figures 3-14

The effect of contact time was investigated with the initial TC drug concentrations of 100 mg L^{-1} at 30 ^{o}C. The adsorption capacity as a

function of contact time and initial concentration. The adsorption increased rapidly in the first 30 min, The uptake rate is initially fast until an equilibrium constant value is reached after 2hr of contact(Waleed K. Abdulsahib 2020). When the initial concentration of TC drug increased of 100 mg/L at 30 oC , the adsorption capacity increased from 106.88 to 215.67 mg/g while the removal percentage increased from 42,72 % to 86.26 %. At a higher concentration range the fractional removal is always higher whereas for low concentration ranges the percentage removal of the drug is higher (Yao 2011).

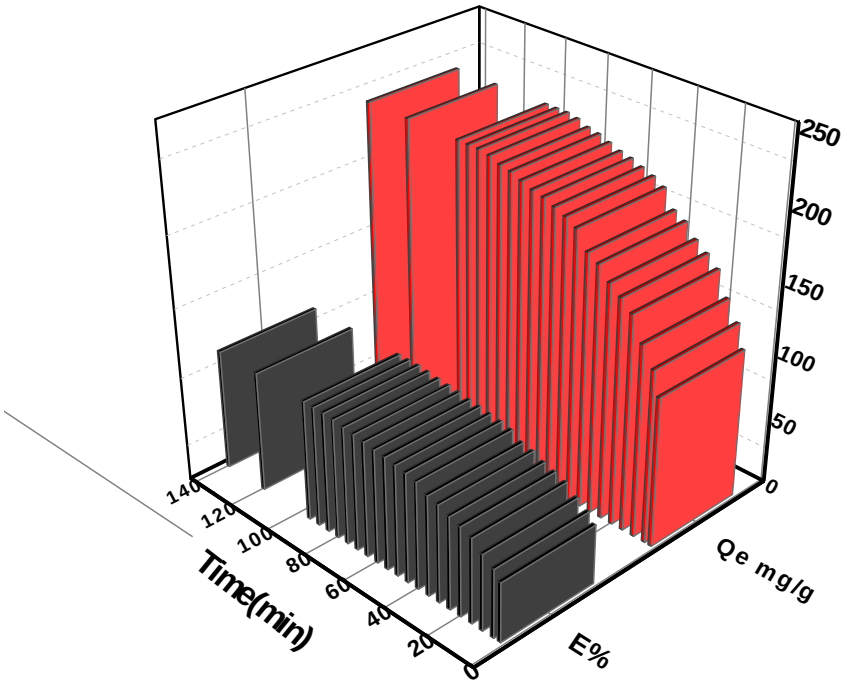

Figure (3-14) Effect of contact time on removal percentage and adsorption capacity for removal of TC drug by (SA-g-(PAAC-co-VBS)/ZnO) at pH 4, Temp. 30 ^{o}C and mass adsorbent 0.04 g .

3-5-2 Effect of dose of adsorbent

The effect of the amount of the adsorbents was necessary to observe the minimum possible amount, which shows the maximum adsorption stoichiometric. The amounts of the adsorbent was varied from (0.01-0.1g/100mL) of (SA-g-(PAAC-co-VBS)/ZnO). The results are illustrated in Table (3-6) and shown in Figures 3-15 .

Table (3-6): Effect of adsorbent dose on the removal percentage of TC drug onto (SA-g-(PAAC-co-VBS)/ZnO).

Co(mg.L^{-1})	W(g)	Abs.	Ce(mg.L^{-1})	E%	Qe mg/g
100	**0.01**	0.7777	39.36022	60.63978	606.3978
100	**0.02**	0.599	29.75269	70.24731	351.2366
100	**0.04**	0.311	14.26882	85.73118	214.328
100	**0.06**	0.211	8.892473	91.10753	151.8459
100	**0.08**	0.123	4.16129	95.83871	119.7984
100	**0.1**	0.0999	2.919355	97.08065	97.08065

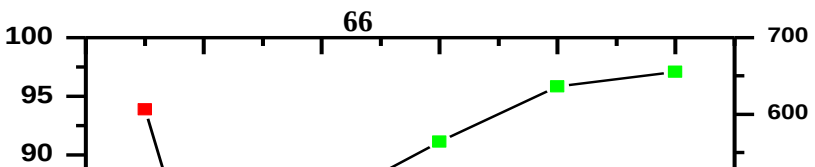

Figure (3-15): Effect of the mass amount of adsorbent (SA-g-(PAAC-co-VBS)/ZnO) on the percent removal and amount of adsorbed TC drug , initial concentration = 100 $mg.L^{-1}$, Temp. = 30°C, contact time 2hr., pH=4.

The effect of the (SA-g-(PAAC-co-VBS)/ZnO) dosage on the percentage % of TC drug adsorbed from aqueous solutions showed that increasing the (SA-g-(PAAC-co-VBS)/ZnO) dosage steadily improved the removal potential of TC drug., increasing the weight of (SA-g-(PAAC-co-VBS)/ZnO)from 0.01 g to 0.1 g are followed via increasing the percentage % adsorbed from 60.639% - 97.085% . Increasing the masses of SA-g-(PAAC-co-VBS)/ZnO) data in decreasing the adsorption capacity of the same series of TC drug from 606.39 – 97.08 mg/g . This may be because increasing the volume of adsorbent produced a larger surface area or more adsorption sites for the drug (Farabi Temel 2020).Further increasing in the quantity of SA-g-(PAAc-co-VBS)/ZnO NPs) utilized from 0.08 g to 0.1

g had no effect on the percentage of TC drug removed (Sotelo, Rodriguez et al. 2012; Layth S. Jasim 2018; Ayad F. Alkaim 2020) .

3-5-3 Effect of pH

pH is one of the basic factors that have to be accounted for when analyzing the adsorption behavior of sorbate sorbent methods. The results are illustrated in Table (3-7) and shown in Figures 3-16

Table (3-7): Effect of solution pH on adsorption TC drug onto (SA-g-(PAAc-co-VBS)/ZnO NPs)

Co(mg/L)	pH	Abs	Ce(mg/L)	E%	Qe (mg/g)
100	3	0.765	38.67742	61.32258	153.3065
100	4	0.311	14.26882	85.73118	214.328
100	6	0.232	10.02151	89.97849	224.9462
100	8	0.0933	2.564516	97.43548	243.5887
100	10	0.0555	0.532258	99.46774	248.6694

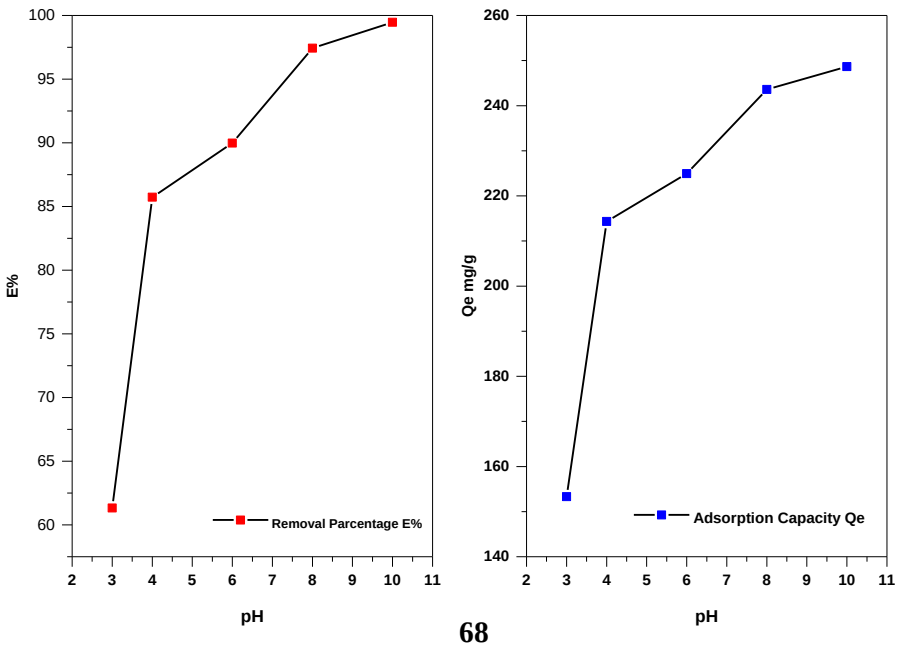

Figure (3-16): Effect of solution pH on the adsorption of TC drug on (SA-g-(PAAc-co-VBS)/ZnO NPs) (Exp. Condition: Temp. = 30°C, contact time 2 h, and pH of solution 4.6).

presents the effect of primary pH solution ranging from about 3 to 10 on the removal capacity of TC drug on SA-g-(PAAc-co-VBS)/ZnO NPs). At the operational conditions of the study (100 ml of 100 mg L^{-1}) TC drug adsorbed on 0.04 g SA-g-(PAAc-co-VBS)/ZnO NPs), 120 min contact time and 120 rpm shaking rate) (Bahareh Tanhaei 2020).The equilibrium sorption efficiency for TC drug was lowest at pH 3 (153.306 mg/g) , maximum adsorption was achieved at pH 10 (248.66 mg/g) (Basam W. Mahde 2018; Salam H. Alwan Altaa 2018; Aljeboree, Alshirifi et al. 2020; Aljeboree;, Alshirifi; et al. 2020).

3-5-4 Effect of temperature

To determine whether the ongoing adsorption process was endothermic or exothermic in nature. The adsorption isotherms were determined for various drug-adsorbent systems. The removal of TC drug has been studied at different temperature (283.15, 293.15, 303.15 and 313.15 K) in the presence of various initial drug concentrations (10-100 $mg.L^{-1}$) . results are illustrated in Tables (3-8), and presented in Figures (3-17) .

Table (3-8)Adsorption isotherm for adsorption of TC drug on the (SA-g-(PAAC-co-VBS)/ZnO) **at different temperatures. (pH 4.6, mass adsorbent 0.04 gm/ 100 ml, contact time 2h).**

C_0 mg.L^{-1}	10 °C			20 °C			30 °C			40°C		
	C_e mg.L^{-1}	Q_e mg.g^{-1}	E%	C_e mg.L^{-1}	Q_e mg.g^{-1}	E %	C_e mg.L^{-1}	Q_e mg.g^{-1}	E%	C_e mg.L^{-1}	Q_e mg.g^{-1}	E%
10	0.236	24.40	97.6	0.112	24.717	98.8	0.0596	24.85	99.4	0.0537	24.86	99.4
20	0.532	48.66	97.3	0.417	48.955	97.9	0.2204	49.44	98.8	0.1182	49.70	99.4
30	2.919	67.70	90.2	1.731	70.672	94.2	1.1935	72.01	96.0	0.2956	74.26	99.0
40	4.827	87.93	87.9	4.000	90.00	90.0	2.9838	92.54	92.5	0.5967	98.50	98.5
50	7.763	105.5	84.4	5.967	110.08	88.0	5.3709	111.5	89.2	1.7903	120.5	96.4
60	10.69	123.2	82.1	8.978	127.55	85.0	6.5591	133.6	89.0	2.6881	143.2	95.5
70	13.67	140.8	80.4	11.34	146.63	83.7	8.3333	154.1	88.0	4.7311	163.1	93.2
80	14.99	162.5	81.2	13.73	165.65	82.8	10.752	173.1	86.5	6.4516	183.8	91.9
90	17.31	181.7	80.7	16.72	183.19	81.4	12.543	193.6	86.0	9.4623	201.3	89.4
100	22.09	194.7	77.9	20.26	199.32	79.7	14.892	212.7	85.1	11.344	221.6	88.6

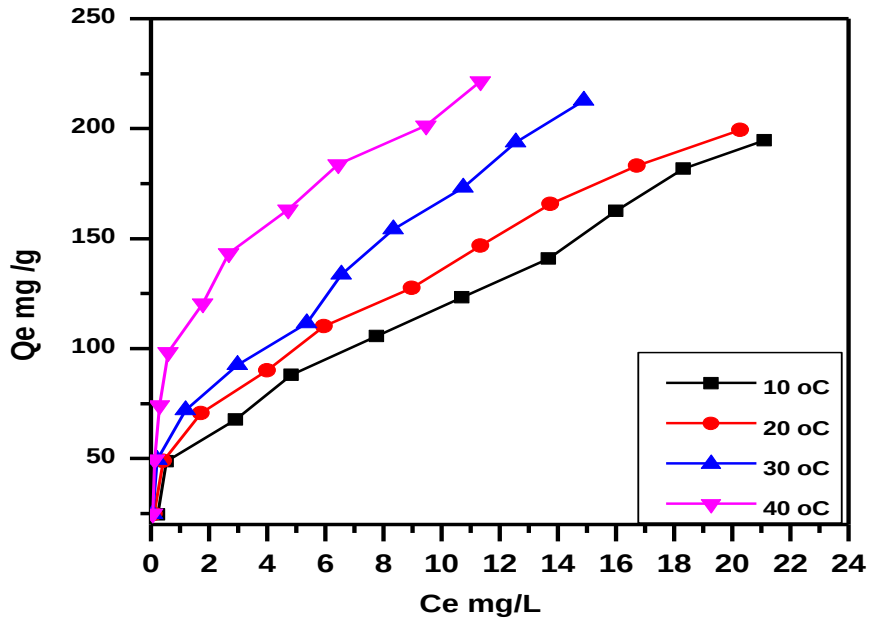

Figure (3-17) Effect of temperature on the adsorption of TC drug on the surface of (SA-g-(PAAc-co-VBS)/ZnO NPs)**. (pH 4.6, mass adsorbent 0.04 gm/ 100 ml).**

The study of the temperature effect on adsorption will also help in the calculation of the basic thermodynamic functions such as Gibbs free energy (ΔG), change enthalpy (ΔH), and change entropy (ΔS) of the adsorption process (Yahya A. Faleh 2021). The equilibrium constant (K_e) of the adsorption process at each temperature, was calculated from the equations (3-2) (A. F. AlKaim 2007):

$$K_e = \frac{(Q_{max}) * Wt\ (0.04\ gm)}{(C_e) * V(0.1L)} \qquad 3-1$$

Where Q_{max} is the amount adsorbed in ($mg.gm^{-1}$), C_e is the equilibrium concentration of the adsorbent expressed in ($mg.L^{-1}$), 0.04 gm represents the weight of the (SA-g-(PAAc-co-VBS)/ZnO NPs) adsorbent, and 0.1L represents the volume of the TC drug solution used in the adsorption process (Huda Salim Al-Niaeem 2022). The change in the free energy could be determined from the equation (3-2) :(Huda Salim Al-Niaeem 2022)

$$\Delta G = -RT \ln K_e \qquad 3-2$$

Where ΔG: Gibbs free energy ($J.K^{-1}.mol.^{-1}$), R is the gas constant (8.314 $J.K^{-1}.mole^{-1}$), T is the absolute temperature in Kelvin.

The enthalpy of adsorption may be obtained from the following equation (3-3) (Abdalghaffar M Osman 2020):

$$\ln X_m = -\frac{\Delta H^{\circ}}{RT} + Cons. \qquad 3-3$$

When $X_{m:}$ is the maximum value of adsorption at a certain value of equilibrium concentration (Ce). Table (3-9) gives X_m values at different temperatures TC drug. Plotting $\ln X_m$ versus (1/T) should produce a straight line with a slope -ΔH/R as shown in Figures (3-18). The value of ΔH and ΔS can be calculated from the slope and intercept respectively (Nasseh 2019).

Table (3-9) Maximum adsorption quantity Xm values of TC drug onto (SA-g-(PAAc-co-VBS)/ZnO NPs) surfaces at different temperatures.

T(K)	1000/T(K^{-1})	C_e = 11.2	
		X_m	ln X_m
283	3.5335	130	4.867534
293	3.4129	142	4.955827
303	3.3003	179	5.187386
313	3.1948	220	5.393628

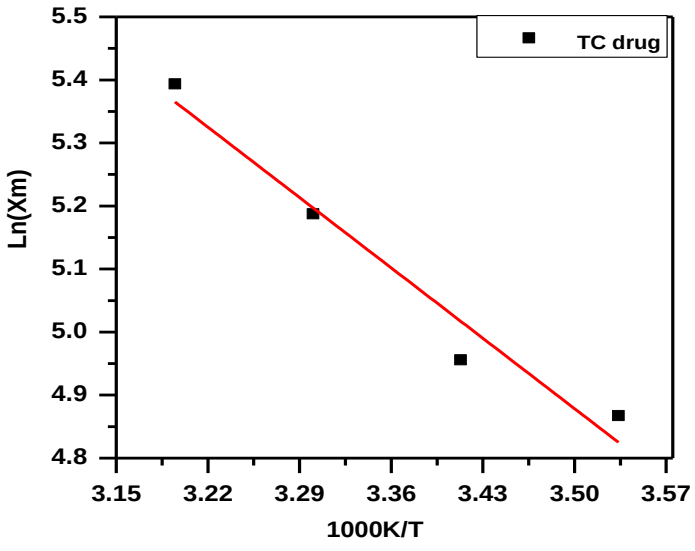

Figure (3-18) Plot ln X_m against the absolute temperature. of the adsorption TC drug onto (SA-g-(PAAc-co-VBS)/ZnO NPs).

The negative value of ΔG^o indicates the feasibility and spontaneity of the adsorption process. The value of ΔS^o had been estimated to be so large which indicated an increase of entropy as a result of adsorption. Before adsorption, the ions of drug near the adsorbent surface were in ordered form than in the subsequent adsorbed state and the ratio of free drug ions to the interacting drug ions with the adsorbent will be higher than in the adsorbed state. As a result the distribution of rotational and translational energy will increase with increasing adsorption by producing a positive entropy value and at solid–liquid interface there will be increased randomness(Sakin 2019; Shumei Zhao 2020.).

The Table 3.10 show the ΔH values of TC drug is positive indicating that the adsorption process is endothermic reaction. All process of adsorption considered spontaneous from the negative value of ΔG. While, ΔS have positive value for TC drug that refer the interaction of molecules caused random of the total system (Abdalghaffar M. 2020; Adheem 2020).

Table 3.10: Thermodynamic functions ΔG, ΔS and, ΔH of TC drug adsorbed on the (SA-g-(PAAc-co-VBS)/ZnO NPS)**..**

(SA-g-(PAAC-co-VBS)/ZnO). adsorbent/ TC adsorbate				
Thermodynamics parameters **T/K**	**K_e**	**$-\Delta G^o$/ kJ.mol^{-1}**	**ΔH^o/ kJ.mol^{-1}**	**ΔS^o/ J.K^{-1}.mol^{-1}**
283	11607.14	-22.0213	13.26	86.97275

293	12678.57	-23.0145		
303	15982.14	-24.3833		
313	19642.86	-25.7248		

3-6 Effect of different parameters on the adsorption process for the removal PH :

3-6-1 Effect of contact time:

100 ml of PH solution (100 mg.L^{-1}) is to be prepared and placed in a conical flask with an adsorbent (0.04g/100ml) from (SA-g-(PAAc-co-VBS)/ZnO NPs and put in a shaker water bath at controlled temperature. A spectrophotometer will be used to estimate PH concentration spectrophotometrically at the wavelength equivalent to maximal absorbance, . Centrifugation is used to isolate samples at various time intervals. The results are illustrated in and shown in Figures 3-19

The effect of contact time was investigated with the initial PH concentrations of 100 mg L^{-1} at 30 ^{o}C. The adsorption capacity as a

function of contact time and initial concentration. The adsorption increased rapidly in the first 40 min, The uptake rate is initially fast until an equilibrium constant value is reached after 2hr of contact(Waleed K. Abdulsahib 2020). When the initial concentration of PH increased of 100 mg/L at 30 oC , the adsorption capacity increased from 79.45 to 203.44 mg/g while the removal percentage increased from 15.90 % to 81.34 % and the same order . At a higher concentration range the fractional removal is always higher whereas for low concentration ranges the percentage removal of the PH is higher (Yao 2011).

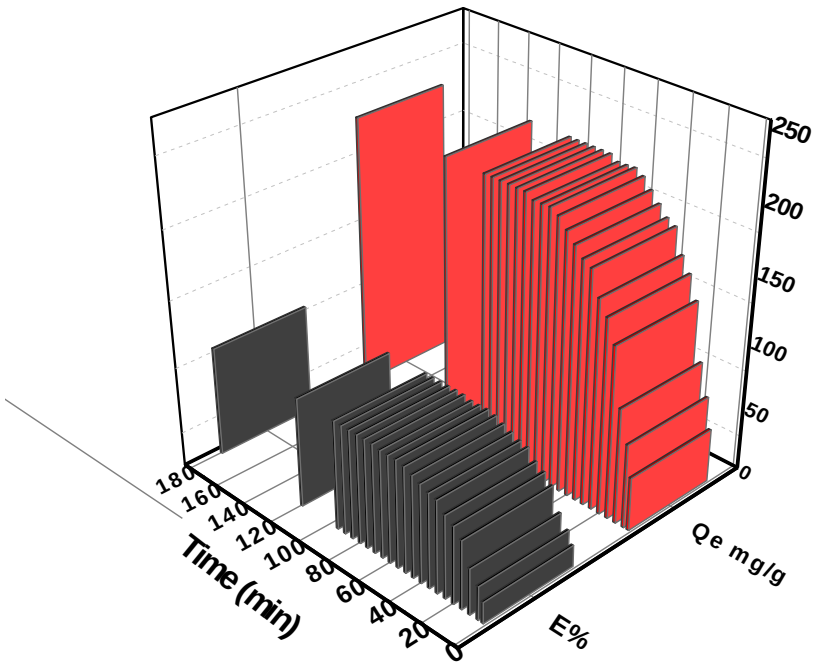

Figure (3-19) Effect of contact time on removal percentage and adsorption capacity for removal of PH by (SA-g-(PAAc-co-VBS)/ZnO NPs) at pH 4.6, Temp. 30 ^{o}C and mass adsorbent 0.04 g .

3-6-2 Effect of dose of adsorbent

The effect of the amount of the adsorbents was necessary to observe the minimum possible amount, which shows the maximum adsorption stoichiometric. The amounts of the adsorbent was varied from (0.01-0.1g/100mL) of (SA-g-(PAAc-co-VBS)/ZnO NPs). The results are illustrated in Table (3-11) and shown in Figure 3-20.

Table (3-11): Effect of adsorbent dose on the removal percentage of PH onto (SA-g-(PAAc-co-VBS)/ZnO NPs).

Co(mg.L^{-1})	W(g)	Abs.	Ce(mg.L^{-1})	E%	Qe mg/g
100	**0.01**	0.444	51.28169	48.71831	487.1831
100	**0.02**	0.276	27.61972	72.38028	361.9014
100	**0.04**	0.212	18.60563	81.39437	203.4859
100	**0.06**	0.166	12.12676	87.87324	146.4554
100	**0.08**	0.144	9.028169	90.97183	113.7148
100	**0.1**	0.122	5.929577	94.07042	94.456

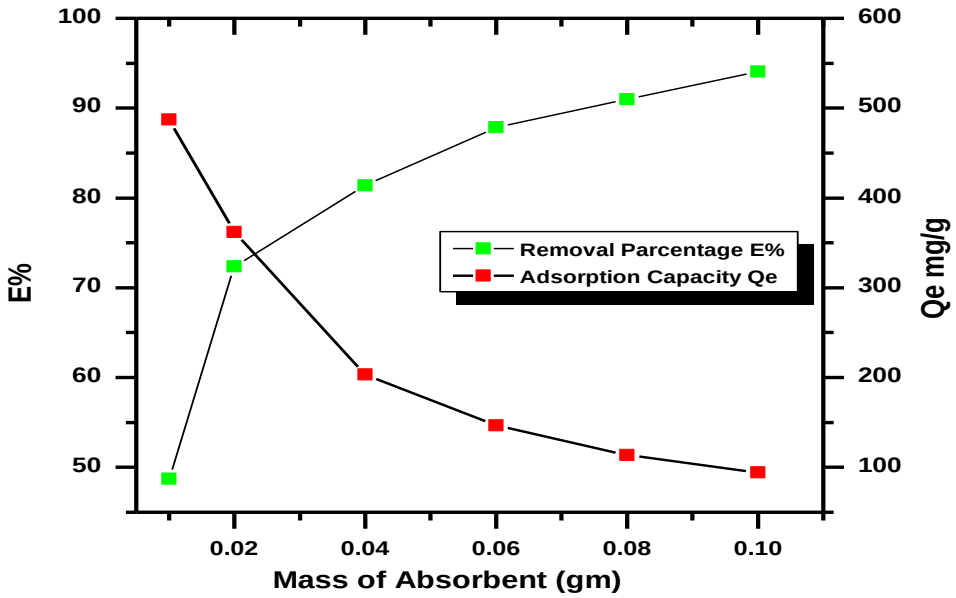

Figure (3-20): Effect of the mass amount of adsorbent (SA-g-(PAAC-co-VBS)/ZnO) on the percent removal and amount of adsorbed PH , initial concentration = 100 mg.L^{-1}, Temp. = 30°C, contact time 2hr., pH=4.6.

The effect of the (SA-g-(PAAC-co-VBS)/ZnO) dosage on the percentage % of PH adsorbed from aqueous solutions showed that increasing the (SA-g-(PAAC-co-VBS)/ZnO) dosage steadily improved the removal potential of PH., increasing the weight of (SA-g-(PAAC-co-VBS)/ZnO)from 0.01 g to 0.1 g are followed via increasing the percentage % adsorbed from (48.71% - 94.05%) . Increasing the masses of SA-g-(PAAC-co-VBS)/ZnO) data in decreasing the adsorption capacity of the same series of PH from 487.1831- 94.456 mg/g . This may be because increasing the volume of adsorbent produced a larger surface area or more adsorption sites for the drug (Sotelo, Rodriguez et al. 2012; Layth S. Jasim 2018; Ayad F. Alkaim 2020; Farabi Temel 2020) .

3-6-3 Effect of pH

pH is one of the basic factors that have to be accounted for when analyzing the adsorption behavior of sorbate sorbent methods. The results are illustrated in Table (3-12) and shown in Figures 3-21

Table (3-12): Effect of solution pH on adsorption PH onto (SA-g-(PAAC-co-VBS)/ZnO)

Co(mg/L)	pH	Abs	Ce(mg/L)	E%	Qe (mg/g)
100	3	0.544	65.3662	34.6338	86.58451
100	4	0.444	51.28169	48.71831	121.7958
100	6	0.212	18.60563	81.39437	203.4859
100	8	0.1111	4.394366	95.60563	239.0141
100	10	0.0999	2.816901	97.1831	242.9577

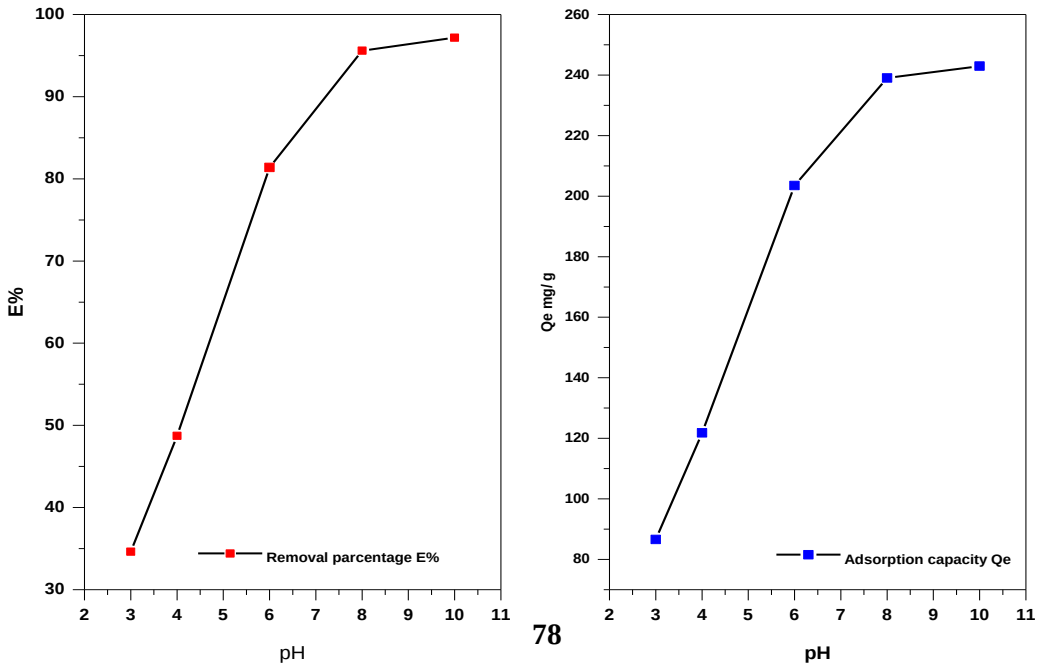

Figure (3-21): Effect of solution pH on the adsorption of PH on (SA-g-(PAAC-co-VBS)/ZnO) (Exp. Condition: Temp. = 30°C, contact time 2 h, and pH of solution 4.6).

presents the effect of primary pH solution ranging from about 3 to 10 on the removal capacity of PH on SA-g-(PAAc-co-VBS)/ZnO NPs). At the operational conditions of the study (100 ml of 100 mg L^{-1}) PH adsorbed on 0.04 g SA-g-(PAAc-co-VBS)/ZnO NPs), 2hr contact time and 120 rpm shaking rate) (Bahareh Tanhaei 2020).The equilibrium sorption efficiency for PH was lowest at pH 3 (86.85 mg/g), maximum adsorption was achieved at pH 10 (242.95 mg/g) (Basam W. Mahde 2018; Salam H. Alwan Altaa 2018; Aljeboree, Alshirifi et al. 2020; Aljeboree;, Alshirifi; et al. 2020).

3-6-4 Effect of temperature

To determine whether the ongoing adsorption process was endothermic or exothermic in nature. The adsorption isotherms were determined for various pollutant-adsorbent systems. The removal of PH has been studied at different temperature (283.15, 293.15, 303.15 and 313.15 K) in the presence of various initial PH concentrations (10-100 $mg.L^{-1}$) . results are illustrated in Tables (3-9), and presented in Figures (3-13) .

Table (3-13)Adsorption isotherm for adsorption of PH on the (SA-g-(PAAC-co-VBS)/ZnO) **at different temperatures. (pH 4.6, mass adsorbent 0.04 gm/ 100 ml, contact time 2h).**

C_0 mg.L^{-1}	10 ºC			20 ºC			30 ºC			40ºC		
	C_e mg.L^{-1}	Q_e mg.g^{-1}	E%	C_e mg.L^{-1}	Q_e mg.g^{-1}	E %	C_e mg.L^{-1}	Q_e mg.g^{-1}	E%	C_e mg.L^{-1}	Q_e mg.g^{-1}	E%
10	0.3239	24.190	96.7	0.295	24.260	97.0	0.1549	24.612	98.4	0.014	24.964	99.5
20	1.1408	47.147	94.2	1.000	47.5	95	0.7183	48.204	96.4	0.295	49.260	98.5
30	2.4084	68.978	91.9	1.732	70.669	94.2	1.5633	71.091	94.7	0.859	72.852	97.1
40	7.0563	82.359	82.3	5.647	85.880	85.8	4.2394	89.401	89.4	2.126	94.683	94.6
50	9.0845	102.28	81.8	7.211	106.97	85.5	5.9295	110.17	88.1	4.380	114.04	91.2
60	10.154	124.61	83.0	8.605	128.48	85.6	7.6197	130.95	87.3	5.788	135.52	90.3
70	13.014	142.46	81.4	11.56	146.09	83.4	10.774	148.06	84.6	7.478	156.30	89.3
80	15.169	162.07	81.0	13.67	165.80	82.9	12.971	167.57	83.7	12.12	169.68	84.8
90	16.915	182.71	81.2	16.21	184.47	81.9	15.929	185.17	82.3	15.36	186.58	82.9
100	24.239	189.40	75.7	21.14	197.14	78.8	18.605	203.48	81.3	16.91	207.71	83.0

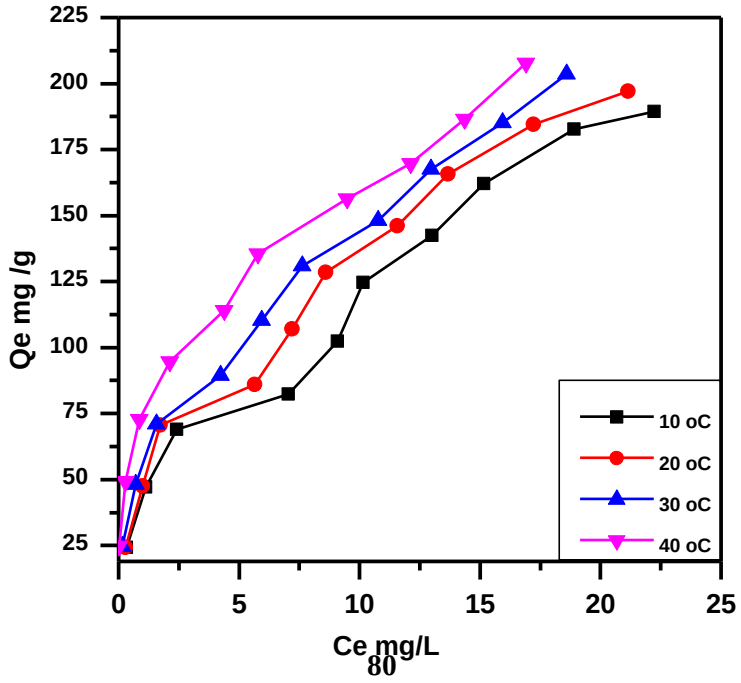

Figure (3-22) Effect of temperature on the adsorption of PH on the surface of (SA-g-(PAAc-co-VBS)/ZnO NPs)**. (pH 4.6, mass adsorbent 0.04 gm/ 100 ml).**

The study of the temperature effect on adsorption will also help in the calculation of the basic thermodynamic functions such as Gibbs free energy (ΔG), change enthalpy (ΔH), and change entropy (ΔS) of the adsorption process (Yahya A. Faleh 2021). The equilibrium constant (K_e) of the adsorption process at each temperature, was calculated from the equations (3-2) (A. F. AlKaim 2007):

$$K_e = \frac{(Q_{max}) * Wt\ (0.04\ gm)}{(C_e) * V(0.1L)} \qquad 3-1$$

Where Q_{max} is the amount adsorbed in ($mg.gm^{-1}$), C_e is the equilibrium concentration of the adsorbent expressed in ($mg.L^{-1}$), 0.04 gm represents the weight of the (SA-g-(PAAC-co-VBS)/ZnO) adsorbent, and 0.1L represents the volume of the PH solution used in the adsorption process (Huda Salim Al-Niaeem 2022). The change in the free energy could be determined from the equation (3-2) :(Huda Salim Al-Niaeem 2022)

$$\Delta G = -RT \ln K_e \qquad 3-2$$

Where ΔG: Gibbs free energy ($J.K^{-1}.mol.^{-1}$), R is the gas constant (8.314 $J.K^{-1}.mole^{-1}$), T is the absolute temperature in Kelvin.

The enthalpy of adsorption may be obtained from the following equation (3-3) (Abdalghaffar M Osman 2020):

$$\ln X_m = -\frac{\Delta H^{\circ}}{RT} + Cons. \qquad 3-3$$

When $X_{m:}$ is the maximum value of adsorption at a certain value of equilibrium concentration (Ce). Table (3-11) gives X_m values at different temperatures PH. Plotting $\ln X_m$ versus (1/T) should produce a straight line with a slope -ΔH/R as shown in Figures (3-14). The value of ΔH and ΔS can be calculated from the slope and intercept respectively (Nasseh 2019).

Table (3-14) Maximum adsorption quantity Xm values of PH onto (SA-g-(PAAc-co-VBS)/ZnO NPs) surfaces at different temperatures.

T(K)	1000/T(K^{-1})	C_e = 17	
		X_m	ln X_m
283	3.5335	169	5.129899
293	3.4129	182	5.204007
303	3.3003	194	5.267858
313	3.1948	205	5.32301

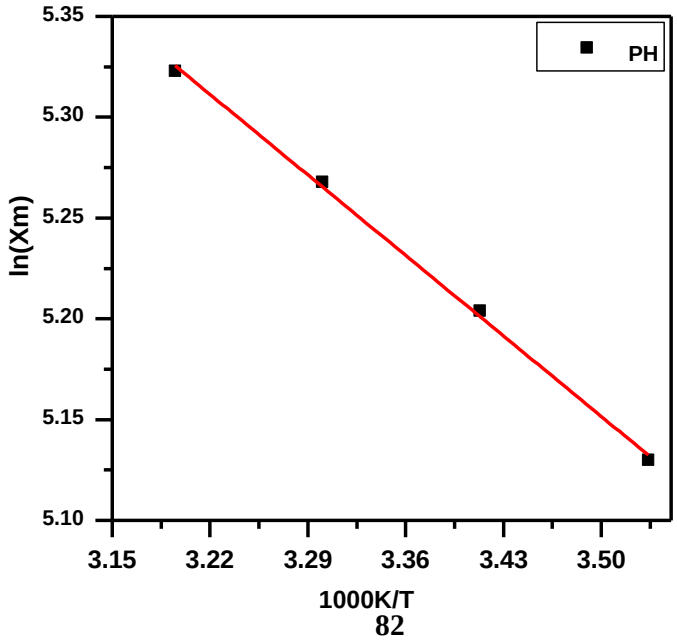

Figure (3-23) Plot ln X_m against the absolute temperature. of the adsorption PH onto (SA-g-(PAAc-co-VBS)/ZnO NPs).

The negative value of ΔG^o indicates the feasibility and spontaneity of the adsorption process. The value of ΔS^o had been estimated to be so large which indicated an increase of entropy as a result of adsorption. Before adsorption, the ions of pollutant near the adsorbent surface were in ordered form than in the subsequent adsorbed state and the ratio of free drug ions to the interacting PH ions with the adsorbent will be higher than in the adsorbed state. As a result the distribution of rotational and translational energy will increase with increasing adsorption by producing a positive entropy value and at solid–liquid interface there will be increased randomness(Sakin 2019; Shumei Zhao 2020.).

The Table 3-15 shows the ΔH values of PH is positive indicating that the adsorption process is endothermic reaction. All process of adsorption considered spontaneous from the negative value of ΔG. While, ΔS have positive value for PH that refer the interaction of molecules caused random of the total system (Abdalghaffar M. 2020; Adheem 2020).

Table 3.15: Thermodynamic functions ΔG, ΔS and, ΔH of PH adsorbed on the (SA-g-(PAAC-co-VBS)/ZnO)..

(SA-g-(PAAC-co-VBS)/ZnO). adsorbent/ PH adsorbate				
Thermodynamics parameters / T/K	K_e	$-\Delta G^o$/ kJ.mol^{-1}	ΔH^o/ kJ.mol^{-1}	ΔS^o/ J.K^{-1}.mol^{-1}
283	9941.176	21.6568		
293	10705.88	22.6026		
303	11411.76	23.5348		
313	12058.82	24.4551	4.742	59.43013

3-7 Adsorption Isotherms

3-7-1 Freundlich Isotherm:

The Freundlich isotherm is defined through the following equation 3-4 (Freundlich H 1939).

$$q_e = K_f C_e^{1/n} \qquad (3-4)$$

qe: Amount adsorbed per unit weight of adsorbent at equilibrium (mg/g), (mol/g), Ce: Equilibrium concentration of adsorbate in solution after adsorption (mg.L^{-1}), (mol/L), K_f: Empirical Freundlich constant or capacity factor (L/mg) or the dye quantity adsorbed for unit equilibrium

concentration, 1/n: Freundlich exponent, if the value of n is equal to unity, the adsorption is linear; if below to unity, then adsorption process is chemical and if the value is above unity, then adsorption is a physical process (Kim 2019; Yongde Liu 2019).

3-7-2 Langmuir Isotherm:

The Langmuir isotherm is mostly used for pollutants adsorption from liquid solutions. The nature of the adsorption process was derived by Langmuir alternative equation 3-5 (Langmuir 1918)

$$q_e = \frac{q_m K_L C_e}{1 + K_L C_e} \qquad (3-5)$$

qe: amount adsorbed per unit weight of adsorbent at equilibrium (mg/g), Ce: equilibrium concentration of adsorbent in solution after adsorption ($mg.L^{-1}$), qm: Empirical Langmuir constant which represents maximum adsorption capacity (mg/g) of the total number of surface sites per mass of adsorbent and it may vary among different compounds because of differences in adsorbate sizes, K_L: empirical Langmuir constant (L/mg) or the equilibrium constant of the adsorption reaction (Zaheer 2019).

The coefficients of determination (R^2) and isotherm parameters from the nonlinear regressive method were listed in Table (3-15 , 3-16 &3-17). A comparison of nonlinear fitted curves from experimental data and two different isotherms at 30 ^oC are shown in Figures (3-24 , 3-25 &3-26).

A plot of q_e versus C_e Figures (3-24 , 3-25 &3-26) where the values of K_F and 1/n are obtained from the intercept and slope of the linear regressions (Table 3-16 to 3-18).

the correlation coefficient, R^2 values for the Freundlich model at tempracher 30 oC are (R^2=0.9969) , (R^2=0.9899) and (R^2=0.9697) of

CV, TC and PH onto (SA-g-(PAAC-co-VBS)/ZnO) respectively (E. Alipanahpour Dil 2015; Nadavala Siva Kumar 2019).

Table 3-16: different parameters isotherm models for the adsorption study of CV dye on to (SA-g-(PAAc-co-VBS)/ZnO NPs).

(SA-g-(PAAC-co-VBS)/ZnO)			
Freundlich	K_f	152.0695	±8.3613
	1/n	0.3917	±0.0133
	R^2	0.9969	
Langmuir	q_m (mg/g)	1056.623	±122.632
	K_L (L/mg)	0.05124	±0.01907
	R^2	0.9185	

Table 3-17: different parameters isotherm models for the adsorption study of TC drug on to (SA-g-(PAAc-co-VBS)/ZnO NPs) .

(SA-g-(PAAC-co-VBS)/ZnO)			
Freundlich	K_f	50.4058	±2.9264
	1/n	0.4675	0.0234±
	R^2	0.9899	
Langmuir	q_m (mg/g)	259.156	±33.4566

	K_L (L/mg)	0.1465	±0.0474
	R^2	0.93009	

Table 3-18: different parameters isotherm models for the adsorption study of PH on to (SA-g-(PAAc-co-VBS)/ZnO NPs).

(SA-g-(PAAc-co-VBS)/ZnO NPs)			
Freundlich	K_f	60.9307	±5.6381
	1/n	0.4444	±0.0408
	R^2	0.9697	
Langmuir	q_m (mg/g)	282.599	±53.845
	K_L (L/mg)	0.1581	±0.0716
	R^2	0.8862	

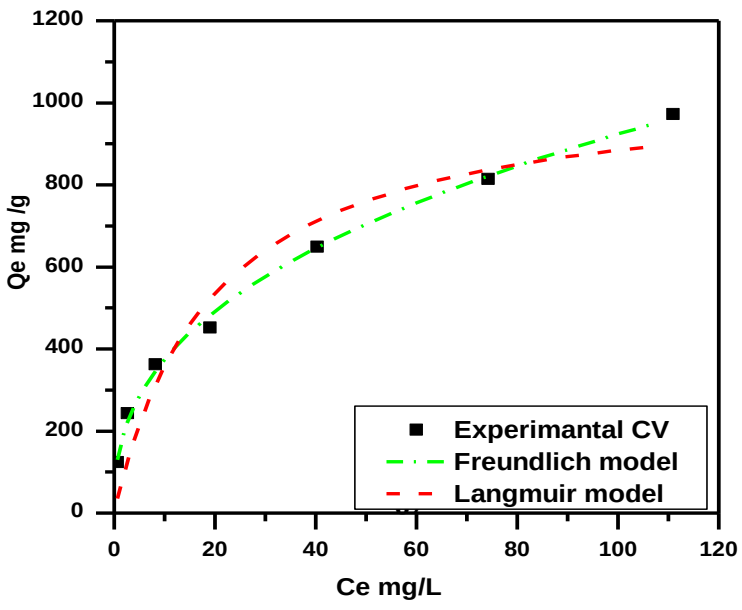

Figure 3-24: Several adsorptions models nonlinear fit of adsorption CV onto (SA-g-(PAAc-co-VBS)/ZnO NPs) at temperatures 30 oC , conc. = 200 mg. L^{-1}, pH of solution 6.6 and weight of surface 0.04 g/100ml).

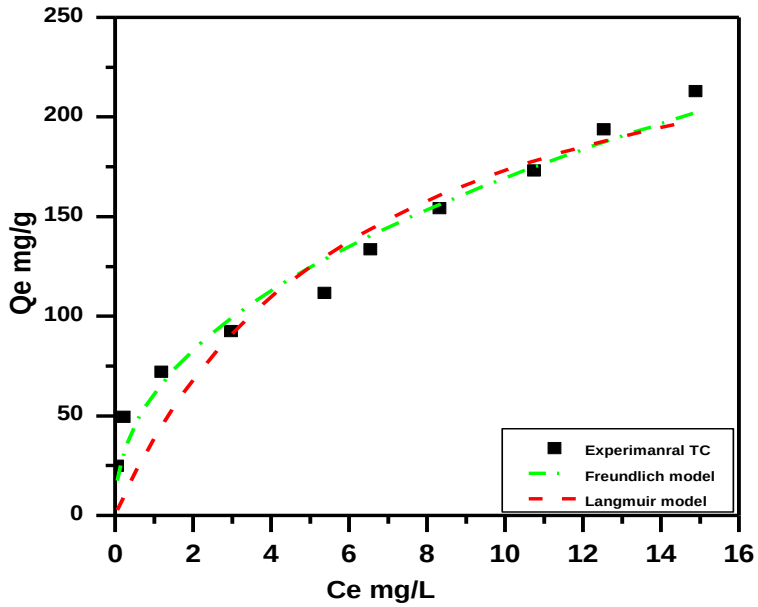

Figure 3-25: Several adsorptions models nonlinear fit of adsorption TC onto (SA-g-(PAAC-co-VBS)/ZnO) at temperatures 30 oC , conc. = 100 mg. L^{-1}, pH of solution 4.6 and weight of surface 0.04 g/100ml).

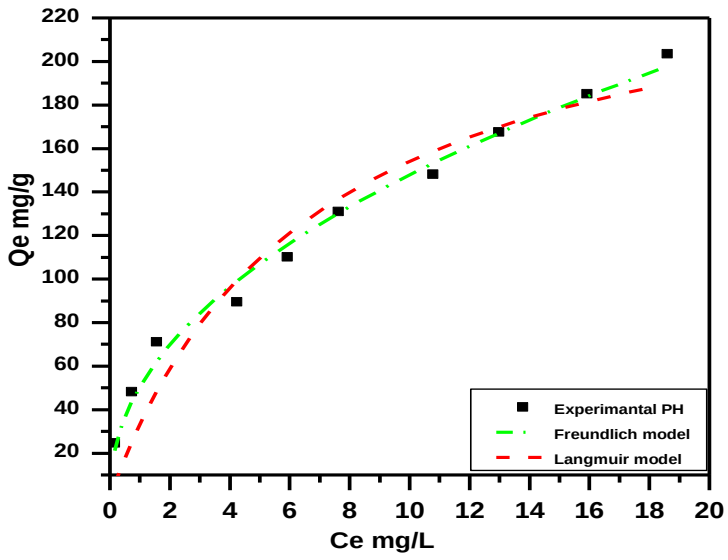

Figure 3-26: Several adsorptions models nonlinear fit of adsorption PH onto (SA-g-(PAAC-co-VBS)/ZnO) at temperatures 30 oC , conc. = 100 mg. L^{-1}, pH of solution 4.6 and weight of surface 0.04 g/100ml).

3-8 Kinetic study

The mechanism of adsorbate–adsorbent interaction is best described by studying the rate expression for dye adsorption on (SA-g-(PAAC-co-VBS)/ZnO); this can be shown by examining the effect of time on the adsorption process and fitting the experimental findings to different conventional models. The agreed function for model suitability for good prediction of experimental data at different times , which is validated by a low relative error among the orchid and experimental adsorption potential (Abdalghaffar M Osman 2020). The rate expression can be calculated by analyzing the adsorption data with three different kinetic models: Lagergren first-order ,pseudo-second-order , and Chemisorption (Aseel M. Aljeboree 2021) . The fitting results are seen in Table 3-19,3-20 and 3-21 .

A simple kinetic description of adsorption (pseudo-first-order equation) is as follows :

$$q_t=q_e[1-\exp(k_f t)] \quad (3\text{-}6)$$

where qt is the total amount of adsorbate adsorbed at time t (mg^{-1}), qe is the equilibrium adsorption potential (mg g^{-1}), kf is the pseudo-first-order rate constant (min^{-1}), and t is the contact time (min).

Lagergren's usability deviates from its linear form, according to the results. This means that the new kinetic model is inadequate for forecasting pseudo-first order sorption kinetics on (SA-g-(PAAC-co-VBS)/ZnO). We wanted to apply the experimental data to models because the first-order kinetic model failed to represent the sorption effects (Saeed U J 2020).

The following is an example of a pseudo-second-order equation based on adsorption equilibrium capacity:

$$qt = \frac{K2qe2t}{1+K2qet} \qquad (3\text{-}7)$$

k_2 and qe were estimated from qt versus t; shows the pseudo-second-order plot; it can be seen that the sorption data maintains its linear profile over the entire period; however, higher values of correlation coefficients and qe determined using the pseudo-second-order model were more compatible with the experimental data (Del Mar Orta 2019; Shumei Zhao 2020.).

Both of these findings indicate that the model can be used to describe adsorption data over time. Furthermore, the model supports the theory that the sorption process is caused by chemisorption.

The non-linear structure of the Elovich (Chemisorption kinetic formula) [49] model equation is usually written as:

$$qt = \frac{1}{\beta} 1\beta \ln(\alpha\beta) + \frac{1}{\beta} \ln t \qquad (3-8)$$

The kinetic data from the Elovich model. The nonlinear plots of qt versus t for various initial concentrations demonstrated good consistency between the experimental and calculated qe values. Furthermore, the pseudo-second-order kinetic model has higher correlation coefficients than the Chemisorption model. As a result, the adsorption is best suited to

the pseudo-second-order model than the Chemisorption kinetic model. Adsorption kinetics are associated with the intraparticle diffusion concept.

The gap in three pollution adsorption on an (SA-g-(PAAC-co-VBS)/ZnO) with shaking time (0–240 min) and initial solution concentration (100 mg/L) is visualized in Figure (3-27,3-28 and 3-29). Although pollutant adsorption was initially very high, the rate of adsorption slowed over time and gradually reached a constant value, as shows in Figure (3-28,3-29 and 3-20) (equilibrium time). As the concentration rose, this process was gradually repeated. The initial faster rate may be due to the adsorbents' exposed surface region being available (Kim 2019; Nasseh 2019; Arif Chowdhury 2020).

Table 3-19:Pseudo first-order, pseudo-second-order, and Elovich including correlation coefficients for (CV dye) adsorption onto (SA-g-(PAAc-co-VBS)/ZnO NPs).

Type	Parameters	**Value**	**Stand. Error**	***R*2**
Pseudo-First-order	q*e* (mg g^{-1})	463.86	6.659	0.9774
	k*f* (min^{-1})	0.0508	0.003	
pseudo-second-order	q*e* (mg g^{-1})	538.69	19.83	0.9311
	ks (gmg^{-1} min^{-1})	0.063	0.0089	
Elovich	α (mg g^{-1} min^{-1})	268.60	24.042	0.8491
	β (g min^{-1})	1.155	0.151	

Table 3-20:Pseudo first-order, pseudo-second-order, and Elovich including correlation coefficients for (TC drug) adsorption onto (SA-g-(PAAc-co-VBS)/ZnO NPs).

Type	Parameters	Value	Stand. Error	*R*2
Pseudo-First-order	qe (mg g^{-1})	206.185	6.464	0.9566
	kf (min^{-1})	0.127	0.0233	
pseudo-second-order	qe (mg g^{-1})	218.954	5.444	0.8555
	ks (gmg^{-1} min^{-1})	0.2403	0.0410	
Elovich	α (mg g^{-1} min^{-1})	86.537	7.054	0.8123
	β (g min^{-1})	4.5677	1.301	

Table 3-21:Pseudo first-order, pseudo-second-order, and Elovich including correlation coefficients for (PH) adsorption onto (SA-g-(PAAc-co-VBS)/ZnO NPs).

Type	Parameters	Value	Stand. Error	*R*2
Pseudo-First-order	qe (mg g^{-1})	20.423	1.6308	0.9894
	kf (min^{-1})	0.0615	0.0022	
pseudo-second-order	qe (mg g^{-1})	234.45	4.256	0.9567
	ks (gmg^{-1} min^{-1})	0.0810	0.0067	
Elovich	α (mg g^{-1} min^{-1})	104.792	8.241	0.8844
	β (g min^{-1})	1.4958	0.1988	

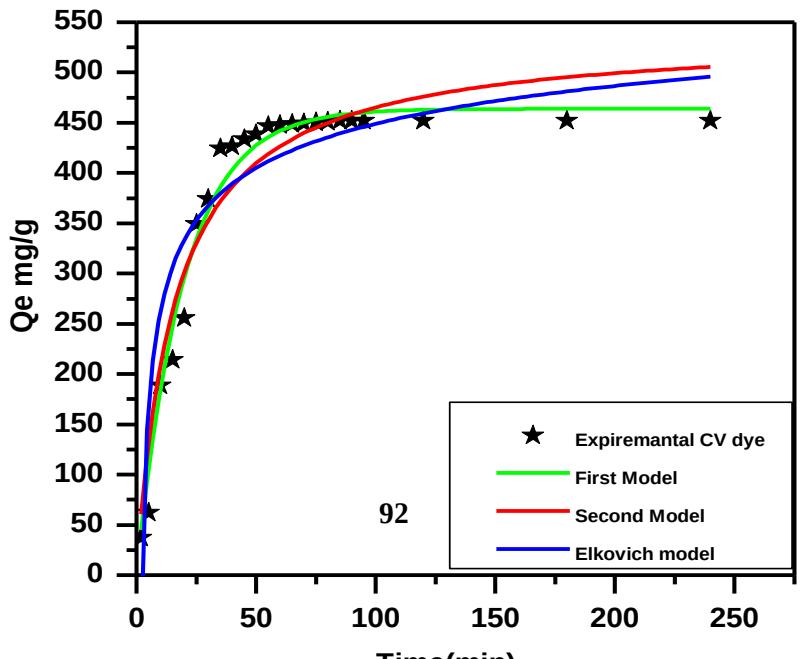

Figure 3-27 . Adsorption rate curve models fitted to experimental CV dye adsorption on the surface of (SA-g-(PAAc-co-VBS)/ZnO NPs). a) first-order kinetic; b) second-order kinetic; and c) Elkovich kinetic (pH 6.6, Temp. 30 oC , mass dosage 0.04 g).

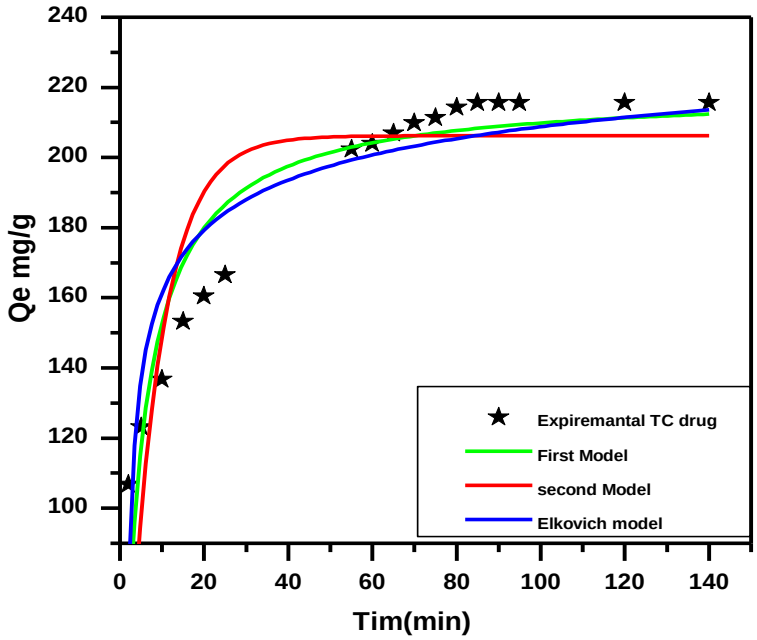

Figure 3-28 . Adsorption rate curve models fitted to experimental TC drug adsorption on the surface of (SA-g-(PAAc-co-VBS)/ZnO NPs). a) first-order kinetic; b) second-order kinetic; and c) Elkovich kinetic (pH 4.6, Temp. 30 oC , mass dosage 0.04 g).

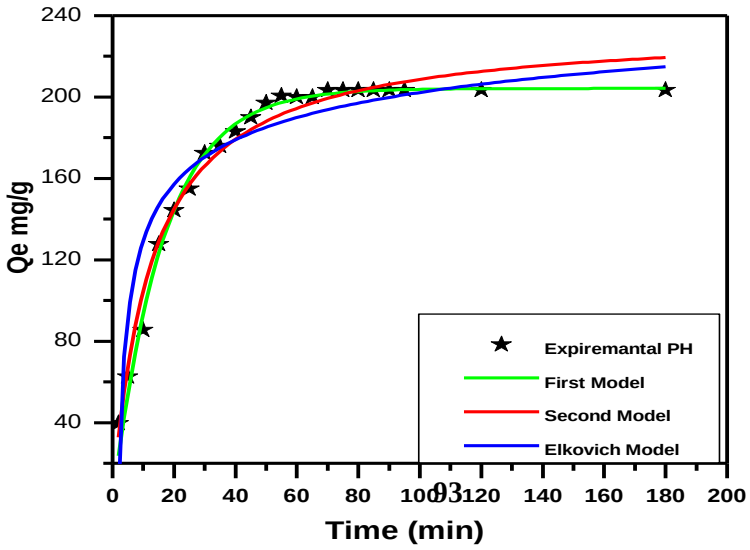

Figure 3-29 . Adsorption rate curve models fitted to experimental PH adsorption on the surface of (SA-g-(PAAc-co-VBS)/ZnO NPs). a) first-order kinetic; b) second-order kinetic; and c) Elkovich kinetic (pH 4.6, Temp. 30 oC , mass dosage 0.04 g).

3-9 Removal of laboratory sample Aqueous Pollutants by Using (SA-g-(PAAc-co-VBS)/ZnO NPs).

A laboratory sample 100 mL of pollutants(dyes and drugs) with a refry concentration were using in this study, then added to a conical flask (Erlenmeyer) in the presence of 0.04 g from prepared (SA-g-(PAAc-co-VBS)/ZnO NPs)., after that the mixture were putting in a Shaker water bath for 1 hr, after that the supernatant were separated by centrifuge and measured the remaining concentration by using UV-Visible spectrophotometer at the λmax 595nm, 272nm and 270 nm for CV , TC and PH at the same order (Xiong, Di et al. 2020; Shoaib Nawa 2022) the result show in figure (3-30 , 3-31 and 3-32).

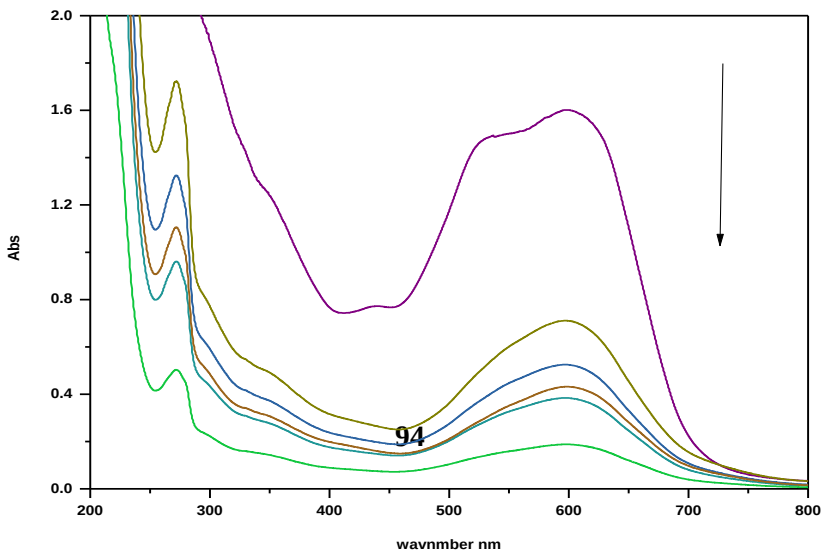

Figure (3-30): Spectra of removal pollutants (dyes and drugs) by using (SA-g-(PAAc-co-VBS)/ZnO NPs) , (Exp. Condition: Temp. = 30°C, contact time 2 h, and mass absorbent 0.04 g).

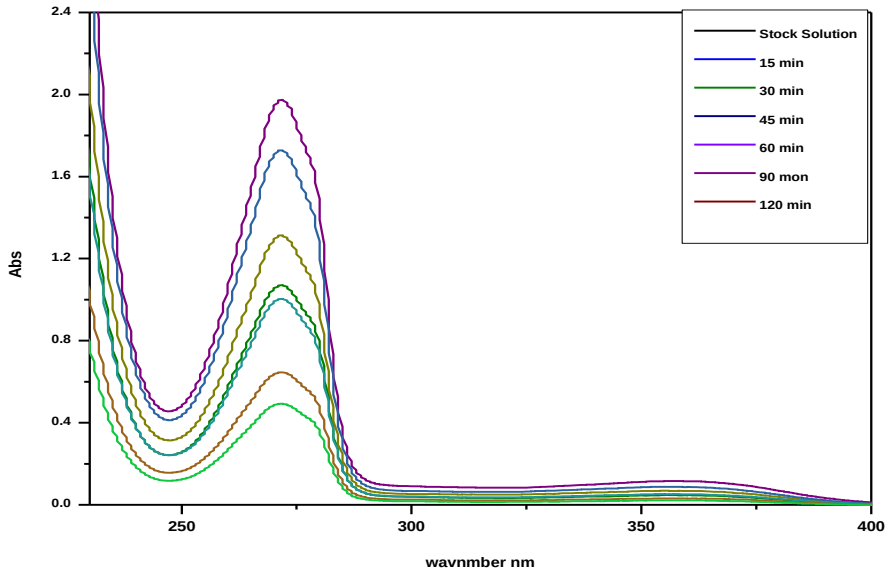

Figure (3-31): Spectra of removal pollutants (drugs) by using (SA-g-(PAAc-co-VBS)/ZnO NPs) , (Exp. Condition: Temp. = 30°C, contact time 2 h, and mass absorbent 0.04 g).

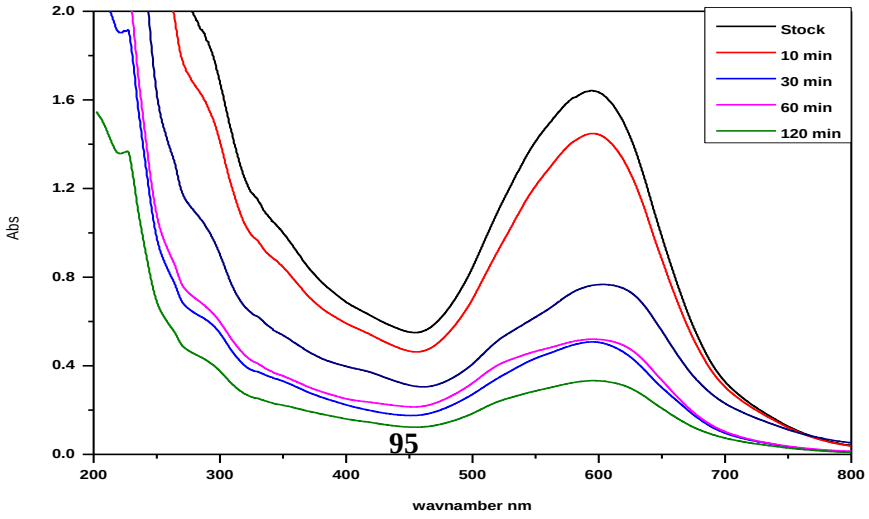

Figure (3-32): Spectra of removal pollutants (dyes) by using (SA-g-(PAAC-co-VBS)/ZnO) , (Exp. Condition: Temp. = 30°C, contact time 2 h, and mass absorbent 0.04 g).

3-10 Regeneration and Desorption of (SA-g-(PAAc-co-VBS)/ZnO NPs).

The regeneration of hydrogels ,after sorption, is one of the significant economic parameter for the treatment method. It helps in elucidating the mechanism of removal three pollutant(CV,TC and PH) from Pollutant -loaded adsorbent, regeneration mechanism and recycling of spent adsorbents, which in turn may reduce operational cost and protect the environment from secondary pollution. Three pollutant(CV,TC and PH) desorption studies were carried out using different desorption agents at concentration (0.01 N) such as H_2SO_4, NaOH, H_3PO_4 , HCl , HNO_3, and water(Sevda Pashaei-Fakhri ; Hoppen 2019; Zhang 2019; Al-Bayati 2020) .The (SA-g-(PAAc-co-VBS)/ZnO NPs)., was regeneration with 100% can be desorbed in diluted HCl solution because the –COO− is converted into –COOH in acidic solutions, and correspondingly, the electrostatic interactions between (SA-g-(PAAC-co-VBS)/ZnO) and three pollutant(CV,TC and PH) are weakened .The performance and reuse of (SA-g-(PAAc-co-VBS)/ZnO NPs) by using HCl solution in the three pollutant(CV,TC and PH) adsorption process was investigated up to 3 steps under optimal conditions . After the 3 cycle of using (SA-g-(PAAc-co-VBS)/ZnO NPs), the efficiency is still significant (>80%) and this shows (SA-g-(PAAc-co-

VBS)/ZnO NPs)., is probable renewable adsorber (Sukul 2019; Hemant Mittal 2021) as shown in Figure (3-33), (3-34) and (3-35) .

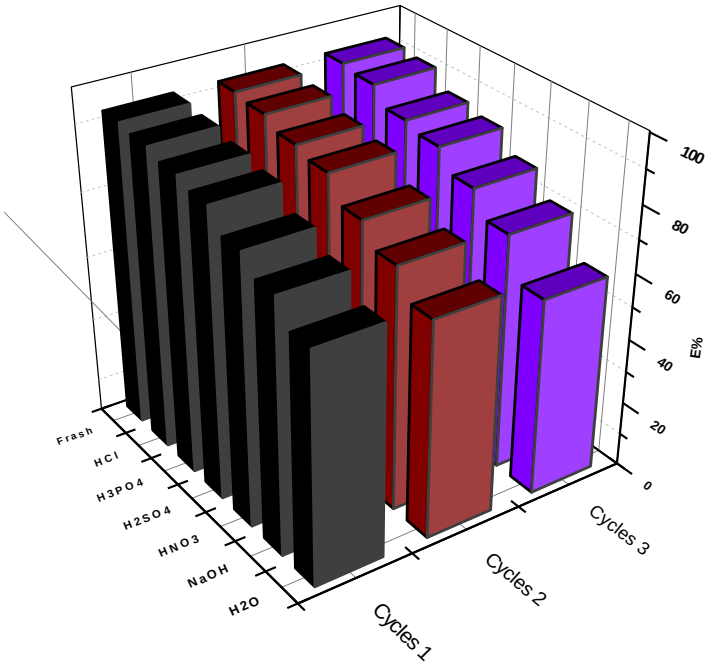

Figure 3-33: Comparison of CV dye removal efficiency (%) using fresh and three Cycles regenerated (SA-g-(PAAC-co-VBS)/ZnO).

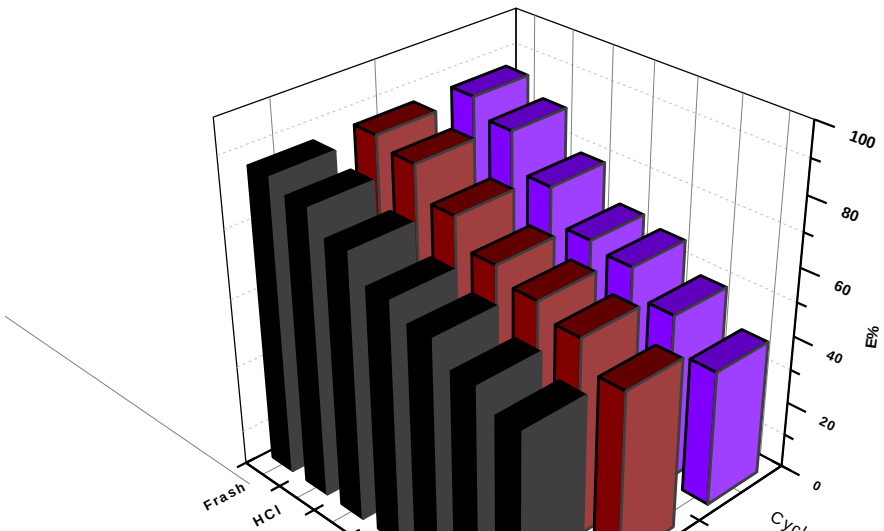

Figure 3-34: Comparison of TC drug removal efficiency (%) using fresh and three Cycles regenerated (SA-g-(PAAc-co-VBS)/ZnO NPs).

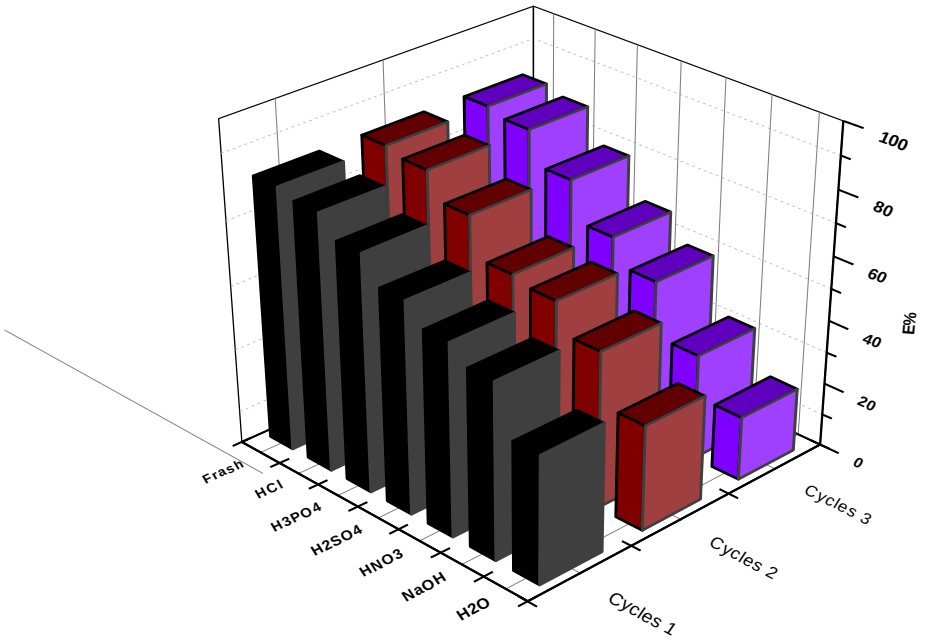

Figure 3-35: Comparison of PH removal efficiency (%) using fresh and three Cycles regenerated (SA-g-(PAAc-co-VBS)/ZnO NPs).

3-11 A Comparative adsorption between different surfaces and comparison between the amount of Zinc oxide to removal Three pollutant :

A Comparative study between (ZnO NPs , (SA-g-(PAAc-co-VBS) , (SA-g-(PAAc-co-VBS/ZnO NPs)) surfaces as Adsorbents wear carried out. A sample of 100 mL of three pollutant concentration(100 $mg.L^{-1}$) are used in this study, then added to a conical flask (Erlenmeyer) in the presence of 0.04g from prepared (ZnO NPs, (SA-g-(PAAC-co-VBS) , (SA-g-

(PAAC-co-VBS/ZnO)) ,and put in a shaker water bath for 2 hr., after that the supernatant was separated by centrifuge and measured the remaining concentration by using UV-Visible spectrophotometer at the λ_{max} nm (Xiong, Di et al. 2020; Aljeboree, Al-Gubury et al. 2019) .The best results of the percentage of removal (E%) for three pollutant the order increasing: (SA-g-(PAAC-co-VBS)/ZnO) > (SA-g-(PAAC-co-VBS)> ZnO NPs. shows in Figure (3-36).

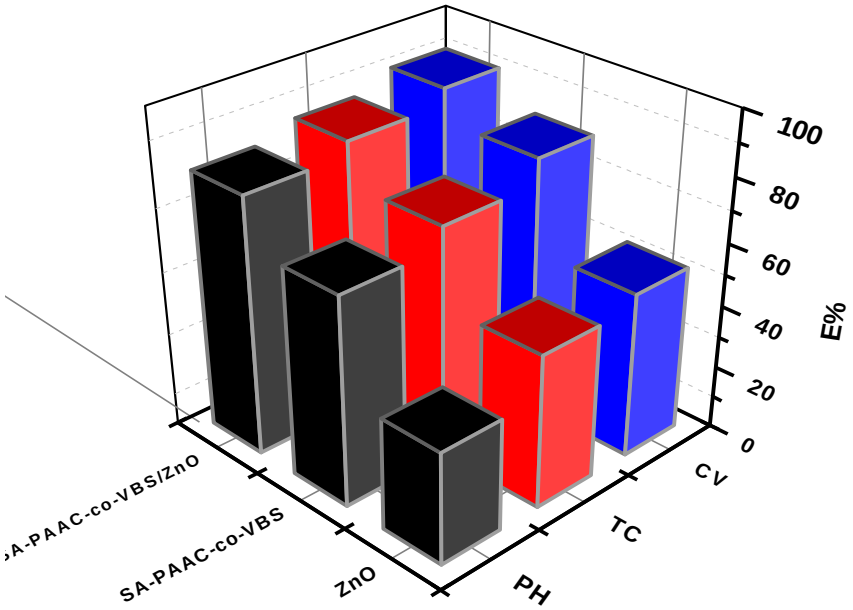

Figure (3-36): Effect comparative between (SA-g-(PAAc-co-VBS)/ZnO NPs) , (SA-g-(PAAC-co-VBS), ZnO. (Exp. Condition: mass of absorbent 0.04 g, conc. 100 mg.L^{-1} Temp. = 30°C, contact time 2 h).

Also comparative between the amount of Zinc oxide (ZnO NPs) decorated of (SA-g-(PAAC-co-VBS) by using (0.05,0.08, 0.1 and 0.15 g) shown in figure (3-37). The good results of the percentage of removal (E%) of three pollutant (CV,TC, PH) about 0.1 g ZnO,(92,451%, 88.55% and , 82.44%) at the same order .

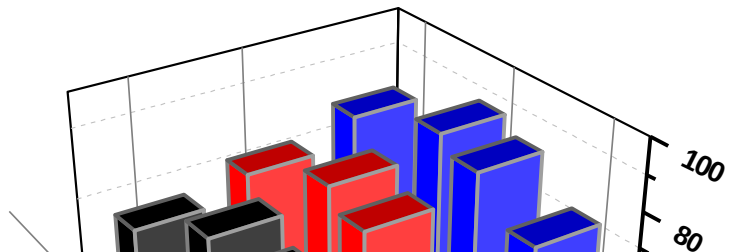

Figure (3-27) Effect comparative between the amount of ZnO decorated (SA-g-(PAAC-co-VBS) (Exp. Condition: mass of absorbent 0.04 g, conc. 100 mg.L^{-1} Temp. = 30°C, contact time 2 hr.)

3-12 Effect pH on Release Ratio of Tetracycline Drug In Vitro

The release of Tetracycline was studied in conditions similar to the human body in terms of acidity and temperature. It was found that the speed of amoxicillin release was higher when the acidity function (pH=7.5), and this is due to the degree of swelling of the hydrogel and the dissolution of Tetracycline depends on the acidity function. The speed of release of Tetracycline in the alkaline medium as a result of the increase in the rate of swelling more than in the acidic medium (Bhavesh D. Kevadiya 2021). As for the acid function (pH=1.2), the concentration of (H+) increases, which competes with the unlinked amino group, and thus the percentage of hydrogel swelling decreases, and thus the percentage of drug release decreases. The initial burst release of 28% and 21.56% , in the first 1 h was observed for Tetracycline . The cumulative release of Tetracycline in 3 h was 50.65 %, 42.33% from pH=7.5 and pH 1.2 at the

same order(Aguzzi ; Bhavesh D. Kevadiya 2021) , as shown in figure 3-38 .

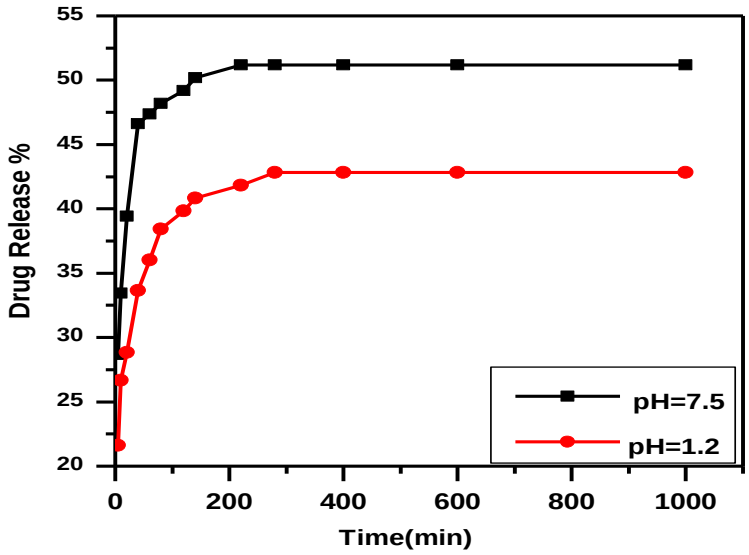

Figure 3-38. Drug Release profiles of TC from the (SA-g-(PAAC-co-VBS)/ZnO) in(pH 1.2) and (pH 7.4) at 37± 0.5 °C .

3-13 Biological Activity

In this study, the two types of bacteria were Gram-positive bacteria (*staphylococcus aureus* and *Staphylococcus epidermidi*) and Gram-negative bacteria (*klebsiella spp and E coli*), using four isolates depending on the method of disc diffusion, where concentrations (0.1 gm) from the three surfaces (SA-g-(PAAc-co-VBS)/ZnO NPs), (SA-g-(PAAc-co-

VBS)) , (ZnO NPs), the results showed that the surface (SA-g-(PAAc-co-VBS)/ZnO NPs),and (SA-g-(PAAc-co-VBS)) have antibacterial activity against the Gram- positive bacteria compared to the gram- negative bacteria with an inhibition area ,More than ZnO NPs where the results showed that it has very little antibacterial activity against two types of bacteria (Asmaa H. Hammadi 2020) as shown in the Figure 3-39 .

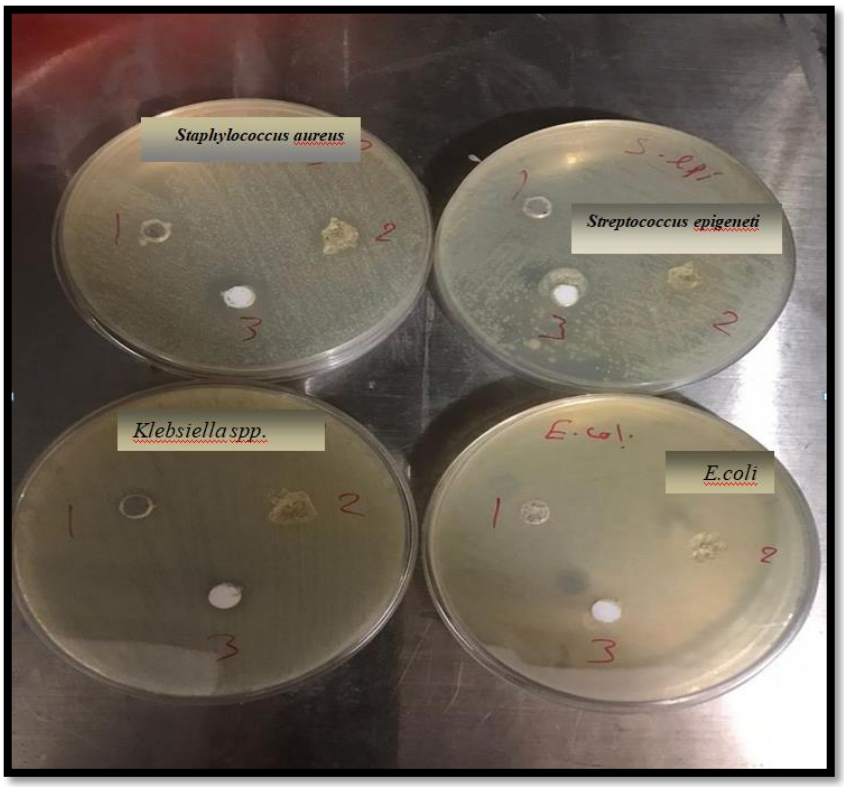

Figure 3-39: Antibacterial activity of three compounds using disc diffusion method.

the inhibition regions of the three compounds (SA-g-(PAAc-co-VBS)/ZnO NPs, SA-g- (PAAC-co-VBS),and ZnO NPs), where it was given that the compound (SA-g-(PAAc-co-VBS)/ZnO NPs) had high antibacterial activity, (30mm) against *Staphylococcus aureus*, (25 mm) against *Streptococcus epigenetics*, (13 mm, 12 mm) against E.coli, and *Klebsiella spp*. That is, it had a higher effect on the Gram-positive

bacteria than on the Gram-negative bacteria, respectively(R.V. Mundra 2014; Mukha IP 2019).

The compound ((SA-g-(PAAc-co-VBS)) hydrogel compound) has antibacterial activity against *Staphylococcus aureus* (15 mm), against Streptococcus epigenetics (20 mm), had no activity against E coli and *Klebsiella spp*. That is, it had an effect on the Gram-positive bacteria and had low effect on the Gram-negative bacteria . The compound (ZnO NPs) had very low anti-bacterial activity for Gram-positive bacteria and Gram-negative bacteria as shown in Figure 3-40 (Adam 2010; Asmaa H. Hammadi 2020).

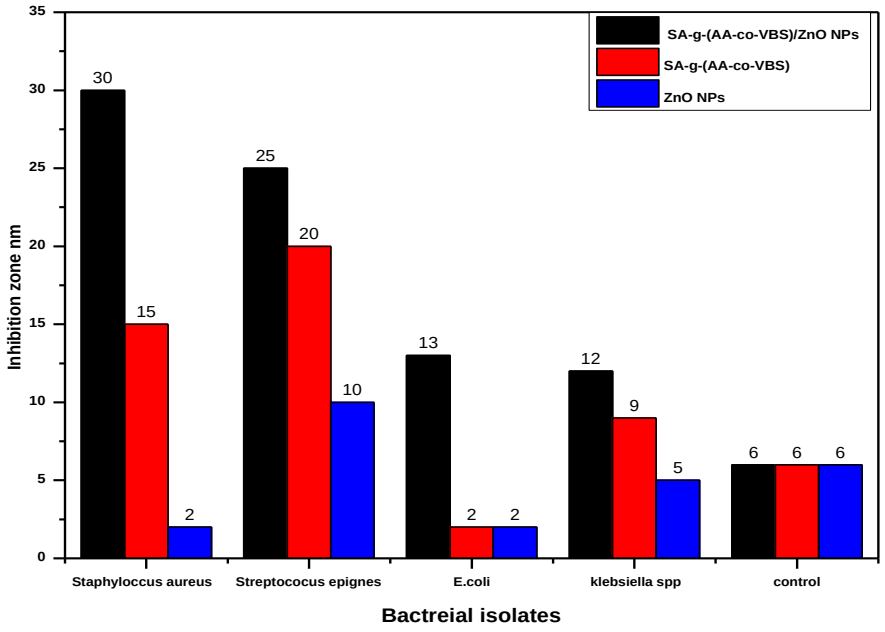

Figure (3-40): Effect of inhibition zones against pathogenic bacteria isolates.

Surface efficacy in Mice healing

Figure (3-41) shows the stages of recovery of wounded mice, as (0.1)g was treated from the surface SA-g-(PAAc-co-VBS)/ZnO NPs, where mice were incised in the animal house at Al-Qadisiyah University, College of Science, and the results were obtained as shown in Figure (3-41)

On the first day, mice were clearly injured on the first day of wounding, and they were treated with about (0.1 gm) from the surface SA-g-(PAAc-co-VBS)/ZnO NPs as shown in image (A)

On the second day, a clear improvement was observed in the treatment of Mice, where the rate of healing and improvement of wounds was at the beginning, as shown in image (B)

On the third day, an improvement was observed in the mice, where the rate of healing and improvement of mice was very clear, with some redness in the skin surrounding the mice as shown in image (C) .

On the four and five day, the clear results in image showed a clear healing of the mice and the return of the skin to its natural pink color, a clear evidence of the surface's efficiency in mice healing, as shown in image (D, E)

On the seven day, according to the results shown in image (F), there is a complete healing of the mice and the return of the skin to its natural color. This is due to the fact that SA-g-(PAAc-co-VBS)/ZnO NPs has a high effective efficiency in treating and healing mice. It is considered environmentally friendly, non-toxic and also considered an anti-inflammatory. In addition, there is a biocompatibility with mammalian cells (Evelina Vågesjö 2018; Dehui Xu 2020; Samia Afrin 2022).

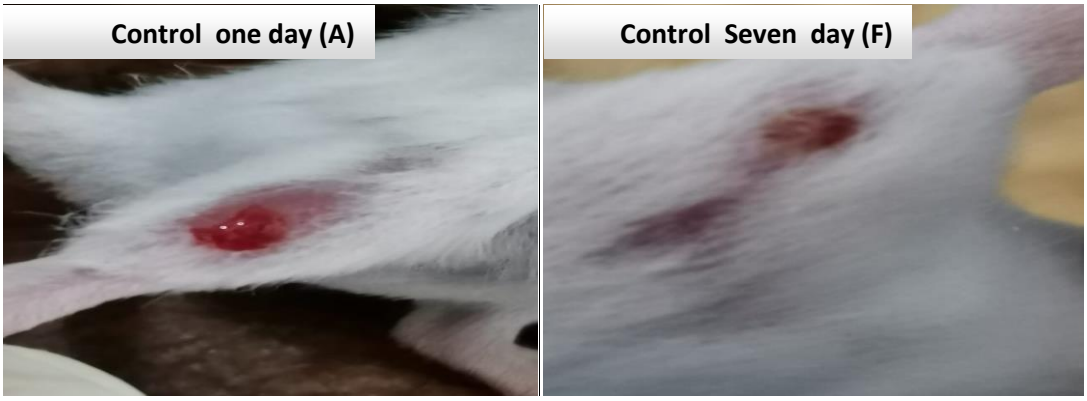

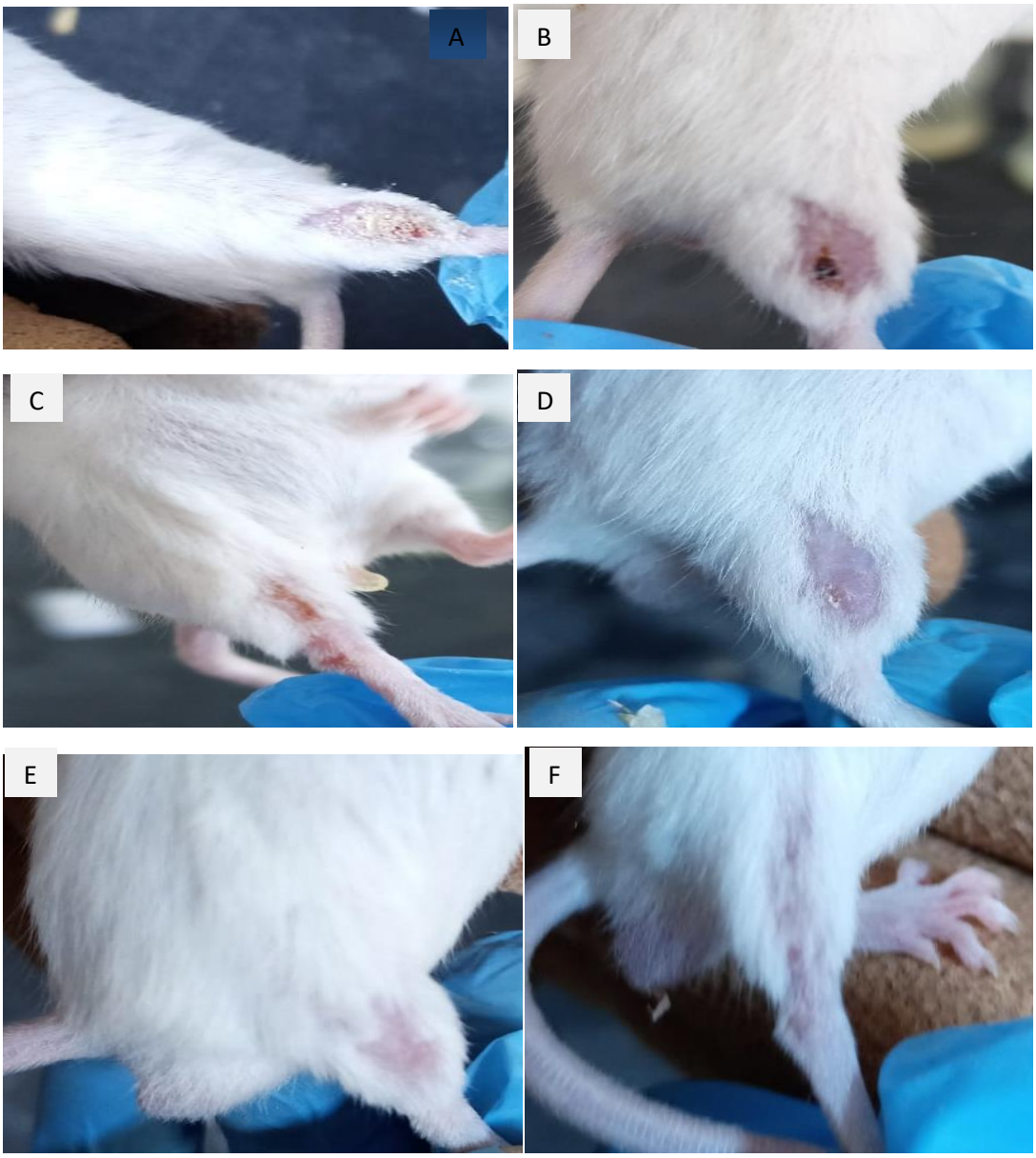

Figure 3-41: Effect of the surface SA-g-(PAAc-co-VBS)/ZnO NPs on the wound healing of mice during seven days

Conclusions:

Studies have been conducted to gain understandings and generic knowledge of the equilibrium aspects of adsorption of adsorbents ,(SA-g-(PAAc-co-VBS)/ZnO NPs, (SA-g-(PAAc-co-VBS) ,ZnO NPs surfaces. Removal of three pollutant (crystal violet CV dye , Tetracycline TC drug , Phenol PH) from aqueous solutions by adsorption with ,(SA-g-(PAAc-co-VBS)/ZnO NPs surfaces have been experimentally determined. The best results have been found in temperature 30 oC, and adsorbent dosage 0.04gm of ,(SA-g-(PAAc-co-VBS)/ZnO NPs for both studying adsorption capacity and removal percentage" and the following observations are made:

1. The adsorption capacity and percentage of three pollutant removal increase with increasing contact time, surface area, and temperature. But adsorption capacity has decreased with the increase of adsorbent dosage.
2. The optimum contact time for equilibrium to be achieved is found to be 2 hr. It is basically due to saturation of the active site which does not allow further adsorption to take place.
3. For CV dye on adsorbent surfaces, maximum adsorption was found to be at pH = 6.6. Adsorption was found to decrease with an increase in the pH of the solution. but tetracycline drug and phenol were to increase with an increase in the pH of the solution in the base medium .
4. The negative value of ΔG confirms the spontaneous nature adsorption process. The positive value of ΔS showed the increased randomness at the solid-solution interface during adsorption and the positive value of ΔH indicated the adsorption process was endothermic.

5. The interaction between dose and initial concentration showed a significant effect on the adsorption process. Adsorbent showed fits better to Freundlich isotherm which suggests that adsorption is heterogeneous.
6. The adsorption efficiency for removal of three pollutant (SA-g-(PAAC-co-VBS)/ZnO NPs surface was found better than the (SA-g-(PAAC-co-VBS) and ZnO NPs .
7. Removal of real aqueous pollutants(dyes , drugs) by using (SA-g-(PAAC-co-VBS)/ZnO NPs to give low absorbance (0.0001) by using UV-Visible spectrophotometer for at a chosen wavelength for 60 minutes .
8. The chemisorption, pseudo-first-order, and pseudo-second-order kinetic models were applied to test the experimental data. The pseudo-first-order exhibited the best fit for the kinetic studies.
9. The release values of tetracycline from the hydrogel are in the hypothetical bowel fluid (pH=7.5).
10. The (SA-g-(PAAc-co-VBS)/ZnO NPs was regeneration with 100% can be desorbed in diluted HCl solution in the three pollutant(CV,TC and PH) adsorption process was investigated up to 3 steps under optimal conditions .
11. SA-g- (PAAc-co-VBS)/ZnO NPs had high antibacterial activity, That is, it had a higher effect on the Gram-positive bacteria than on the Gram-negative bacteria.
12. In two to seven days, according to the results, there is complete healing of the mice and the return of the skin to its natural color.

Future Works:

A study of adsorption of three pollutant using SA-g(PAAc-g-VBS)/ZnO NPs work needs to be done to further understand the science behind the adsorption processes.

1-The possibility of using these surfaces SA-g(PAAc-g-VBS)/ZnO NPs and SA-g(PAAc-g-VBS) to remove many contaminants such as heavy elements and pesticides and herbicides.

2-Preparing new surfaces that are inexpensive, environmentally friendly, and the possibility of replacing Zinc oxide with titanium dioxide.

3-Synthesizing new polymeric complexes adsorbent on the Activated carbon surfaces AC , CNT, GO .

4-Studying the possibility of loading the surface with more than one drug so that it does not interfere or contradict medically.

5-A comparison between the method of loading the drug used in this study and other methods of loading.

6-Completing the study of drug release inside the body of an organism (in vivo) and following up on changes by drawing blood from the body.

References

Reference

A. F. AlKaim, A. N. AlShirifi, and A. H. AlDujaili (2007). "Kinetic study of adsorption of phenol on the novel polymer prepared AUFP from aqueous solution." National Journal of Chemistry **27**: 428-455.

A. H. Al-muhtaseb and T.Magee (2021). "Moisture Sorption Isotherm Characteristics of Food Products: A Review." Food Bioprod. Process. **1**: 1-22.

Abd-Elhamid, A. I. (2021). "Fabrication and characterization of a novel (GO/PAA/PAM) nanocomposite as effective adsorbent for cationic dyes." Journal of Materials Research and Technolog **2**: 1-20.

Abdalghaffar M Osman, A. H. H., Tawfik A.Saleh (2020). "Simultaneous adsorption of dye and toxic metal ions using an interfacially polymerized silica/polyamide nanocomposite: Kinetic and thermodynamic studies." Journal of Molecular Liquids **314**(15): 113640.

Abdalghaffar M. , O. A. H., Tawfik A.S (2020). "Simultaneous adsorption of dye and toxic metal ions using an interfacially polymerized silica/polyamide nanocomposite: Kinetic and thermodynamic studies." Journal of Molecular Liquids **314**(15): 113640.

Abdoon, F. M., Yahyaa, S Y. (2018). "Validated spectrophotometric approach for determination of salbutamol sulfate in pure and pharmaceutical dosage forms using oxidative coupling reaction." Journal of King Saud University - Science **1**: https://doi.org/10.1016/j.jksus.2018.11.002.

Adam, A. M. A. (2010). "Structural, thermal, morphological and biological studies of proton-transfer complexes formed from 4-aminoantipyrine with quinol and picric acid." Spectrochimica Acta Part A: Molecular and Biomolecular Spectroscopy **104**: 1-13.

Adheem, H. M., Jasim, L.S. (2020). "Preparation and Characterization of a three-component hydrogel composite and study of kinetic and thermodynamic applications of adsorption of some positive and

negative dyes from their aqueous solutions." IOP Conference Series: Materials Science and Engineering **928**(5): 052027.

Aguzzi, C., Capra, P.,Bonferoni, C.,Cerezo, P.,Salcedo, I.,Snchez, R.,Caramella, C.,Viseras, C. "Chitosanâ silicate biocomposites to be used in modified drug release of 5-aminosalicylic acid (5-ASA)." Applied Clay Science, 2020 **50**(1): 106-111.

Ahmed EM (2019). "Hydrogel: preparation, characterization, and applications: a review." J Adv Res **6**(2): 105-121.

Akeem Adeyemi Oladipo, M. G. (2019). "Enhanced removal of crystal violet by low cost alginate/acid activated bentonite composite beads: Optimization and modelling using non-linear regression technique." journal of Water Process Engineering **2**: 43-52.

Al-Bayati, R. A. (2020). "Adsorption-desorption isotherm of one of antidibetic drug from aqueous solutions on some pharmaceutical adsorbents." Eur. J. Sci. Res. **40**: 580-588.

Ali M. El Shafey, M. K. A.-L., H.M. Abd El-Salam (2021). "The facile synthesis of poly(acrylate/acrylamide) titanium dioxide nanocomposite for groundwater ammonia removal." Desalination and Water Treatment **212** 61-70.

Aljeboree, A. M., H. Y. Al-Gubury, et al. (2019). "THE EFFECT OF DIFFERENT PARAMETERS ON THE REMOVAL OF VITAMIN B12 DRUG (AS A MODEL BIOCHEMICAL POLLUTANTS) BY AC/ CLAY." ***Biochem. Cell. Arch.*** **19**(1): 755-759.

Aljeboree, A. M., Alrazzak, N.A., Alqaraguly, M.B., Jasim, L.S., Alkaim, A.F. (2021). "Adsorption of pollutants by using low-cost (Environment-Friendly): Equilibrium, kinetics and thermodynamic studies: A review." Systematic Reviews in Pharmacy **11**(12): 1988-1997.

Aljeboree, A. M., A. N. Alshirifi, et al. (2017). "Kinetics and equilibrium study for the adsorption of textile dyes on coconut shell activated carbon." Arabian Journal of Chemistry **10**: S3381-S3393.

Aljeboree, A. M., A. N. Alshirifi, et al. (2020). "REMOVAL OF AMOXICILLIN DRUG ONTO NANO COMPOSITES SURFACE USING ULTRASOUND ASSISTANCE." Plant Archives **20**(1): 3135-3140.

Aljeboree, A. M. R., Nadher D;Jasim, Layth Sameer ;Alwarthan, Abdulrahman A.;Khadhim, Mustafa M.;Washeel Salman, Abbas ;Alkaim, Ayad F. (2022). "Synthesis of a new nanocomposite with the core TiO2/hydrogel: Brilliant green dye adsorption, isotherms, kinetics, and DFT studies." Journal of Industrial and Engineering Chemistry **109**: 475 - 485.

Aljeboree;, A. M., A. N. Alshirifi;, et al. (2020). "REMOVAL OF PHENYLEPHRINE HYDROCHLORIDE AS A MODEL OF PHARMACEUTICAL COMPOUNDS BY USING ULTRASONICATED

ADSORPTION TECHNIQUE IN THE PRESENCE OF NANO COMPOSITES." Plant Archives **20**(1): 3149-3153.

Amer M. Alshamri, A. M. A., Mohammed B. Alqaragully, Ayad F. Alkaim (2021). "Removal of toxic textile dyes from aqueous solution through adsorption onto coconut husk waste: Thermodynamic and isotherm studies." Caspian J. Environ. Sci. **19**(3): 513~522

Arif Chowdhury, S. K., Afaq Ahmad Khan, M. Ravi Chandra, and Sahid Hussain (2020). "Activated carbon loaded with Ni-Co-S nanoparticle for Superior Adsorption Capacity of Antibiotics and Dye from Wastewater: Kinetics and Isotherms." Journal Pre-proof **1**: https://doi.org/10.1016/j.colsurfa.2020.125868.

Arif Chowdhury, S. K., Afaq Ahmad Khan, M. Ravi Chandra, and Sahid Hussain (2020). "Activated carbon loaded with Ni-Co-S nanoparticle for SuperiorAdsorption Capacity of Antibiotics and Dye from Wastewater: Kinetics and Isotherms." Journal Pre-proof **20**: https://doi.org/10.1016/j.colsurfa.2020.125868.

Aseel M Aljeboree, A. Y. A.-B., Saifaldeen M Abdalhadi, Ayad F Alkaim (2021). "Investigation Study of Removing Methyl Violet Dye From Aqueous Solutions Using Corn-Cob as A Source of Activated Carbon." Egyptian Journal of Chemistry: DOI: 10.21608/EJCHEM.2021.55274.3159.

Aseel M. Aljeboree , A. B. M. (2021). "Synthesis highly active surface of ZnO/AC nanocomposite for removal of pollutants from aqueous solutions: thermodynamic and kinetic study." Applied Nanoscience: https://link.springer.com/article/10.1007%2Fs13204-021-01946-w.

Ashour, S. and R. Bayram (2019). "Selective and validated kinetic spectrophotometric method for the determination of irbesartan in pure and pharmaceutical formulations." Annales Pharmaceutiques Fran¦§aises **77**(2): 101-111.

Asmaa H. Hammadi, S. A. H., Lena Fadhil Al-Jibouri, Falah H. Hussien (2020). "Synthesis, Characterization and Biological Activity of Zinc Oxide Nanoparticles (ZnO NPs)." Sys Rev Pharm **11**(5): 431 439.

Ayad F. Alkaim, A. M. A. (2020). "White Marble as an Alternative Surface for Removal of Toxic Dyes (Methylene Blue) from Aqueous Solutions " International Journal of Advanced Science and Technology **29**(5): 5470 - 5479.

Aziz RK, K. M. (2018). "Rise and persistence of global M1T1 clone of Streptococcus pyogenes. ." Emerg Infect Dis **14**: 1511-1517.

Bahareh Tanhaei , A. A., Evgenia Iakovleva , Mika Sillanp (2020). "Efficient carbon interlayed magnetic chitosan adsorbent for anionic dye removal: Synthesis, characterization and adsorption study." International Journal of Biological Macromolecules **164**: 3621-3631.

Banerjee, S. and M. C. Chattopadhyaya (2017). "Adsorption characteristics for the removal of a toxic dye, tartrazine from aqueous solutions by a low cost agricultural by-product." Arabian Journal of Chemistry **10**: S1629-S1638.

Basam W. Mahde , N. D. R., Layth S. Jasim ,Hayder O. Jamel (2018). "Synthesis and characterization of polyacrylamide hydrogel for the controlled release of aspirin." J. Pharm. Sci. & Res. **10**(11): 2850-2854.

Bhavesh D. Kevadiya, G. V. J., Haresh M. Mody, Hari C. Bajaj (2021). "Biopolymer–clay hydrogel composites as drug carrier: Host–guest intercalation and in vitro release study of lidocaine hydrochloride." Applied Clay Science **52**: 364-367.

Bo Gao, H. Y., Jingya Wen, Hongju Zeng, Ting Liang, Fang Zuo, Changjing Cheng (2021). "Super-adsorbent poly(acrylic acid)/laponite hydrogel with ultrahigh mechanical property for adsorption of methylene blue." Journal of Environmental Chemical Engineering **24**: 18-24.

Chen J.P., C. M. L., Zhang B. (2012). "Effects of competitive ions, humic acid, and pH on removal of ammonium and phosphorous from the synthetic industrial effluent by ion exchange resins." Waste. Manage. **22** 711-719.

Clement Yaw Efah, T. S., Shaohua Liu ,Yongjun Wu (2020). "Klebsiella pneumoniae: an increasing threat to public health." Ann Clin Microbiol Antimicrob **19**: 1.

Dalia Khalid Mahmoud, M. A. M., Wan Azlina Abdul Karim (2012). "Langmuir model application on solidliquid adsorption using agricultural wastes: Environmental application review." Journal of Purity, Utility Reaction and Environment **4**: 170-199.

Dehui Xu, S. W., Bing Li, Miao Qi, Rui Feng, Qiaosong Li, Hao Zhang, Hailan Chen, and Michael G Kong (2020). "Effects of Plasma-Activated Water on Skin Wound Healing in Mice." Microorganisms **7**(8): 1091.

Del Mar Orta, M., Martn, Julia,Medina-Carrasco, Santiago,Santos, Juan Luis,Aparicio, Irene,Alonso, Esteban (2019). "Adsorption of propranolol onto montmorillonite: Kinetic, isotherm and pH studies." Applied Clay Science **173**: 107-114.

E. Alipanahpour Dil , M. G., A.M. Ghaedi , A. Asfaram, A. Goudarzi , S. Hajati , M. Soylak, Shilpi Agarwal, Vinod Kumar Gupt (2015). "Modeling of quaternary dyes adsorption onto ZnO-NR-AC artificial 3 neural network: Analysis by derivative spectrophotometry " Journal of Industrial and Engineering Chemistry **1**: 22.

Evelina Vågesjö, E. Ö., Anneleen Mortier, Hava Lofton, Fredrik Huss, Paul Proost, Stefan Roos, Mia Phillipsona, (2018). "Accelerated wound healing in mice by on-site production and delivery of CXCL12 by transformed lactic acid bacteria." National Center for Biotechnology Information **7**(8): 1-9.

Farabi Temel , M., SezenKucukcongar (2020). "Removal of methylene blue from aqueous solutions by silica gel supported calix[4]arene cage: Investigation of adsorption properties." European Polymer Journal **125**(15): 109540.

Freundlich, H. (1906). "Over the adsorption in solution." J. Phys. Chem **57**(385471): 1100-1107.

Freundlich H, W. (1939). "The Adsorption of cis- and trans-Azobenzene " J Am Chem Soc **61**: 2228-2230.

Gamoudi, S. and E. Srasra (2019). "Adsorption of organic dyes by HDPy+-modified clay: effect of molecular structure on the adsorption." Journal of Molecular Structure.

Gaofeng Pan , K.-I. K., Yutaka Yamad (2021). "Application of hydrogel for the removal of pollutant phenol in water." Journal of the Chinese Institute of Chemical Engineers **39** 361-366.

Garg S and Garg A (2016). "Hydrogel: classification, properties,preparation and technical features. ." Asian J Biomater Res **2**(6): 163-170.

Gui-Bing Hong , T.-J. Y., Hsueh-Chia Lee , Chih-Ming Ma (2021). "Using Rice Bran Hydrogel Beads to Remove Dye from Aqueous Solutions." Sustainability **13**: 5640.

H.M. Xiong, Y. X., Q.G. Ren, Y.Y. Xia (2008). Journal of the American Chemical Society **130**: 7522-7523.

Hameed , B. H. (2019). "Batch adsorption of methylene blue from aqueous solution by garlic peel, an agricultural waste biomass." J. Hazard. Mater **164**: 870-875.

Hameed, K. S., Muthirulan, P., Meenakshi, S.M. (2017). "Adsorption of chromotrope dye onto activated carbons obtained from the seeds of various plants: Equilibrium and kinetics studies." Arabian J. Chem **10**: S2225-S2233.

Hanieh Gharehbakhsh , H. A. P., Mohammad Reza Toosi , Amir Hessam Hassani , Elham Moniri (2022). "Adsorptive removal of toluenediamine from aqueous solution by polysulfone/graphene oxide/TiO2 membrane functionalized by allylamine " Chemical Data Collections **37**: 100800.

Hanieh Gharehbakhsh , H. A. P., Mohammad Reza Toosi ,Amir Hessam Hassani , Elham Moniri (2022). "Adsorptive removal of toluenediamine from aqueous solution by polysulfone/graphene oxide/TiO2 membrane functionalized by allylamine." Chemical Data Collections **37**: 100800.

Hany El-Hamshary , S. E.-S., Manal F. Abou Taleb , Nabil A. El-Kelesh (2007). "Removal of phenolic compounds using (2-hydroxyethyl methacrylate/acrylamidopyridine) hydrogel prepared by gamma radiation." Separation and Purification Technology **57**: 329-337.

Hazem Hassan , A. S., Ahmed K. El-ziaty , Mohamed El-Sakhawy (2019). "New chitosan/silica/zinc oxide nanocomposite as adsorbent for dye removal." International Journal of Biological Macromolecules **131**: 520-526.

Heloise Beatriz Quesada, A. T. A. B., Luís Fernando Cusioli,Daiana Seibert,Charleston de Oliveira Bezerra,Ros^angela Bergamasco, (2021). "Surface water pollution by pharmaceuticals and an alternative of removal by low-cost adsorbents: A review." Chemosphere **222**: 766e780.

Hemant Mittal , A. A., Pranay P. Morajkar , Saeed M. Alhassan (2021). "Graphene oxide crosslinked hydrogel nanocomposites of xanthan gumm for the adsorption of crystal violet dye." Journal of Molecular Liquids **323**: 115034.

Hemant Mittal , A. A. A., Pranay P. Morajkar , Saeed M. Alhassan (2021). "Graphene oxide crosslinked hydrogel nanocomposites of xanthan gum for the adsorption of crystal violet dye." ournal of Molecular Liquids **323**: 115034.

Hoppen, M. I., Carvalho, K. Q.,Ferreira, R. C.,Passig, F. H.,Pereira, I. C., Rizzo-Domingues, R. C. P.,Lenzi, M. K.,Bottini, R. C. R. (2019). "Adsorption and desorption of acetylsalicylic acid onto activated

carbon of babassu coconut mesocarp." Journal of Environmental Chemical Engineering **7**(1): 102862.

Huda Salim Al-Niaeem , A. A., Whidad Hanoosh (2022). "Preparation of Semi IPNs-Hydrogel Composite for Removing Congo Red and Bismarck Brown Y from Wastewater: Kinetic and Thermodynamic Study." Egypt. J. Chem. **56**(1): 19 - 34.

Inas A. Ahmed , M. K. S., Eder C. Lima , Michael A. Badawi , Zichao S. Liaa , Adrián B. Petriciolet , Ioannis A. Anastopoulos (2022). "Outstanding Performance of a New Exfoliated Clay Impregnated with Rutile TiO2 Nanoparticles Composite for Dyes Adsorption: Experimental and Theoretical Studies." Coatings **12**: 22.

Jinsong He , F. N., Anan Cui , Xianli Chen , Shihuai Deng , Fei Shen , Churui Huang , Gang Yang ,Chun Song , Jing Zhang , Dong Tian , Lulu Long , Ying Zhu , Ling Luo (2020). "New insight into adsorption and co-adsorption of arsenic and tetracycline using a Y-immobilized graphene oxide-alginate hydrogel: Adsorption behaviours and mechanisms." Science of The Total Environment **70**: 134363.

Jolanta Sarowsk , B. F. K., Agnieszka Jama Kmiecik, Magdalena Frej Madrzak (2019). "Virulence factors, prevalence and potential transmission of extraintestinal pathogenic Escherichia coli isolated from diferent sources: recent reports." Gut Pathogens **10**: 1-11.

Jun, L. Y., Yon, Lau Sie,Mubarak, N. M.,Bing, Chua Han,Pan, Sharadwata,Danquah, Michael K.,Abdullah, E. C.,Khalid, Mohammad (2019). "An overview of immobilized enzyme technologies for dye and phenolic removal from wastewater." Journal of Environmental Chemical Engineering **7**(2): 102961.

Katz AR, M. D. (2019). "Severe streptococcal infections in historical perspective. ." Clin Infect Dis **12**: 14:298-307.

Khan TA, Nazir M, et al. (2018). "Removal of Chromium (VI) from aqueous solution using guar gum-nano zinc oxide biocomposite adsorbent." Arabian J Chem **10**: S2388-S2398.

Kim, Y.-S., Kim, Jin-Hyun (2019). "Isotherm, kinetic and thermodynamic studies on the adsorption of paclitaxel onto Sylopute." The Journal of Chemical Thermodynamics **130**: 104-113.

Kumar T, Thakur A, et al. (2018). " Modified chitosan hydrogels as drug delivery and tissue engineering systems: present status and applications. ." Acta Pharm Sin B **2**(5): 439-449.

Kwinn LA, N. V. (2019). "How group A Streptococcus circumvents host phagocyte defenses. ." Future Microbiol **2**: 75-84.

Lamin Sanyang , K. G., Ruziah Zainudin (2013). "SORPTION OF PHENOL FROM WASTEWATER BY HYDROGEL-BIOCHAR COMPOSITE." International Journal of Engineering and Technology **10**(1): 38-49.

Langmuir, I. (1918). "The adsorption of gases on plane surfaces of glass, mica and platinum." Journal of the American Chemical society **40**(9): 1361-1403.

Layth S. Jasim , N. D. R., Hayder O. Jamel (2018). "Synthesis and Characterization of Poly (Acryl Amide - Maleic Acid) Hydrogel: Adsorption Kinetics of a Malachite Green from Aqueous Solutions." Eurasian Journal of Analytical Chemistry **13**(1b): em74.

Li J, Ma J, et al. (2019). "Adsorption of lysozyme by alginate/graphene oxide composite beads with enhanced stability and mechanical property." Mater Sci Eng C **89**: 25-32.

Liang Y, Zhao X, et al. (2019). "pH-responsive injectable hydrogels with mucosal adhesiveness based on chitosan grafted-dihydrocaffeic

acid and oxidized pullulan for localized drug delivery." J Colloid Interf Sci **536**: 224-234.

Liu, H., Yang, Yongkui, Sun, Huifang, Zhao, Lin, Liu, Yu (2020). "Fate of tetracycline in enhanced biological nutrient removal process." Chemosphere **193**: 998-1003.

Liu L, Gao Q, et al. (2019). "In situ forming hydrogels based on chitosan for drug delivery and tissue regeneration. ." Asian JPharm Sci **11**(6): 673-683.

Mahdi, A. B., Aljeboree, A.M., Alkaim, A.F. (2021). "Adsorption and removal of pollutants (Dyes) from wastewater using different types of low-cost adsorbents: A review." Journal of Chemical Health Risks **11**(2): 203-212.

Makhado E and Hato M (2021). "Preparation and characterization of sodium alginate-based oxidized multi-walled carbon nanotubes hydrogel nanocomposite and its adsorption behaviour for methylene blue dye. ." Front Chem **9**: 576913.

Mariana Alves Leite Dutra , N. d. N. M., Men de Sá Moreira de Souza Filho ,Rosangela de Carvalho Balaban (2021). "Phenol removal from wastewater using eco-friendly hybrid hydrogels." Applied polymer **2**: 1-19.

Mariana Alves Leite Dutra, N. d. N. M., Men de Sá Moreira de Souza Filho, Rosangela de Carvalho Balaban, (2020). "Phenol removal from wastewater using eco-friendly hybrid hydrogels." Applied polymer **2**: 1-22.

Martínez-Huitle, C. A., Brillas, E. (2019). "Decontamination of wastewaters containing synthetic organic dyes by electrochemical methods: A general review. ." Appl. Catal. B Environ., **87**: 105-145.

Metrani, R., G. K. Jayaprakasha, et al. (2018). "Optimized method for the quantification of pyruvic acid in onions by microplate reader and confirmation by high resolution mass spectra." Food Chemistry **242**: 451-458.

Mohamad A Salleh , D. K. M., Wan A Karim , Azni I Salleh (2020). "Cationic and anionic dye adsorption by agricultural solid wastes:A comprehensive review." Desalination **280**: 1-13.

Mohammad, N., Atassi, Y., & Tally, M. (2019). "Synthesis and swelling behavior of metal-chelating superabsorbent hydrogels based on sodium alginate-g-poly (AMPS-co-AA-co-AM) obtained under microwave irradiation." Polymer Bulletin **74**(11): 4453-4481.

Mohammad T. ALSamman, J. S. (2021). "Recent advances on biobased hydrogels based on chitosan and alginate for the adsorption of dyes and metal ions from water." Arabian Journal of Chemistry **2**: https://doi.org/10.1016/j.arabjc.2021.103455.

Mohammed A. Jawad, A. J. K., Aseel M. Aljeboree (2021). "Removal of Direct Dye from Aqueous Solution by a Low-cost Hydrogel: Adsorption Kinetics, and Isotherms Study." International Journal of Pharmaceutical Quality Assurance **12**(3): 191-195.

Mohammed A. Jawad, A. J. K., Nadher D. Radia (2021). "Role of Sodium Alginate-g-poly (Acrylic acid-fumaric acid) Hydrogel for Removal of Pharmaceutical Paracetamol from Aqueous Solutions by Adsorption " International Journal of Pharmaceutical Quality Assurance **12**(3): 202-205.

Mohib Ullah, R. N., Muslim Khan,Waliullah Khan,Mohib Shah,Sahib Gul Afridi,Amir Zada1 (2020). "The effective removal of heavy metals from water by activated carbon adsorbents of Albizia lebbeck and Melia azedarach seed shells " Soil and Water Research **15**(1): 30-37.

Mukha IP, E. A., Smirnova NP, Mikhienkova AI, Korchak GI, Gorchev VF (2019). "Antimicrobial activity of stable silver nanoparticles of a certain size." Appl Biochem Microbio **49** 199-206.

Mustafa T. Yagub ;Tushar Kanti Sen , S. A. H. M. A. (2014). "Dye and its removal from aqueous solution by adsorption: A review." Advances in Colloid and Interface Science **209**: 172-188.

Nadavala Siva Kumar , M. A., Anesh Manjaly Poulose , Madala Suguna and Mansour I. Al-Hazza (2019). "Equilibrium and Kinetic Studies of Biosorptive Removal of 2,4,6-Trichlorophenol from Aqueous Solutions Using Untreated Agro-Waste Pine Cone Biomass." processes **1**: 22-33.

Nadher, D. R., Layth S J. (2019). "Synthesis of Graphene Oxide/Hydrogel Composites and Their Ability for Efficient Adsorption of Crystal Violet." J. Pharm. Sci. & Res. **11**(2): 456-463.

Nasseh, N., Barikbin, Behnam,Taghavi, Lobat,Nasseri, Mohammad Ali (2019). "Adsorption of metronidazole antibiotic using a new magnetic nanocomposite from simulated wastewater (isotherm, kinetic and thermodynamic studies)." Composites Part B: Engineering **159**: 146-156.

Nelly Janira Avire , H. W., Kirstin Ross (2021). "A Review of Streptococcus pyogenes: Public Health Risk Factors, Prevention and Control." pyogenes **10**: 248.

Nompumelelo Malatji, E. M., Kwena D Modibane, Kabelo E Ramohlola,Thabiso C Maponya,Gobeng R Monama , Mpitloane J Hato (2021). "Removal of methylene blue from wastewater using hydrogel nanocomposites: A review." Nanomaterials and Technologies for Environmental Applications **11**: 1-27.

Peter Cass , W. K., Eliana Pereeia, Natalie P. Holmes, Tim Hughes (2010). "Preparation of hydrogels via ultrasonic polymerization." Ultrasonics Sonochemistry **17**: 326-332.

Qiuyan Luo, T. R., Zihua Lei , Yifeng Huang , Yong Huang , Dong Xu ,Caichao Wan , Xin Guo , Yiqiang W (2022). "Non-toxic chitosan-based hydrogel with strong adsorption and sensitive detection abilities for tetracycline " Chemical Engineering Journal **427**: 131738.

Quesada, H. B., A. T. A. Baptista, et al. (2019). "Surface water pollution by pharmaceuticals and an alternative of removal by low-cost adsorbents: A review." Chemosphere **222**: 766-780.

R.V. Mundra, X. W., J. Sauer, J.S. Dordick, R.S. Kane (2014). "Nanotubes in biological applications." Curr. Opin. Biotechnol., **28**: 25-32.

Rangaraju , A. and K. Chaitanya (2018). "Spectrophotometric determination of lamotrignine using oxidative coupling reaction in Pharmaceutical dosage forms." Journal of Innovation in Pharmaceutical Sciences **2**(2): 49-52.

Sadeghi, S., Nasehi, Zohreh (2019). "Simultaneous determination of Brilliant Green and Crystal Violet dyes in fish and water samples with dispersive liquid-liquid micro-extraction using ionic liquid followed by zero crossing first derivative spectrophotometric analysis method." Spectrochimica Acta Part A: Molecular and Biomolecular Spectroscopy **201**: 134-142.

Saeed U J, A. A. K., Saad M, Iftikhar A, Guohua S, Cheng-Meng C, Rashid A (2020). "Removal of azo dye from aqueous solution by a low-cost activated carbon prepared from coal: adsorption kinetics, isotherms study, and DFT simulation." Environmental Science and Pollution Research **1**: https://doi.org/10.1007/s11356-020-11344-4.

Saeed Ullah Jan, A. A., Adnan Ali Khan1, Saad Melhi, Iftikhar Ahmad, Guohua Sun, Cheng-Meng Chen, Rashid Ahmad (2020). "Removal of azo dye from aqueous solution by a low-cost activated carbon prepared from coal: adsorption kinetics, isotherms study, and DFT simulation." Environmental Science and Pollution Research **1**: https://doi.org/10.1007/s11356-020-11344-4.

Sakin, O. A., H. M. ;Belal , H. M.;Arbi,M (2019). "Adsorption thermodynamics of cationic dyes (methylene blue and crystal violet) to a natural clay mineral from aqueous solution between 293.15 and 323.15 K." Arabian Journal of Chemistry **11**(5): 615-623.

Salam H. Alwan Altaa, H. A. H. A., Layth S. Jasim Al-Hayder (2018). "Synthesis and Characterization of rGO/Co3O4 composite as nanoadsorbent for Rhodamine 6G dye removal." Desalin. Water Treat. **114**: 320-331.

Salleh, M., Mahmoud, D.K.,Karim, W.A., Idris, A. (2021). "Cationic and anionic dye adsorption by agricultural solid wastes: A comprehensive review. ." Desalination **280**(1-3): 1-13.

Samia Afrin , M. S., Papia Haque , Md. Sazedul Islam , Shafiul Hossain ,Taslim Ur Rashid , Tanvir Ahmed , Makoto Takafuji , Mohammed Mizanur Rahman (2022). "Advanced CNC/PEG/PDMAA Semi-IPN Hydrogel for Drug Delivery Management in Wound Healing." Gels **8**: 340.

Sarkar, B., Mandal, Sanchita,Tsang, Yiu Fai,Kumar, Pawan,Kim, Ki-Hyun,Ok, Yong Sik (2019). "Designer carbon nanotubes for contaminant removal in water and wastewater: A critical review." Science of The Total Environment **612**: 561-581.

Sevda Pashaei-Fakhri , S. J. P., Rauf Foroutan ,Nasser Arsalani , Bahman Ramavandi "Crystal violet dye sorption over acrylamide/graphene

oxide bonded sodium alginate nanocomposite hydrogel, 2021." Chemosphere **270**: 129419.

Shoaib Nawa , M. S., Romana Khan, Nadia Riaz, Ummara Waheed ,Irum Shahzadi , Asmat Ali (2022). "Ultrasound-Assisted Hydrogen Peroxide and Iron Sulfate Mediated Fenton Process as an Efficient Advanced Oxidation Process for the Removal of Congo Red Dye." Pol. J. Environ. Stud **31**(3): 1-13.

Shumei Zhao, Y. Z., Xinyi Wan, Shuangjiang He, Xulin Yang, Jiaxin Hu, Guiyuan Zhang (2020.). "Selective and efficient adsorption of anionic dyes by core/shell magnetic MWCNTs nano-hybrid constructed through facial polydopamine tailored graft polymerization: Insight of adsorptionmechanism, kinetic, isotherm and thermodynamic study." Journal of Molecular Liquids **319**: 1-6.

Sotelo, J. L., A. R. Rodriguez, et al. (2012). "Adsorption of pharmaceutical compounds and an endocrine disruptor from aqueous solutions by carbon materials." J Environ Sci Health B **47**: 640-652.

Soulaima Chkirid , N. Z., Redouane Achour , Hicham Hassoune , Adil Lacheha, Abou el kacem Qaiss, Rachid Bouhfid (2021). "Highly synergic adsorption/photocatalytic efficiency of Alginate/Bentonite impregnated TiO2 beads for wastewater treatment " Journal of Photochemistry and Photobiology A: Chemistry **412**: 113215.

Soulaima Chkirida , N. Z., Redouane Achour , Hicham Hassoune , Adil Lachehab ,Abou el kacem Qaiss , Rachid Bouhfid (2021). "Highly synergic adsorption/photocatalytic efficiency of Alginate/Bentonite impregnated TiO2 beads for wastewater treatment." Journal of Photochemistry & Photobiology, A: Chemistry **412**: 113215.

Stefaniuk I, Cieniek B, et al. (2019). "Magnetic properties of ZnO:Co layers obtained by pulsed laser deposition method." Mater Sci-Pol **36**(3): 439-444.

Sukul, P., Lamsh, Marc,Zhlke, Sebastian,Spiteller, Michael (2019). "Sorption and desorption of sulfadiazine in soil and soil-manure systems." Chemosphere **73**(8): 1344-1350.

Tariq J. AlMusawi, N. M., Mahmoud Taghavi, Samaneh Mohebi, Davoud Balarak (2021). "Activated carbon derived from Azolla fliculoides fern: a high adsorption capacity adsorbent for residual ampicillin in pharmaceutical wastewater." Biomass Conversion and Biorefnery **1**: https://doi.org/10.1007/s13399-021-01962-4.

Thakur, S. (2017). "Synthesis, characterization and adsorption studies of an acrylic acid-grafted sodium alginate-based TiO2 hydrogel nanocomposite." Adsorption Science & Technology **0**: 1-20.

Thakur S, Pandey S, et al. (2019). "Development of a sodium alginate-based organic/inorganic superabsorbent composite hydrogel for adsorption of methylene blue. ." Carbohydr Polym **135**: 34-46.

V, N. (2020). "Streptococcal beta-hemolysins: genetics and role in disease pathogenesis." Trends Microbiol **10**: 575-580.

Vahidhabanu S, Karuppasamy D, et al. (2018). " Impregnation of zinc oxide modified clay over alginate beads: a novel material for the effective removal of Congo red from wastewater. ." RSC Adv **7**(10): 5669-5678.

Venkatesan Srinivasan, S. T., Kullagounder Subramani, Sibi Srinivasan, Pragathiswaran Chelliah, Stanley Anthuvan Babu (2014). "In Situ Disassembling Behavior of Composite Hydrogels for the Efficient Removal of Crystal Violet Dye from Aqueous Solution." ISRN Polymer Science **2**: 10.

Waleed K. Abdulsahib, S. H. G., Nadher D. Radia, Layth S. Jasim (2020). "New Approach for Sulfadiazine Toxicity Management using Carboxymethyl Cellulose Grafted Acrylamide Hydrogel." International Journal of Drug Delivery Technology **10**(2): 259-264.

Wang, W., Wang, A (2020). "Synthesis and swelling properties of pH sensitive semi-IPN superabsorbent hydrogels based on sodium alginate-g-poly (sodium acrylate) and polyvinylpyrrolidone." Carbohydr Polym **80**(4): 1028-1036.

Wieczerzak, M., Yotova, S. ,Tsakovski, V. ,Simeonov, J. (2019.). "*Impact of inorganic ions and pH variations on toxicity and endocrine potential of selected environmentally relevant pharmaceuticals.* ." Environmental Pollution **237**: 549-558.

X. Zhou, Y. Z. L., T. Peng, W. Xie, X.J. Zhao (2009). Materials Letters **63**: 1747-1749.

Xiong, J., J. Di, et al. (2020). "Hexagonal boron nitride adsorbent: Synthesis, performance tailoring and applications." Journal of Energy Chemistry **40**: 99-111.

Xu J, Liu X, et al. (2019). "The role of chemical and physical crosslinking in different deformation stages of hybrid hydrogels. ." Eur Polym J **100**: 86-95.

Y. Guo, H. S. W., C.L. He, L.J. Qiu, X.B. Cao (2009). Langmuir **25**: 4678-4684.

Yahya A. Faleh , N. D. R. (2021). "Removal of Metformin hydrochloride from Aqueous Solutions by using Carboxymethyl cellulose-g-poly(acrylic acid-co-acrylamide) Hydrogel: Adsorption and Thermodynamic Studies." IOP Conf. Series: Earth and Environmental Science **790**: 012062.

Yang, M., Huang, Y., Cao, H., Lin, Y., Cheng, X. and Wang, X., (2019). "A novel polymeric adsorbent by a self-doped manner: synthesis,

characterization, and adsorption performance to phenol from aqueous solution. ." Polymer Bulletin. **37**(8): 2321-2341.

Yao, Y., Bing, H., Feifei, X., Xiaofeng, C. (2011). "Equilibrium and kinetic studies of methyl orange adsorption on multiwalled carbon nanotubes. ." Chem. Eng. J. **170**(1): 82-89.

Yazidi A Atrous, M. E. S., Felycia S Lotfi , Smadji E Suryadi , Alessandro B Petriciolet , Luiz D Guilherme , Ben L Abdelmottaleb (2020). "Adsorption of amoxicillin and tetracycline on activated carbon prepared from durian shell in single and binary systems: Experimental study and modeling analysis." Chemical Engineering Journal **379**: 122320.

Yiping Feng , G. C., Yijian Zhang , Daguang Li , Chen Ling , Qiaoying Wang ,Guoguang Liu (2022). "Superhigh co-adsorption of tetracycline and copper by the ultrathin g-C3N4 modified graphene oxide hydrogels." Journal of Hazardous Materials **424**: 127362.

Yongde Liu, Y. C., Yahui Shi, Dongjin Wan, Jing Chen, Shuhu Xiao (2019). "Adsorption of toxic dye Eosin Y from aqueous solution by clay/carbon composite derived from spent bleaching earth." *Journal of Hazardous Materials*, **1**: 4656-5544.

Zaheer, Z., Al-Asfar, Aisha,Aazam, Elham Shafik (2019). "Adsorption of methyl red on biogenic Ag@Fe nanocomposite adsorbent: Isotherms, kinetics and mechanisms." Journal of Molecular Liquids **283**: 287-298.

Zhang, G., Feizbakhshan, Mohammad,Zheng, Shuilin,Hashisho, Zaher,Sun, Zhiming,Liu, Yangyu (2019). "Effects of properties of minerals adsorbents for the adsorption and desorption of volatile organic compounds (VOC)." Applied Clay Science **173**: 88-96.

Zhang M, Chang L, et al. (2019). "Fabrication of Zinc Oxide/ Polypyrrole Nanocomposites for brilliant green removal from aqueous phase." Arabian J Sci Eng **44**(1): 111-121.

Zhao Ying, C. Y., Zhao Jian, Tong Zongrui, Jin Shaohua (2019). "Preparation of SA-g-(PAA-co-PDMC) polyampholytic superabsorbent polymer and its application to the anionic dye adsorption removal from effluents." Separation and Purification Technology **2**: 123.

Zhao Ying, C. Y., Zhao Jian, Tong Zongrui, Jin Shaohua (2020). "Preparation of SA-g-(PAA-co-PDMC) polyampholytic superabsorbent polymer and its application to the anionic dye adsorption removal from effluents.Ultrasonics Sonochemistry " **25**: 12-18.

Zhou, M., He, J. (2013). "Uniform hamburger-like mesoporous carbon-incorporated ZnO nanoarchitectures: One-pot solvothermal synthesis, high adsorption and visible-light photocatalytic decolorization of dyes." Applied Catalysis B: Environmental **138**: 1-8.